

# Swamp Launch IREC – TropoGator Technical Report

Team 109 Project Technical Report for the 2022 IREC



Bilal Hassan<sup>1</sup> and Gavin Gamble<sup>2</sup>

*University of Florida, Gainesville, Fl, 32608, United States*

Matthew Estenoz<sup>3</sup> & Wiler A. Sanchez<sup>4</sup>

*University of Florida, Gainesville, Fl, 32608, United States*

Tsz Pan Chu<sup>5</sup> and Cristian A. Edgar<sup>6</sup>

*University of Florida, Gainesville, Fl, 32608, United States*

Nurettin K. Aslan<sup>7</sup> and Joshua T. Carson<sup>8</sup>

*University of Florida, Gainesville, Fl, 32608, United States*

---

<sup>1</sup> Project Manager, Aerospace Engineering, Senior 22', NAR Level 2.

<sup>2</sup> Structures Lead, Senior Consultant, Aerospace Engineering, Senior 22', NAR Level 2.

<sup>3</sup> Flight Dynamics Lead, Quality Consultant, Aerospace Engineering, Senior 22'.

<sup>4</sup> Payload Electronics Lead, Aerospace Engineering, Senior 22'.

<sup>5</sup> Payload Control Lead, Aerospace Engineering, Junior 23'.

<sup>6</sup> Payload Structures Lead, Aerospace Engineering, Senior 22'.

<sup>7</sup> Avionics & Recovery Lead, Aerospace Engineering, Sophomore 24'.

<sup>8</sup> Manufacturing Lead, Aerospace and Mechanical Engineering, Junior 23'.

The design of a high-powered rocket utilizing several Student Researched and Developed subsystems for the Spaceport America Cup 2022 in Las Cruces, NM is presented. The designed rocket features SRAD avionics (inertial measurement unit and altimeter), a carbon fiber reinforced polymer airframe, CNC machined modular aft section, and a reaction control wheel stabilizing payload. All systems are bench validated before flight through finite element models and physical testing. The rocket mission profile was developed through a SRAD flight simulation model to estimate the apogee of the flight and compare it to commercially available flight simulators. Test flight data is recorded through the avionics and compared to simulated flight to validate the model.



Fig. 1 External view of the TropoGator Launch Vehicle and Payload.

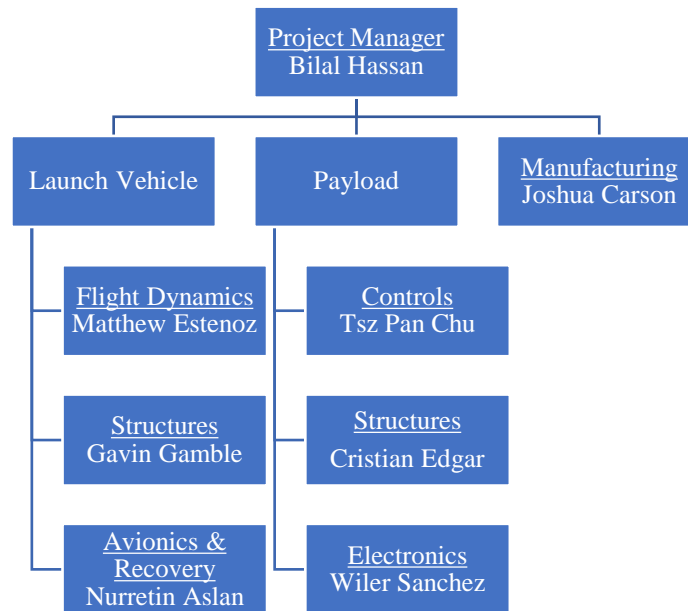
### I. Nomenclature

- APRS = Automatic Packet Reporting System
- BLDC = Brushless Direct Current Motor
- CFRP = Carbon fiber reinforced polymer
- COTS = Commercial Off-The-Shelf
- CPU = Central Processing Unit
- DTEG = Design, Test, & Evaluation Guide
- ESRA = Experimental Sounding Rocket Association
- GFRP = Glass Fiber Reinforced Polymer
- GPS = Global Positioning System
- HPR = High Powered Rocket
- IDE = Integrated Development Environment
- IMU = Inertial Measurement Unit
- KE = Kinetic Energy
- PCB = Printed Circuit Board
- PID = Proportional-Integral-Derivative
- PMI = Project Management Institute
- RCS = Reaction Control System
- RF = Radio Frequency
- SRAD = Student Researched and Developed
- UTM = Universal Testing Machine

### II. Introduction

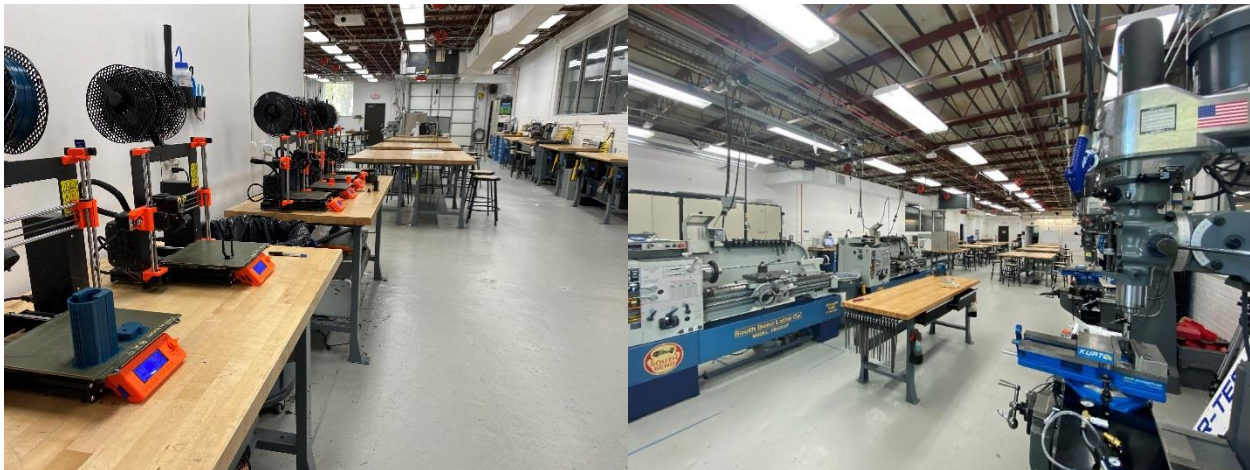
Students at the University of Florida Swamp Launch Rocket Team in Fall 2019 founded the IREC team to pave the path for more ambitious and experimental rocket designs. The team has competed in the NASA Student Launch Initiative since 2010, establishing and accumulating technical knowledge, documentation, and standard operating processes for building High Powered Rockets. Swamp Launch IREC’s mission statement is as follows: “The Swamp Launch IREC Team will develop a payload that will deploy at 10,000 feet using an M-Class COTS Propulsion High-Powered Rocket. The launch vehicle and payload will be exclusively designed and built by students using COTS and custom manufactured components. The entire launch vehicle and payload will be safely recovered after each flight. Experience gained from this experience will be used as an opportunity to provide engineering students at the University of Florida the ability to interact and engage with undergraduate students in a research-based, experiential design project.” The 2022 Spaceport America Cup will be the team’s inaugural visit to Las Cruces, NM to compete in the Intercollegiate Rocket Engineering Competition.

The team has been divided into three subteams each for the payload and launch vehicle and a manufacturing subteam to support manufacturing for both Fig. 2.



**Fig. 2 Breakdown of the Team Structure by subteam and respective lead.**

The team operates out of the Mechanical Design Laboratory and Student Design Center at the University of Florida. Individual subteams hold meetings to mentor and supervise student members on current project designs and simulations. The team uses OpenRocket, SolidWorks, ANSYS Fluent, and MATLAB to model and simulate the launch vehicle for Design for Manufacturing practices, Additive Manufacturing, and Manual Machining.



**Fig. 3 The team conducts team meetings and workshops in the Mechanical Engineering Senior Design Laboratory at the University of Florida. Prusa i3 MK3S 3D printers and Manual Mill and Lathes for manufacturing are shown.**

Team advisors and executives are updated on team progress and project design with monthly design reviews. University advisor Dr. Sean Niemi provides guidance in design and manufacturing, operations, and acts as the liaison between the team and the Mechanical and Aerospace department. University advisor Dr. Richard Lind, provides feedback on reports, launch vehicle design, and integration with the Student Launch team. The team mentor, Jimmy Yawn, provides High Powered Rocketry guidance as a National Association of Rocketry Level 3 member and advises designs and manufacturing to ensure safe and successful design and recovery. The team's safety reviewer, Matthew Reppa, reviews the design and concept of operation to ensure the design is safe and complies with competition rules and regulations.

The team integrated Project Management Institute (PMI) techniques to develop a schedule and budget for the completion of the project. A team charter established milestones and a work breakdown structure for each subteam, highlighting co-dependent tasks and critical tasks to be completed. Subteam leads present their progress with respect to the team's overall milestones at each design review. Leads have broken down their tasks for subteam members to complete, allowing for the documentation of operations over the course of the year. The team's monthly milestones are presented in Table I.

TABLE I  
Team Milestones 2021-2022

MONTH	MILESTONE
July	Subsystem Experimental Design Exploration
August	Literature Review Team Building
September	Project Scoping Chartering Session
October	Preliminary Subsystem Design Machine Training Team Members
November	Detailed Subsystem Design
December	Detailed Subsystem Design Review Order Parts over Winter Break
January	Validate Dimensions of Ordered Parts Revise Designs based on Review
February	Manufacture Subsystem Parts
March	Assemble Subsystems Manufacture Sub-Scale Launch Vehicle
April	Test & Fly Subscale Launch Vehicle Test & Revise Subsystems
May	Integrate Full-Scale Launch Vehicle Parachute and Payload Deployment Testing Full-Scale Test Flight
June	Spaceport America Cup 22

Each subteam is assigned a preliminary budget based on the agreed pre-allocated amounts in the chartering session. The budget is amended after the detailed subsystem design review, based on what is deemed necessary to complete the project. Funding for the team is provided by grants from the University's Student Government. Unfortunately, the team was unable to procure funding from Student Government. This forced the team to rely solely on Aerojet Rocketdyne. The team was subsequently constrained on the manufacturing, delaying the project in the spring 2022 semester.

### III. System Architecture Review



**Fig. 4 Transparent View of the TropoGator Launch Vehicle and Payload.**

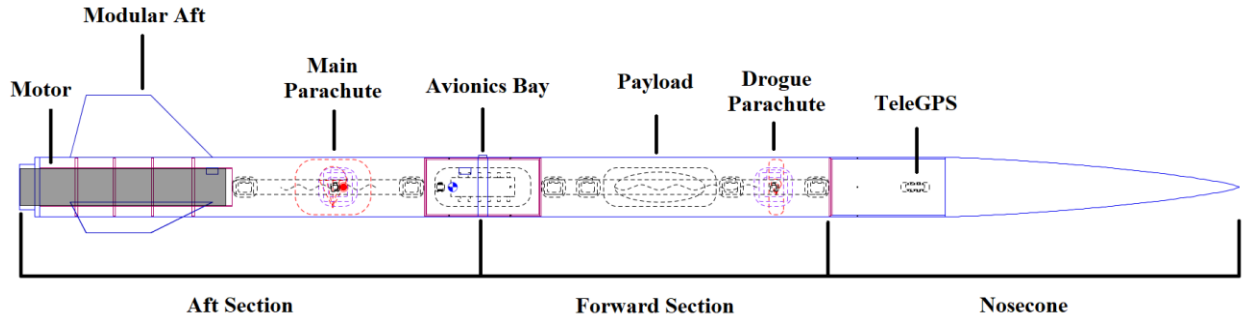
TropoGator is a 6-inch diameter, 10.7-foot tall, High-Powered Rocket propelled by a Cesaroni M2505 motor to deliver a 11.6-pound payload to an altitude of 10,000 feet. Flight simulations are performed in OpenRocket and an SRAD flight simulation code to ensure stability and predict mission performance. Carbon Fiber Reinforced Polymer fins and airframe maximize the strength to weight ratio of the rocket. The aft section utilizes a SRAD modular system, which will allow each component to be able to be replaced in the case of a flight failure. The avionics bay contains a dual redundant system to ensure ignition of the ejection charges if the main altimeter fails. The recovery system utilizes a dual-deployment configuration, with a drogue parachute deploying at apogee, and the main parachute deploying at 1000 feet. This configuration minimizes drift of the rocket during descent, while ensuring recovery of the rocket. An SRAD flight computer tracks the acceleration, orientation, and air properties to resolve the aerodynamics of the vehicle post flight. Finally, the CubeSat payload deploys separately from the rocket at apogee, and utilizes an IMU system, PID controller, and reaction wheel to control the orientation of the payload and mechanically stabilize a video of the payload’s descent.

#### A. Propulsion Subsystems

The objective of the propulsion subsystems experimental design was to select the launch vehicle configuration that would most consistently reach an apogee of 10,000 ft, while meeting the performance and configuration requirements listed in Table II. This resulted in a design with a von Kármán nose cone, three clipped delta fins, the CTI M2505 motor, the payload and drogue parachute in the forward section, and the main parachute in the aft section. The team will use the provided ESRA launch system, which satisfies requirement 1.11.

TABLE II  
Propulsion System Requirements

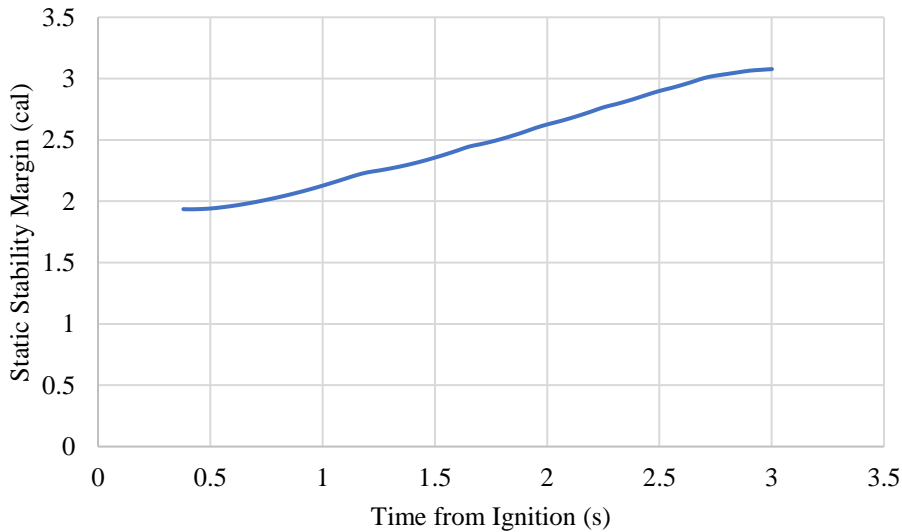
NUMBER	LEVEL	REQUIREMENT
1.1	Design	The launch vehicle must reach an apogee of 10,000 feet
1.2	Design	The thrust-to-weight ratio must be at least 5:1
1.3	Design	The rail departure velocity must be at least 100 ft/s
1.4	Design	The static stability margin must remain above 1.5 cal. throughout ascent
1.5	Design	The static stability margin must not greatly exceed 2 cal. throughout ascent
1.6	Competition	The elevation angle must be nominally 84°
1.7	Competition	The launch vehicle must attach to a 17 ft launch rail at two points
1.8	Competition	The selected motor propellant must be non-toxic
1.9	Competition	The selected motor must be certified by TRA
1.10	Competition	The motor’s total impulse must not exceed 40,960 N·s
1.11	Competition	The propulsion system must be able to arm from 50 ft away



**Fig. 5 OpenRocket model of the vehicle for modeling and simulation.**

Following the design of the other vehicle subsystems, the overall size and partial mass distribution of the vehicle had been determined. Modeling and simulation using OpenRocket as shown in Fig. 5 were then performed to generate mission performance predictions [1]. A von Kármán nose cone and clipped delta fins were then selected to minimize drag [2]. The motor was selected from those available and certified to achieve an apogee as close to the target as possible. The motor uses ammonium perchlorate composite propellant, satisfying requirement 1.8. The CTI M2505 is certified by the TRA, satisfying requirement 1.9. The total impulse of the motor is 7,396 N·s, satisfying requirement 1.10. The thrust-to-weight ratio of the vehicle is 11.2:1, satisfying requirement 1.2. The apogee was then tuned by modifying the fin geometry. However, changing the drag characteristics of the vehicle also perturbed its center of pressure and therefore its static stability margin. The static stability margin was then improved by changing the locations of the parachutes and payload to perturb the center of gravity of the vehicle.

The simulated vehicle has an apogee of 9,553 ft, which approaches design requirement 1.1. A more powerful motor wasn't available due to limited stock near competition. The simulations were performed accounting for an elevation angle of 84°, satisfying requirement 1.6. The simulation was also performed assuming launch from a 17 ft rail and the design includes two rail buttons, satisfying requirement 1.7. The rail departure velocity is 108 ft/s, satisfying requirement 1.3. The minimum static stability margin during ascent is 1.93 cal. and the maximum is 3.08 cal., satisfying requirements 1.4 and 1.5. This is illustrated in Fig. 6.

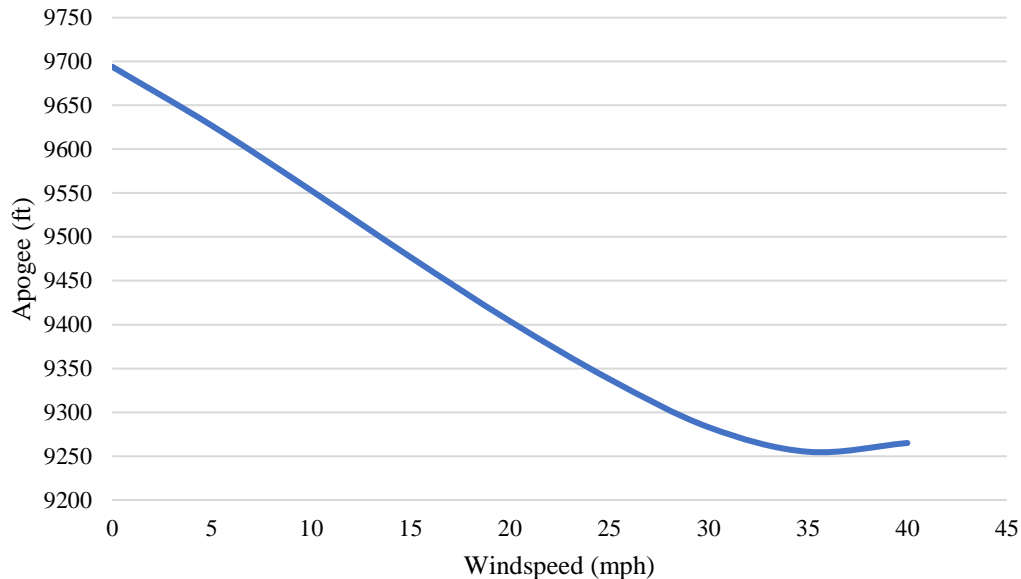


**Fig. 6 Variation of static stability margin during boost.**

The fin design was vetted for fin flutter and divergence. Pines' method for torsion-flexure flutter was applied to determine the critical speeds at which these failures would occur [3]. The method considered the airframe and fin geometries, fin material properties, sea level ambient conditions, and the fin elastic axis and center of gravity. The result was a flutter velocity of 1,555 ft/s and a divergence velocity of 1,111 ft/s, yielding respective factors of safety

of 1.57 and 1.12. The effective fin geometry was taken to be only that beyond the attachment brackets and therefore unsupported.

A sensitivity analysis was performed to determine the robustness of the vehicle under different launch conditions, as seen in Fig. 7. Because the launch hardware and angle are fixed, and changes in the possible range of ambient temperature and pressure would have only minor effects, the effect of different windspeeds on the predicted apogee was studied. The domain was based on historical data for possible windspeeds in Las Cruces, New Mexico in June. The apogee is then expected to range from 9,255 ft to 9,694 ft in the domain of expected windspeeds.



**Fig. 7 Sensitivity analysis of vehicle apogee versus windspeed.**

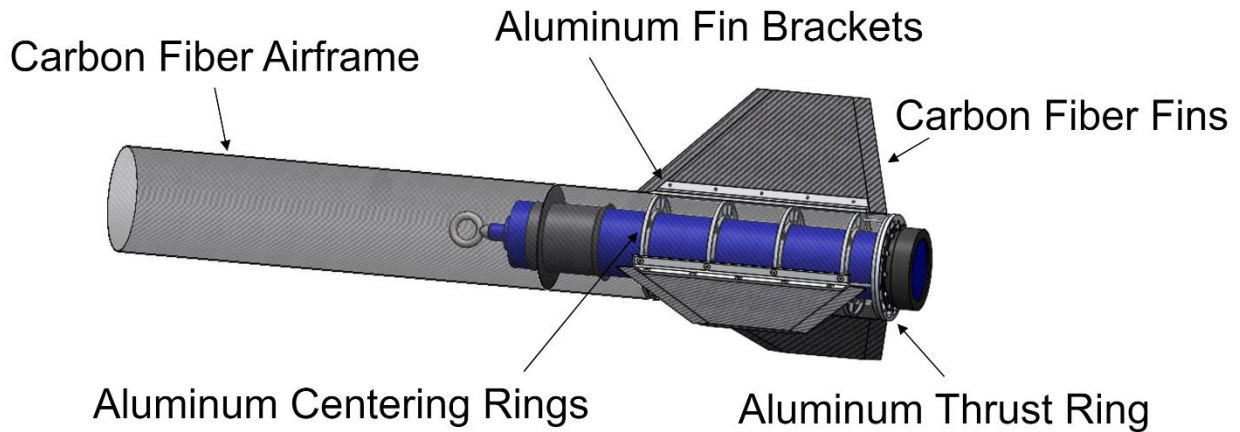
## **B. Aero-structures Subsystems**

The experimental design of the aero-structures subsystems was to design, analyze, manufacture, and test a modular aft system and SRAD CFRP airframe and fins that would allow the team to implement more complex engineering techniques than traditional HPR construction such as FEA, CNC manufacturing, composite manufacturing, and empirical testing. Traditional HPR construction consists of purchasing COTS airframes and coupler sections that are significantly stronger than necessary and epoxying the fins to the airframe using epoxy fillets that are difficult to characterize and do not provide an ideal platform for practicing engineering skills. A modular aft system would also allow the team to replace damaged components after flights or easily swap out fins for unique geometries or stiffness depending on the mission profile. SRAD carbon fiber composites were used to make the airframes and fins which could also be used for traditional HPR construction but allow for even greater weight savings in combination with the modular aft due to the high specific strength that they offer. The design and competition requirements necessary for these subsystems are outlined in Table III were met.

TABLE III  
Structures Subsystems Requirements

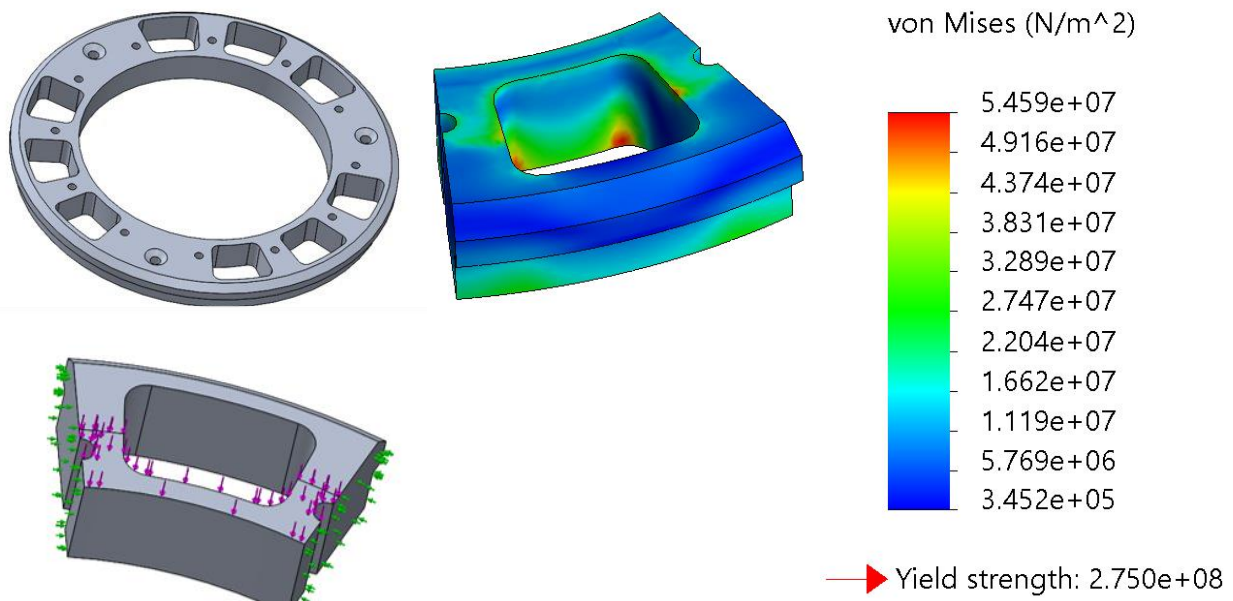
NUMBER	LEVEL	REQUIREMENT
2.1	Design	Be fully modular allowing fins to be easily replaced
2.2	Design	Construct airframe from SRAD carbon fiber
2.3	Design	Construct fins from SRAD carbon fiber
2.4	Competition	Launch vehicles shall be adequately vented to prevent unintended internal pressures developed during flight from causing either damage to the airframe or any other unplanned configuration changes
2.5	Competition	Launch vehicles will be constructed to withstand the operating stresses and retain structural integrity under the conditions encountered during handling as well as rocket flight
2.6	Competition	PVC (and similar low-temperature polymers), Public Missiles Ltd. (PML) Quantum Tube, and stainless-steel components shall not be used in any structural (i.e. load bearing) capacity, most notably as load bearing eye bolts, launch vehicle airframes, or propulsion system combustion chambers.
2.7	Competition	All load bearing eye bolts shall be of the closed-eye, forged type – NOT of the open eye, bent wire type.
2.8	Competition	Airframe joints which implement "coupling tubes" should be designed such that the coupling tube extends no less than one body caliber on either side of the joint – measured from the separation plane.
2.9	Competition	Rail guides should implement "hard points" for mechanical attachment to the launch vehicle airframe.
2.10	Competition	The aft most launch rail button shall support the launch vehicle's fully loaded launch weight while vertical.
2.11	Competition	The team's Team ID (a number assigned by ESRA prior to the IREC), project name, and academic affiliation(s) shall be clearly identified on the launch vehicle airframe, nose cone and other locations where possible.





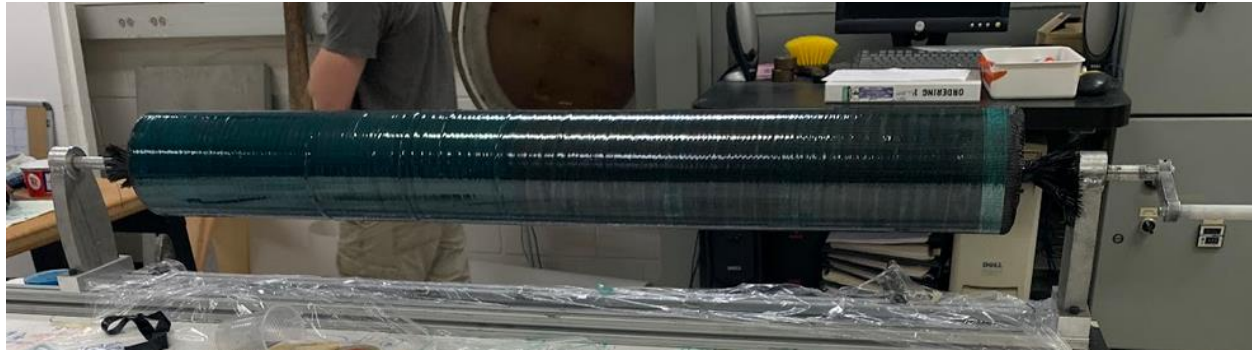
**Fig. 8 CAD of modular aft with the airframe semi-transparent.**

The design requirements for the structure of the rocket that were set in place were to challenge the team to go outside the traditional methods used for high power rockets and utilize engineering tools that are common to industry to build a more optimized rocket that is capable of being easily modified and repaired. To implement the modular design, satisfying requirement 2.1, and keep the components as light as possible, SolidWorks FEA was heavily utilized to remove as much material as possible until the maximum stresses on all components was kept above a factor of safety of 2.5 (Fig. 9). Mesh convergence was used in the FEA studies to model the system most accurately, however due to the complex nature of the boundary conditions introduced by the loading structure, empirical testing will also be used to validate the system when the components are fully integrated [4]. All metal components in the modular aft are made of Aluminum 6061-T6 due to its low cost and ease of manufacturing. The thrust ring, centering rings, and aft centering ring were all cut on an abrasive waterjet cutter and finished on manual lathes and milling machine. The nosecone for the rocket is a COTS G12 filament wound fiberglass. The nosecone was chosen to be COTS because of the difficulty of creating contoured composite structures, and to maintain RF transparency where the telemetry system will be housed.



**Fig. 9 SolidWorks FEA Von-Mises Stress of Thrust Ring. A small cutout of the part was selected to reduce computation time.**

Composites have become more commonplace in the aerospace industry in the last few decades due to their high specific strength that provides desirable weight savings over traditional metals. In the past, the rocket team has used COTS G12 airframes, which is a filament wound fiberglass tube, however there is room to reduce the weight and optimize the strength of the airframes by manufacturer them in house with carbon fiber epoxy composite materials. To satisfy requirement 2.2, a process to fabricate custom carbon fiber airframes was developed that utilized carbon fiber sleeves on a polycarbonate mandrel. It was found the optimal construction of the carbon fiber airframes was achieved with a 3-ply layup, with the first ply being a 3k bidirectional sleeves, the second ply a 12k unidirectional sleeve, and the third ply was an additional 3k bidirectional sleeve, all sourced from Soller Composites. The sleeves were pulled over the mandrel one at a time and wetted out with Soller Composites 820 epoxy system, which combines exceptional wet-out characteristics with a high strength and a slow cure time. After fully wetted out, the entire mandrel was helically wrapped in PET flash tape, which has a silicon-based adhesive and will not adhere to the epoxy. By wrapping the entire mandrel with this semi-elastic tape, excess epoxy is squeezed from one end of the airframe to the other, seen in Fig. 10, resulting in a more optimal fiber-volume fraction that has been measured between 50 and 55%. The exact manufacturing process for the airframes was refined over a period of 2 years and over 7 iterations of experimentation before the final airframe was suitable for use in a high-power rocket. The airframes were tested in compression using a UTM and the results were compared against the performance of the COTS G12 tubes as well as a 4-ply layup using two unidirectional layers for additional strength. It was found that the 3-ply tubes provided the optimal strength to weight ratio, compared to the fiberglass COTS tubes, and were significantly easier to manufacture than the 4-ply airframe. The testing setup can be seen in Appendix B and the results are detailed in Table IV.



**Fig. 10 Carbon fiber airframe after being wrapped with PET tape**

TABLE IV  
Load Testing of Airframes

AIRFRAME	MAX LOAD IN PURE COMPRESSION	MAX LOAD WITH THRUST RING	AVERAGE THICKNESS	WEIGHT PER INCH
3 Ply	11,530 lbf	7,380 lbf	0.056"	0.75 oz
4 Ply	14,380 lbf	7,052 lbf	0.066"	0.99 oz
COTS G12	25,000 lbf **	8,470 lbf	0.088"	2.02 oz

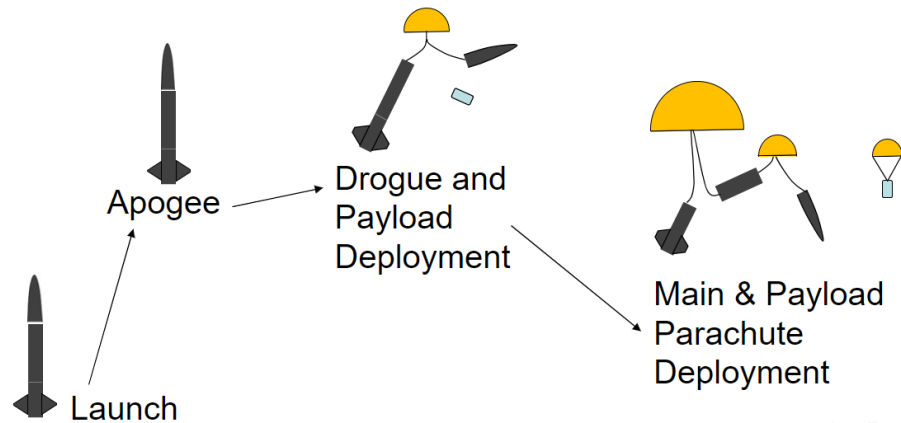
\*\* The max load until failure for the COTS G12 was not able to be determined due to reaching the force limits of the testing machine.

Traditionally, the fins of high-powered rockets are cut from isotropic or quasi-isotropic COTS sheet materials, however this year the team set out to create CFRP fins with a custom layup of pre-impregnated carbon fiber fabric cured in a vacuum bag and oven. This method of manufacturing achieves fiber volume fractions on the order of 60%, has less voids than wet layups, and can be used to optimize the stiffness of a material specific to the directions that are required for the specific application. The fins on an HPR, which are mounted as cantilever beams, experience a bend-twist coupling force during flight that results from aerodynamic forces. The layup for the fins utilized three unique fabrics for optimizing the strength and reducing manufacturing time. The fabrics used were a 3k unidirectional fabric, a 3k plain weave fabric, and a 12k 2x2 twill fabric. The unidirectional plies were used to give the fins strength in the bending direction, while the woven fabrics were used to give the fins strength in torsion. The layup was customized for the fins using a composite laminate theory program that was written in MATLAB to simulate the ideal composition

of the fins [5]. Using stiffer materials than the traditional G10 fiberglass fins, the thickness of the fins was reduced by 16% while having a higher stiffness, and the density is 22% less, improving the overall weight of the fins as well. The layup used for the fins is as follows:  $[45_{3k}/0_{3k}/(0_{1k})^4/(45_{3k})^2/0_{12k}/45_{12k}]_S$  resulting in a total thickness of 0.157”.

The airframe of the flight vehicle has 1/8” holes located in each isolated section to prevent premature separation during ascent, which satisfies requirement 8.1 of the DTEG. Requirement 8.2 was met by load testing the airframe and structures components with a high factor of safety before failure to ensure they could withstand the forces expected during flight. All bulkheads and load bearing components use G10 fiberglass, aluminum T6-6061, carbon fiber, and high strength steel to satisfy requirement 8.3. To satisfy requirement 8.4, all load bearing eye-bolts are of the closed-eye, forged-type capable of withstanding a minimum of 50 G’s of acceleration of the flight vehicle against the shock chords, based on the weight after motor burnout. All coupler tubes being used are COTS G12 fiberglass, which extend 6 inches from the plane of separation into the respective connecting airframe section, satisfying requirement 8.5. For requirements 8.6 and 8.7, the two rail buttons being used are COTS nylon parts and are attached to the airframe using a wooden hardpoint to transfer the load to a larger area on the airframe, which allows the weight of the entire rocket to be supported by the aft-most rail button.

### C. Avionics & Recovery Subsystem



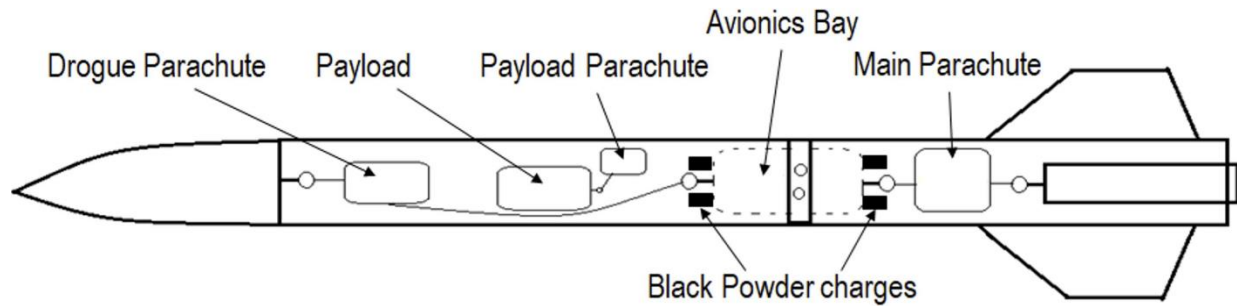
**Fig. 11 Recovery Events Diagram including Payload Deployment**

The objective of the avionics and recovery subteam was to design a parachute configuration, an assembly that houses the recovery electronics and flight computer, and GPS tracking system to retrieve the launch vehicle safely. The launch vehicle recovery system was integrated with the payload recovery such that the drogue and payload can be deployed at apogee as shown in Fig. 11. The electronics that are responsible for deploying the parachutes are housed in the avionics bay which is designed to be easily accessible for adjusting any of its components on the field. The flight computer is a SRAD microcontroller housed in the avionics bay utilized to record acceleration, angular velocity, magnetic field, ambient pressure, and temperature data of the launch vehicle for post-flight analysis. A TeleGPS is placed in the nosecone of the rocket to improve the likelihood of recovering the launch vehicle post-flight and satisfy requirement 3.7. Table V further details all the design and competition requirements that were followed for the design process.

TABLE V  
Avionics & Recovery System Requirements

NUMBER	LEVEL	REQUIREMENT
3.1	Design	Easy to access Avionics Bay
3.2	Design	Utilize a standard Dual Deploy Recovery Configuration
3.3	Design	Eject a payload and payload parachute with drogue parachute at the apogee event
3.4	Design	Impact the ground at no more than 20 ft/sec descend rate
3.5	Design	Adjustable flight computer sled to change location according to the CG of the launch vehicle when the motor propellant mass is exhausted.
3.6	Design	Place COTS telemetry GPS tracker in the nose cone to avoid RF interference from the carbon fiber airframe.
3.7	Competition	All rockets are required to have a GPS tracking solution on their rockets.
3.8	Competition	GPS Tracking Options 70cm – To avoid significant delays in potentially launching, teams should utilize 70cm/APRS systems for their GPS tracking systems. Requires a HAM license, or a similar international licensing.
3.9	Competition	Each independent recovered launch vehicle body anticipated to reach an apogee above 1,500 ft shall follow a "dual-event" recovery
3.10	Competition	The initial deployment event shall occur at or near apogee to stabilize the vehicle's attitude to prevent or eliminate ballistic re-entry; appropriate speeds between 75 and 150 ft/s
3.11	Competition	The main deployment event for any recovery method shall occur at an altitude no higher than 1,500 ft (457 m) AGL and reduce the vehicle's descent rate sufficiently to prevent excessive damage upon impact with ground (< 30 ft/s or 9 m/s)
3.12	Competition	The recovery system shall implement adequate protection to prevent hot ejection gases from causing burn damage to retaining chords, parachutes, and other vital components as the specific design demands.
3.13	Competition	The recovery system rigging shall implement appropriately rated swivel links at connections to relieve twist/torsion as the specific design demands.
3.14	Competition	Launch vehicles shall implement completely independent and redundant recovery systems to include arming switches, sensors/flight computers, power supply, energetics, and "electric initiators". And at least one of the systems shall include a COTS flight Computer.
3.15	Competition	All safety critical wiring shall implement a cable management solution which will prevent tangling and excessive free movement of significant wiring/cable lengths due to expected launch loads.
3.16	Competition	All safety critical wiring/cable connections shall be sufficiently secure as to prevent disconnecting due to expected launch loads.
3.17	Competition	All energetics shall be "safe" until the rocket is in the launch position, at which point they may be "armed".
3.18	Competition	All energetic device arming features shall be externally accessible/controllable.

The dual-deployment recovery configuration consists of two parachutes deployed at two separate events, satisfying competition requirement 3.2. This configuration consists of the launch vehicle descending under a drogue parachute deployed at apogee until the launch vehicle is closer to the ground, minimizing drift, and satisfying competition requirement 3.10. The first event takes place at apogee where the ignition of the e-charges pressurizes the inside of the airframe causing the nose cone to separate and push the payload and the RocketMan 48” drogue parachute out of the forward section of the launch vehicle. The drogue parachute is located on top of the payload, so to connect the drogue parachute to the avionics bay, a slit was made on the payload body to create a gap between the payload and the airframe through which the shock cord falls through and connects to the avionics bay. To reduce potential failures due to tangling during deployment, this deployment configuration was tested in a subscale design which proved to be a success validating the design. The second event takes place when the launch vehicle descends to 1000 feet where the second e-charges are fired to separate the aft section from the avionics bay which ejects the main parachute. The main parachute that is used is a Fruity Chutes IRIS Ultra 96” parachute which slows the launch vehicle to 20 ft/second descent speed to recover with no major damage to its components, satisfying competition requirement 3.11.



**Fig. 12 Recovery configuration diagram. The shock cord in the forward airframe bypasses the payload.**

To calculate the black powder charge mass to eject the components from both the forward and aft sections, the pressure to separate the sections was calculated using Equation 1. The force required to separate the sections is estimated by using an upper limit of 1334.5 N [4]. The upper limit is used due to the large diameter of the airframe.

$$P = \frac{F}{\pi * \left(\frac{D}{2}\right)^2} \quad (1)$$

Where  $F$  is the approximated upper limit of force of ejection,  $g$  is gravitational acceleration, and  $D$  is the inner diameter of the airframe in meters. The pressure necessary for ejection is calculated to be 73.2 kPa. The amount of black powder to create sufficient pressure to reliably cause separation and deploy the payload can be estimated using the ideal gas law assumption in which the black powder charge mass necessary is solved for. This assumes a combustion temperature of 1739 K, and a gas constant of 12.1579 m-K<sup>-1</sup> for FFFFg black powder [4].

$$PV = mRT \quad (2)$$

Where  $P$  is the pressure required to push the payload out,  $T$  being the combustion temperature and  $R$  being the gas constant for FFFFg black powder. The volume  $V$  will be calculated considering only the empty cavity the ejection charge is fired within. For the forward section, this volume would be between the avionics bay forward bulkhead and the payload bottom bulkhead. For the main section, this volume would be between the avionics bay aft bulkhead, and the modular aft sealing disk. After plugging in the volume calculated for the respective sections into Equation 2, the mass of black powder necessary is found to be 2.48 g for the forward section, and 2.79 g for the aft section. During ejection testing, the black powder ejection mass is tested to verify the mass calculated and adjust based on the results of the test.

The deployment of both main and drogue parachute generates a force that is transferred through all the recovery components of the launch vehicle equal to the drag of the parachute added to the weight of the launch vehicle:

$$F = D + W \quad (3)$$

$$F = \frac{1}{2} \rho \cdot V^2 \cdot A \cdot C_d + m \cdot g \quad (4)$$

Where F is for deployment force, D is for drag, W for weight,  $\rho$  for density of air, V for descent velocity, A for area of the parachute,  $C_d$  for drag coefficient of the respective parachute, m for mass of the rocket and g is the acceleration due to gravity. The descent velocities are measured from the OpenRocket simulation of the launch vehicles flight at the respective event for each parachute deployment. The deployment force for the drogue parachute is 500 N, and the main is 1440 N.

A steel eyebolt is fastened into the nose cone bulkhead and motor casing for each section. A steel quick-link and swivel are attached to fasten the eyebolt to the 1-inch Kevlar shock cord. A HPR rule of thumb stating that the shock cord should be at least 3 times the length of the launch vehicle airframe leads the shock cord length for both sections to be 32 feet. Swivels are added to the eyebolts on the nose cone bulkhead and motor casing eyebolt to prevent twisting from parachutes unthreading eyebolts, satisfying requirement 3.13. An additional quick-link fastened at a third of the shock cord length attaches each parachute via its respective swivel. Load from the deployment force is transferred through the 1/4" threaded rod. The recovery hardware is rated for strength in Table VI using the main deployment force of 1440 N to ensure a factor of safety greater than 1.

TABLE VI  
Recovery Hardware Strength Rating

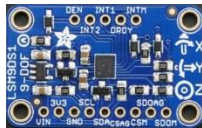





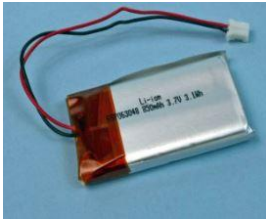

COMPONENT	DESCRIPTION	RATED STRENGTH*	FACTOR OF SAFETY
Eyebolt	3/8" Steel Eyebolt	5780 N	4.0
U-bolt	1/4" x 2-1/4" National Hardware U-bolt	1890 N	1.3
Threaded Rod	1/4" High-Strength Steel Threaded Rod	32800 N	22.8
Quick-Links	9/32" Thickness Steel Quick Link	4450 N	3.1
Swivel	RocketMan 3,000 lbf Stainless Steel Swivel	13400 N	9.3
Shock Cord	RocketMan 1" Kevlar Shock Cord	24500 N	17.0

\* Values are converted from the manufactured provided units in lbf. to N.

Ejection gases created due to the burning of the black powder are flammable and can damage the parachutes and the parachute lines. To prevent burning of the recovery equipment and comply with requirement 3.12, parachutes are folded inside a DinoChutes parachute protector flame-retardant fabric. For the same reason, Kevlar shock cord is selected due to its flame resistance. As an extra layer of safety, an insulating flame-resistant recovery wadding is placed between the ejection charges and the parachutes inside the airframe.

The purpose for the avionics is to be able to perform dual-deployment and determine the location of the launch vehicle after it has landed on the ground. The launch vehicle is equipped with a telemetry module in the nose cone and avionics bay responsible for payload deployment and recovery. The avionics bay houses a flight computer used to inertially track the vehicle's position and orientation during flight. The flight computer records acceleration, orientation, magnetic field, pressure, and temperature to an external storage unit. The telemetry module uses a COTS TeleGPS to relay the real-time position of the launch vehicle to a ground station for recovery and mid-flight tracking. The key electrical components that make up the avionics and recovery electronics are listed in Table VIII.

TABLE VII  
Avionics & Recovery Electronic Equipment

DEVICE	SPECIFICATIONS	IMAGE
Adafruit LSM9DS1 Inertial Measurement Unit	$\pm 2/\pm 4/\pm 6/\pm 8/\pm 16 \text{ g's}$ $\pm 2/\pm 4/\pm 8/\pm 16 \text{ Gauss}$ $\pm 245/\pm 500/\pm 2000 \text{ }^\circ/\text{s}$ $1.3'' \times 0.8'' \times 0.1''$ $2.5 \text{ g} / 0.1 \text{ oz}$	
Adafruit BMP388 Precision Barometric Pressure Altimeter	$\pm 8 \text{ Pa}$ $\pm 0.5 \text{ }^\circ\text{C}$ $1.0'' \times 0.7'' \times 0.1''$ $1.2 \text{ g} / 0.1 \text{ oz}$	
Altus Metrum TeleGPS	$16 \text{ mW}$ Transmit Power $2 \text{ Mb}$ Flash Memory $1.5'' \times 1.0'' \times 0.3''$ $12.3 \text{ g} / 0.4 \text{ oz}$	
Altus Metrum TeleDongle	$433 \text{ MHz}$ Yagi Antenna $70 \text{ cm}$ wavelength	
Stratologger SL100 Altimeter	$20 \text{ Hz}$ sample rate $1.5 \text{ mA}$ consumption $12.8 \text{ g} / 0.5 \text{ oz}$ $2.8'' \times 0.9'' \times 0.5''$	
Featherweight Raven Flight Computer 3	$20 \text{ Hz}$ sample rate $440 \text{ Hz}$ axial accelerometer $220 \text{ Hz}$ lateral accelerometer $1.8'' \times 0.8''$	
Lithium Polymer Battery	$3.7\text{V}$ $900 \text{ mAh}$ $24.1 \text{ g} / 0.9 \text{ oz}$ $2.0'' \times 1.2'' \times 0.3''$	
Lithium Polymer Battery	$3.7\text{V}$ $2000 \text{ mAh}$ $2.2'' \times 1.4'' \times 0.5''$ $40 \text{ g} / 1.4 \text{ oz}$	

To meet requirement 3.14, a redundant avionics system is designed such that if the primary altimeter fails, a secondary altimeter entirely interdependent from the first system will fire the ejection charges. Both altimeters selected are COTS to maximize reliability of the system. A decision matrix of altimeters in the team’s inventory was made to select the altimeters used in the avionics bay and payload.

TABLE VIII  
Altimeter Decision Matrix

Altimeter			Raven 3			StratoLogger SL100			Entacore AIM			TeleMetrum		
			Mag	Score	Value	Mag.	Score	Value	Mag.	Score	Value	Mag.	Score	Value
Objective	Weight Factor	Parameter												
Reliability	0.30	Experience	1.00	10	3.00	1.00	10	3.00	0.50	1.0	0.30	0.67	2.0	0.60
Mass	0.10	Grams	6.6	10	1.0	12.8	4.0	0.40	12.8	4.0	0.40	20.1	1.0	0.10
Volume	0.15	In <sup>3</sup>	0.7	9	1.35	1.2	7.5	1.13	1.4	6.0	0.90	1.8	3.0	0.45
Cost	0.15	USD	155	4.5	0.68	79.9	8	1.2	121.2	5.0	0.75	363.5	1.0	0.15
Sampling Rate	0.30	Hz	20	10	3	20	10	3	10	5.0	1.5	100	10	3
					9.03			8.73			3.85			4.3

Weight factors prioritize reliability based on team experience with the altimeter and sampling rate for post-processing the data. The lowest scoring altimeter is the Entacore AIM, largely due to its unreliability as an altimeter, with two launch failures occurring due to premature triggering of ejection charges by the altimeter. The Raven 3 was selected as the best altimeter due to its small form factor and high sampling rate making it the primary altimeter. The small form factor also enables the Raven 3 to be used in the payload’s avionics bay where space is limited. The StratoLogger SL100 came in second and was therefore selected as the secondary altimeter.

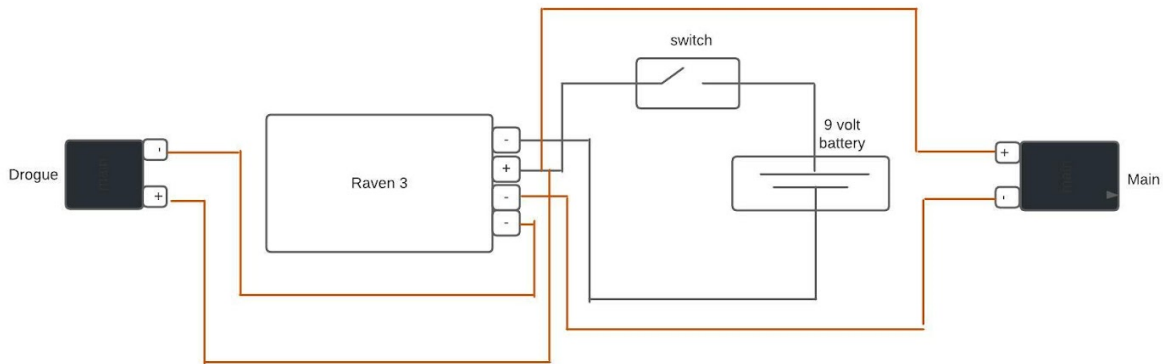
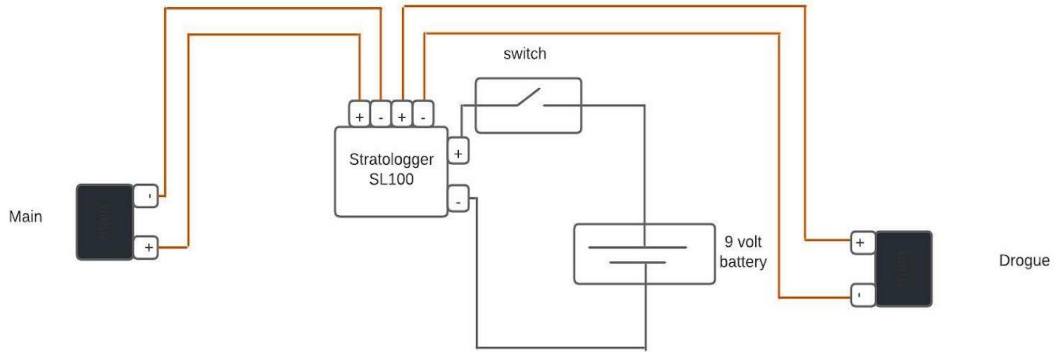


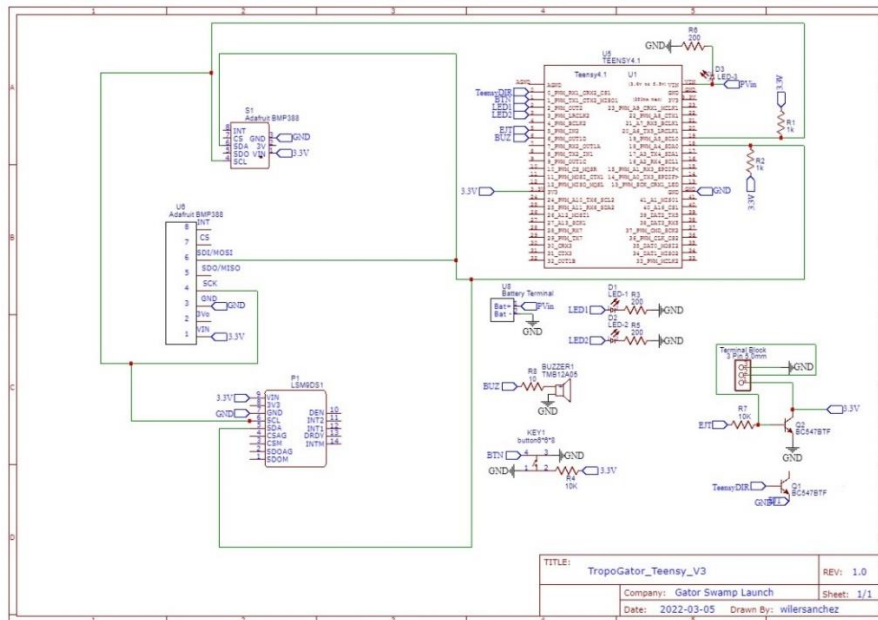
Fig. 13 Wiring Diagram for the main altimeter system using the Raven 3.



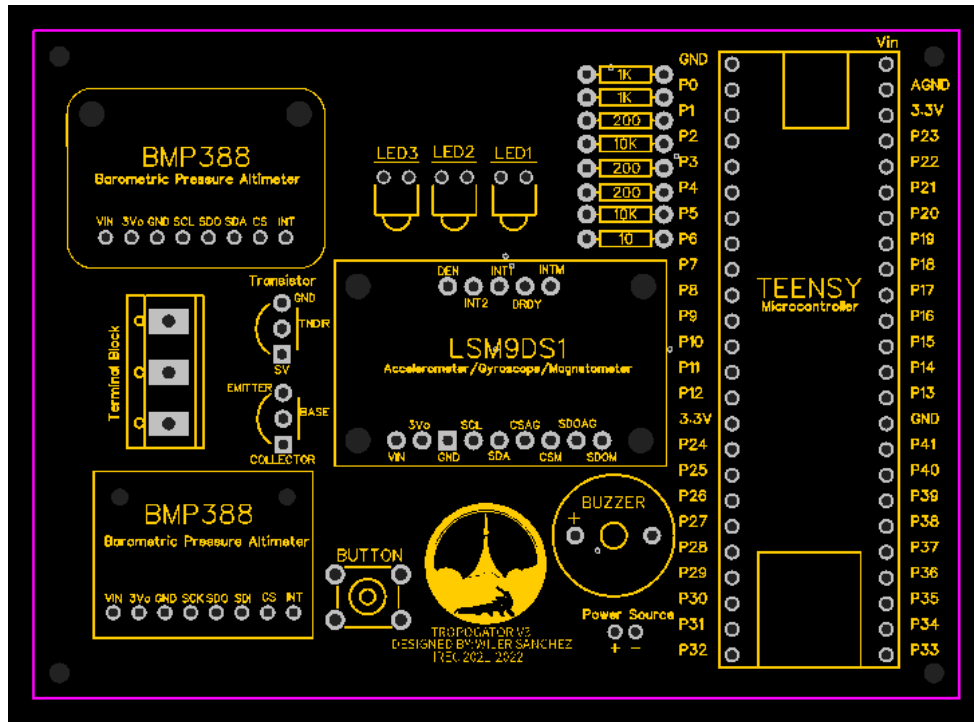


**Fig. 14 Wiring Diagram for the redundant altimeter system using the Stratologger SL100.**

The SRAD flight computer is the third computer housed in the avionics bay, and records the acceleration, orientation, magnetic field, pressure, and temperature of the launch vehicle throughout flight. The data is written to an SD card attached to the Teensy 4.1 microcontroller on the IMU. The recorded raw data is used by the flight dynamics sub team to model the trajectory of the launch vehicle during flight and study the aerodynamic performance of the launch vehicle during post-flight analysis. To ensure electrical and mechanical stability between the connection of all the electrical components housed on the flight computer, a printed circuit board is designed. The software used to design the PCB for the flight computer is EasyEDA, an open-source software for PCB design. Fig. 15 is the schematic which includes all key and minor electrical components. Fig. 16 is the PCB drawing that was exported to JLCPCB for manufacturing.

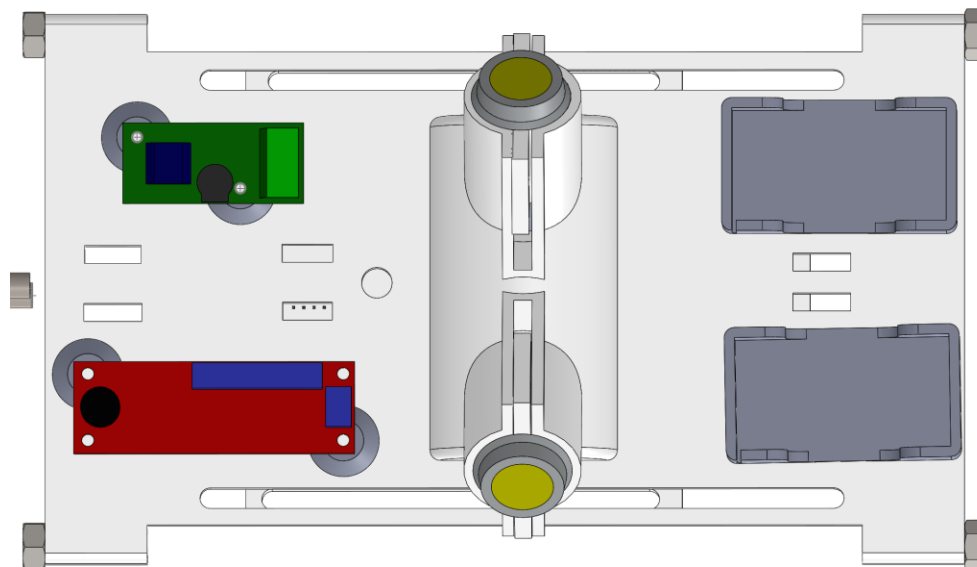


**Fig. 15 The schematic of the flight computer. The drawing is the third version of the flight computer and was exported from EasyEDA.**



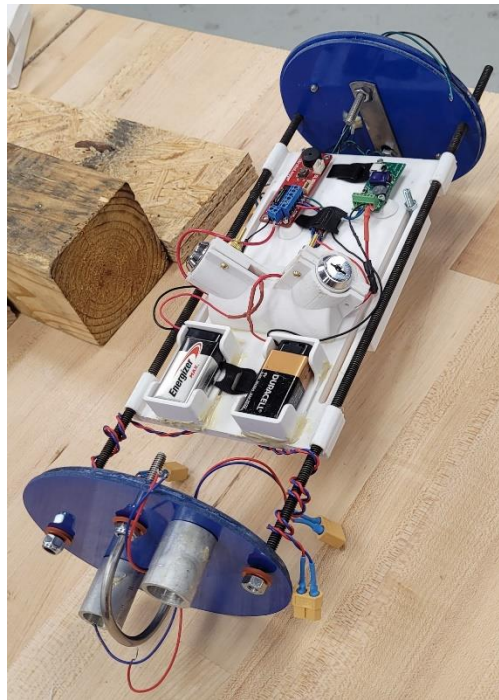
**Fig. 16** The PCB drawing reflects the physical placement of all minor and key components. The drawing is the third version of the flight computer and was exported from EasyEDA.

The flight computer is programmed in C/C++ and developed in Arduino IDE. External libraries derived from each of the devices on the flight computer are utilized in the flight software. A calibration sequence is programmed within the software and is intended to calibrate the IMU when the avionics bay is fully assembled prior to launch. To notify the operator that the calibration sequence has been finished, a buzzer will generate a noise that will indicate the sequence has finished. The flight software is preprogrammed to the Teensy 4.1 microcontroller.



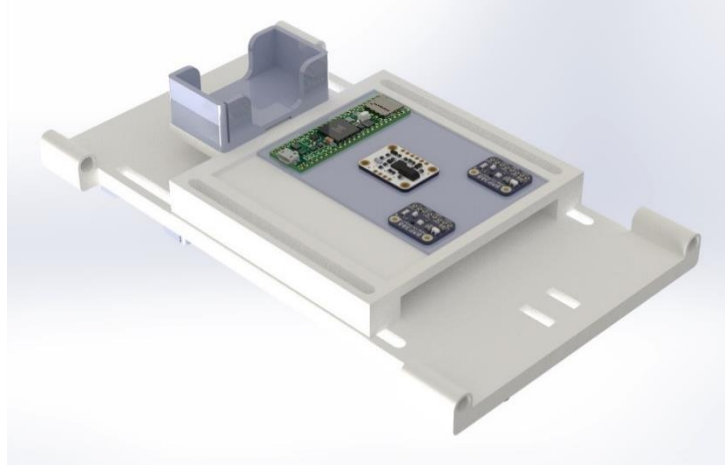
**Fig. 17** Electronics sled CAD located in the avionics bay.

The electronics sled shown in Fig. 17 was designed to fit two 9 V batteries, two key switches, a SL100 StrataLogger and a Raven 3 altimeter. It was 3D printed from the more heat resistant filament PETG. To give clearance to the sensors underneath the altimeters, the altimeters were raised by using conical 2 mm tall raisers which were also 3D printed and glued on to the sled. Threaded inserts were put inside the raisers to fasten the altimeters to the sled. The 9V batteries that power the altimeters are secured inside a hollow rectangular part which has a slit underneath to leave an opening for a Velcro strap to tie the battery down from moving out of the housing. These battery housings are also super glued on the electronics sled. To ensure the wires were secure, all wire connections were soldered and protected through a heat shrink. Zip ties were used to secure loose wires and a wire tug test was performed at all terminals to satisfy competition requirement 3.16. The wires were further braided and wrapped around the threaded rods, and XT60 wiring connectors were used to pass the wires through the bulkhead. The key switches that are responsible for arming and disarming the altimeters are held up by a part that places each key switches with 45-degree angle from the sled mirrored to each other. These key switches held by the part become flush to the airframe, and they are accessed through two holes with 0.629 inches in diameter which are drilled on the airframe, which satisfies competition requirement 3.18.



**Fig. 18 The wired avionics bay prior to testing for redundancy.**

The team's flight simulator is dependent on the center of gravity of the launch vehicle, as it is a key variable in the equations of motions of a moving non-linear rigid body. The IMU records the flight data during the coasting phase, where all the motor propellant has been expended, to resolve the aerodynamic parameters during post-flight analysis. An adjustable sled for the flight computer is designed to place the computer at the estimated center of gravity location during the coasting phase. The adjustable sled is composed of two rounded slots that run through each plate and fits four screws along with a nut for each screw. The screws are tightened when the sled is placed at the desired location. The design allows for the electronics to be shifted within the avionics sled to be moved to a desired location, depicted in Fig. 19.

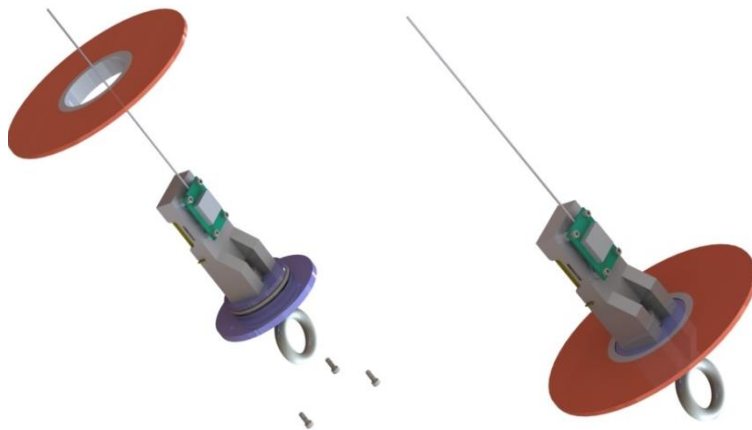


**Fig. 19 A CAD model of the adjustable sled housed in the avionics bay.**

A COTS telemetry system, the AltusMetrum TeleGPS, is selected to track the position of the launch vehicle and satisfy requirement 3.7. The telemetry module is housed in the nose cone of the launch vehicle to avoid RF signal interference from the carbon fiber airframe which satisfies design requirement 3.6. The TeleGPS transmits on a 70 cm band and requires a Ham Radio Technician License for operation which has been acquired by the payload electronics lead. This transmission allows the operator to join an APRS network present during the IREC competition.

A laptop is used to interface as the ground station between the TeleGPS and TeleDongle telemetry modules. The laptop will run AltusOS, the proprietary software that interacts with the TeleGPS; it allows for real-time tracking of the launch vehicle via pre-loaded satellite maps and records the flight data to a spreadsheet.

To ensure the telemetry module remains secure throughout flight and recovery, epoxy was used to fasten the mounting ring to the nosecone, as well as the inner ring to the mounting ring. The bulkhead and electronics mount were secured to the inner ring using three 6-32 screws, fastened into threaded inserts placed in the inner ring as shown in Fig. 20. The battery sits in a 3D-printed containment area and is restrained by Velcro straps. All 3D-printed parts were made with 100% infill for full structural integrity.



**Fig. 20 CAD model of the telemetry model before (left) and after (right) placement into nosecone.**

To fulfill competition requirement 3.14, the bulkhead and electronics mount has a #224 Buna-N O-ring to help contain the deployment gases from reaching the interior volume of the nose cone during ejection. The tolerances for designing the O-ring fitting in the bulkhead, as well as the proper tolerances for the bulkhead and the inner ring, were taken from the Machinery's Handbook [5].

The telemetry module was designed for easy attachment and removal. While the mounting ring and inner ring were secured to the nosecone by epoxy, the bulkhead and electronics mount were fastened to these using three 6-32 screws; this allows for quick assembly before and after launch. This also aided in conserving the TeleGPS battery when not actively being used. The electronics mount was also designed to allow charging of the TeleGPS without removing it from the mount.

The bulkhead that has the electronics module is also used to connect the nosecone to the recovery system through a 3/8" steel eyebolt. The drogue parachute is attached to that eyebolt, and the whole telemetry module is epoxied 12 inches into the nosecone coupler to allow for additional space for the drogue parachute below it. To streamline the manufacturing process, PETG parts were designed with 3D printing in mind and were all manufacturable with the Prusa i3 MK3S printers we have in the lab. The only non-PETG component was the mounting ring, which we made from 1/8" fiberglass using the lab's abrasive waterjet, shown in red in Fig. 20.

#### **D. Payload**

The objective of the payload was to demonstrate an ability to maintain orientation to magnetic north despite disturbances by ejection during deployment and wind during descent. A camera is additionally mounted into the payload structure to record the payload during its operation. The payload's ability to reorient itself is accomplished by utilizing a reaction wheel, which by the law of conservation of angular momentum will cause the payload structure to rotate with respect to its roll axis in response to the reaction wheel's rotation. The payload design is split into three sections described in the sections below: the control system which describe the mechanism with which the payload orients itself, the electronics with which the payload acquires information about its surroundings as well as send commands to actuators, and the structure which house all components. The payload is separated from the launch vehicle at apogee with the payload parachute to satisfy requirement 4.11.

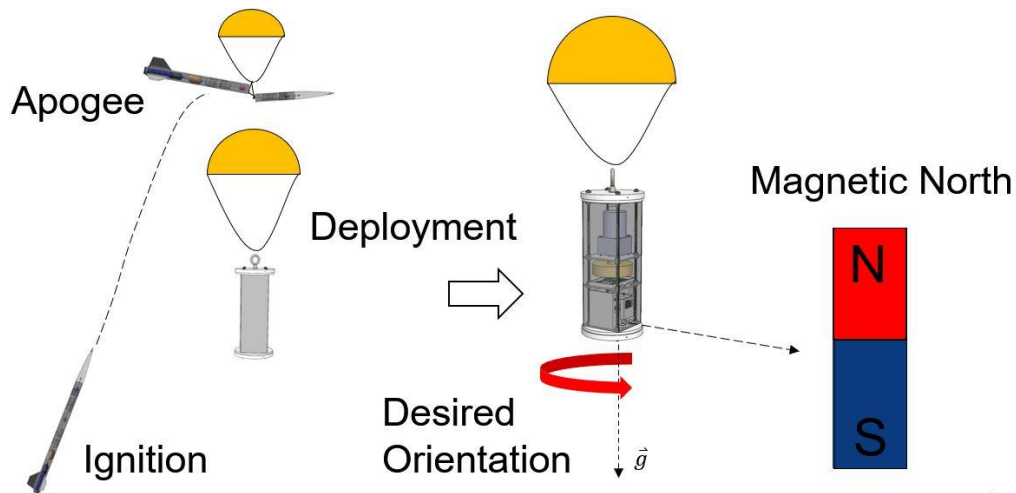


**Fig. 21 Reaction control payload render. The payload follows a 3U CubeSat structure format.**

TABLE IX  
Payload Subsystem Requirements

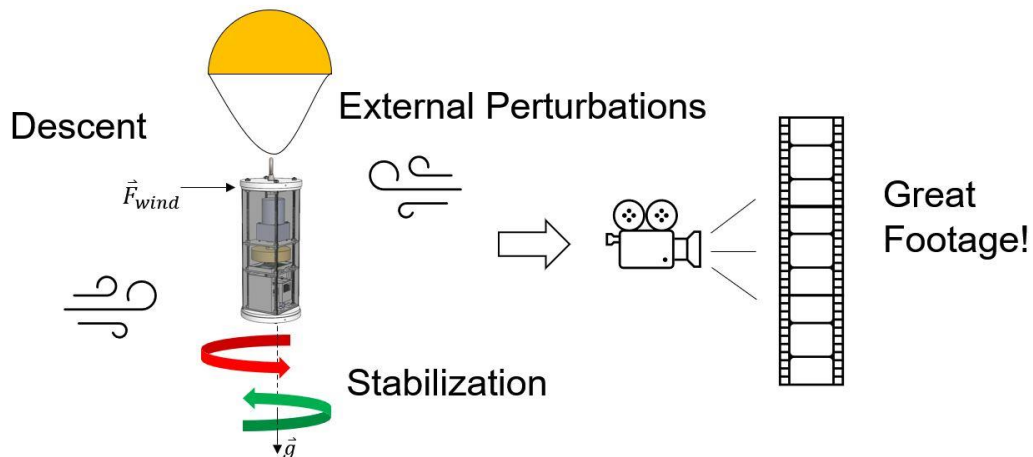
NUMBER	LEVEL	REQUIREMENT
4.1	Design	Must be under 12 lbf., including adapter and reaction wheel.
4.2	Design	Must be able to withstand impact, deployment, and flight forces.
4.3	Design	Must be able to maintain a fixed payload orientation to a degree that the video from the recording camera is stabilized.
4.4	Design	Electronics must be protected from ejection gases.
4.5	Design	Electronics must be powered for duration of mission.
4.6	Design	Altimeter must be powered and accessible from outside the airframe.
4.7	Design	Must be able to deploy at apogee.
4.8	Design	IMU and reaction wheel must be as close to the center of mass as possible.
4.9	Competition	Payload must weigh a minimum 8.8 lbf.
4.10	Competition	Payload must be constructed in a CubeSat form factor.
4.11	Competition	Deployable payload must incorporate an independent recovery system, reducing payload velocity to less than 30 ft/s before 1500 ft.
4.12	Competition	Payloads using independent recovery systems must comply with same requirements for safety critical wiring and redundant electronics.
4.13	Competition	Must implement completely independent and redundant recovery systems.
4.14	Competition	All wiring must be secure to prevent disconnecting during flight.
4.15	Competition	Pyrotechnics must not be used on the payload.
4.16	Competition	Payload cannot drift into White Sands Missile Range.
4.17	Competition	Payload cannot explode inside the rocket.
4.18	Competition	Must be able to deploy on its own without tangling.
4.19	Competition	Payload will operate and leave rocket only at apogee to not affect launch vehicle's angular momentum.

The launch vehicle first ejects the payload at apogee, together with the launch vehicle's drogue parachute and payload parachute. The photoresistor connected to the flight computer decreases its resistance when it has detected an increase in light from being exposed to the sun indicating the payload has exited the launch vehicle. A pyrotechnic charge contained inside the cable cutter is triggered after the flight computer has detected that the payload is outside the launch vehicle. The charge actuates the cable cutter, deploying the payload's parachute satisfying requirement 4.13, stating the payload design must include an independent recovery system. After a programmed delay, the RCS will turn on and begin stabilizing the payload as it descends from the sky. The delay is put in place to minimize the possibility of entanglement between the parachute lines, satisfying requirement 4.18. The RCS's PID control mechanism will compare the direction of magnetic north to the actual direction the payload is facing. The difference is determined to be the error, which is processed by the PID controller to get a command signal that actuates the BLDC motor and spins the brass reaction wheel, inducing a moment on the payload. This action rotates the payload to the direction of magnetic north. The direction of magnetic north is given by the magnetometer and the actual direction the payload is facing is generated by the sensor fusion algorithm from the Mahony filter library [6] in the flight software. A detailed diagram of this phase of the mission is depicted in Fig. 22.



**Fig. 22** The first phase of the payload’s mission. The payload descends from apogee and is rotated to face magnetic north.

As the payload descends down from the sky, external wind forces will hit the payload inducing a non-desired moment on the payload, destabilizing it as it descends. Here, the experiment demonstrates its purpose by using the RCS to mitigate unwanted perturbations on the payload, and mechanically stabilize the payload. This satisfies requirement 4.3 in Table IX. By recording the footage, the reaction control system can be verified to see if it is working as intended and the team can acquire footage of the payload coming down from the sky. A detailed diagram of this phase of the mission is depicted in Fig. 23.



**Fig. 23** The second phase of the payload’s mission. The payload experiences external wind forces, destabilizing it upon descent. The RCS mitigates this destabilization and is verified through camera footage.

Once the payload has descended near the ground, a five-minute timer will deactivate all the powered electronics to minimize any damage resulting from the impact of the payload hitting the ground. The timer will commence once the payload has initiated the experiment. The retrieval of the camera footage and flight data concludes the payload’s mission.

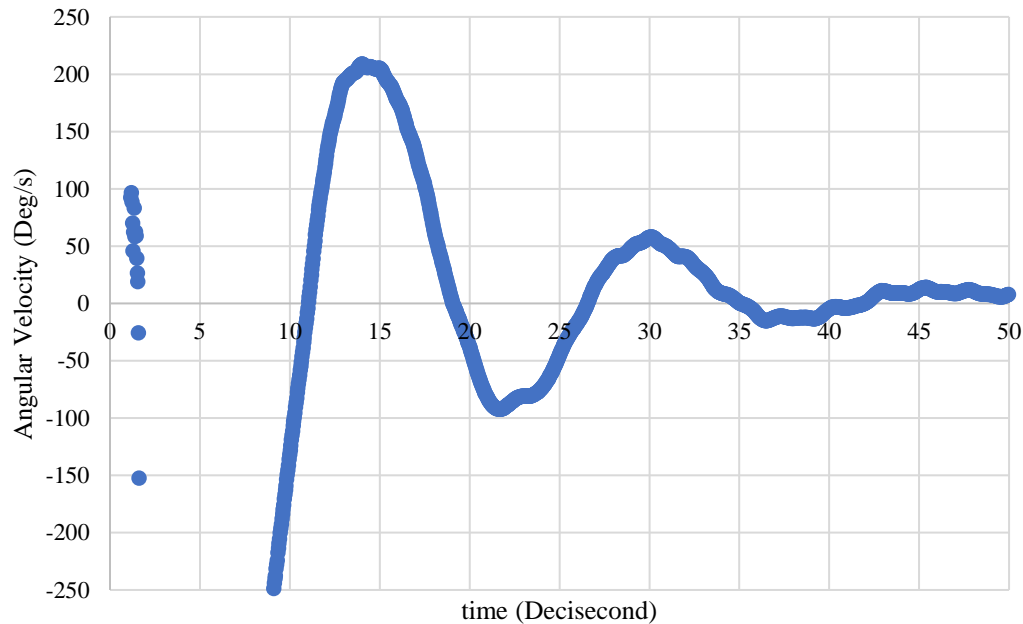
The control system of the payload is composed of a BLDC motor for its actuation, brass reaction wheel, as well as the controller itself. The objective of the system is to track magnetic north as well as mitigate the disturbances to the angular position experienced during the payload’s deployment as well as its descent. To achieve these objectives, a feedback control system using an orientation sensor to monitor position and a reaction wheel to adjust position was used. The reaction wheel and motor used were designed to be able to mitigate the greatest expected disturbance to the

payload which is at its deployment while a PID controller is used to give the motor control command based on the reference position. A goal of  $\pm 10^\circ$  error from the desired position was set as one of the parameters while manually tuning the PID controller gains.

Since the angular momentum of the system is conserved, the components for the control system were sized to have enough angular velocity as well as sufficient moment of inertia about the center of mass to affect the payload. Data recorded from a mockup of the payload is used to determine its peak angular velocity after ejection. The payload was subjected to random disturbances, and it was found that angular velocity would consistently reach between 200 and 300 deg/s despite variations in applied forces after the initial disturbance, shown in Fig. 24 and 25.



**Fig. 24** Experimental setup of the mock-payload. Dummy mass was included to properly replicate moment of inertia of actual payload setup, with angular velocity recorded with a BNO055.



**Fig. 25** Experimental setup of the mock-payload. Dummy mass was included to properly replicate moment of inertia of actual payload setup, with angular velocity recorded with a BNO055.



This peak value was set to be the design angular velocity,  $\omega_D$ . Design angular velocity is multiplied with the known moment of inertia about the roll axis of the payload to obtain the design angular momentum  $H_D$ . The angular velocity output of the motor and the moment of the inertia of the reaction wheel must be greater than or equal to the design angular momentum, so both motor and reaction wheel are sized based off the equation below:

$$\omega_D I_{PL} = H_D \leq \omega_{RW} I_{RW} \quad (5)$$

Equation 5 is now solved to give an estimate for choosing a motor. For the control system, a 30W, 3000 RPM motor was chosen with a 20:1 planetary gear reduction for an output of 150 RPM. A power flow diagram for this motor is shown Fig. 26.

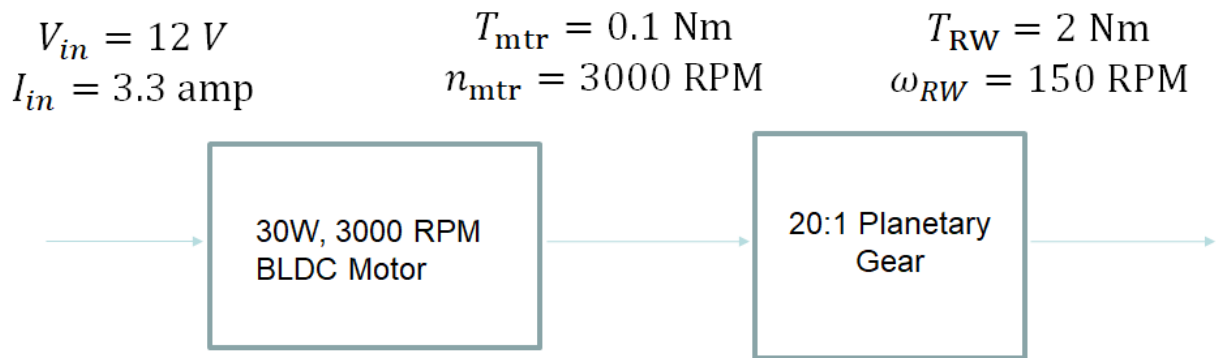


Fig. 26 This combination produces the above power flow diagram for the payload system. Not accounted in this system are any losses due to inefficiencies.

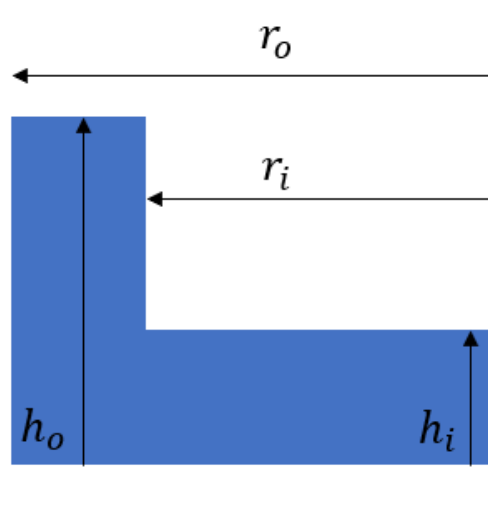


Fig. 27 The dimension  $r_o$  is the outer radius of the reaction wheel,  $r_i$  is the inner radius of the reaction wheel,  $h_o$  is the outer height of the reaction wheel, and  $h_i$  is the inner radius of the reaction wheel.

After the actuator was chosen, the reaction wheel is designed to maximize the moment of inertia while minimizing its weight. To accomplish this, most of the mass of the reaction wheel is placed at the periphery of the reaction wheel. To fit within the payload CubeSat structure and satisfy the design requirement 2.3.5.2, the maximum outer radius of the reaction wheel is set at 1.938 inches and the maximum outer height at 1 inch. The dimensions of inner height and inner radius are chosen based off requirements and found to be 1.05 inch and 0.85 inch respectively. A cross-section of the reaction wheel is shown in Fig. 27.

Inner height and inner radius are adjusted to obtain a moment of inertia for the reaction wheel, which must satisfy equation 5, found to be around 6.30 lbm-in<sup>2</sup> about center of mass with brass as the material. Although both inner height and radius may be adjusted, it is more efficient with respect to mass to adjust inner radius rather than inner height, shown in the table below:

TABLE X  
Comparison of Inner Height versus Inner Diameter Adjustment.

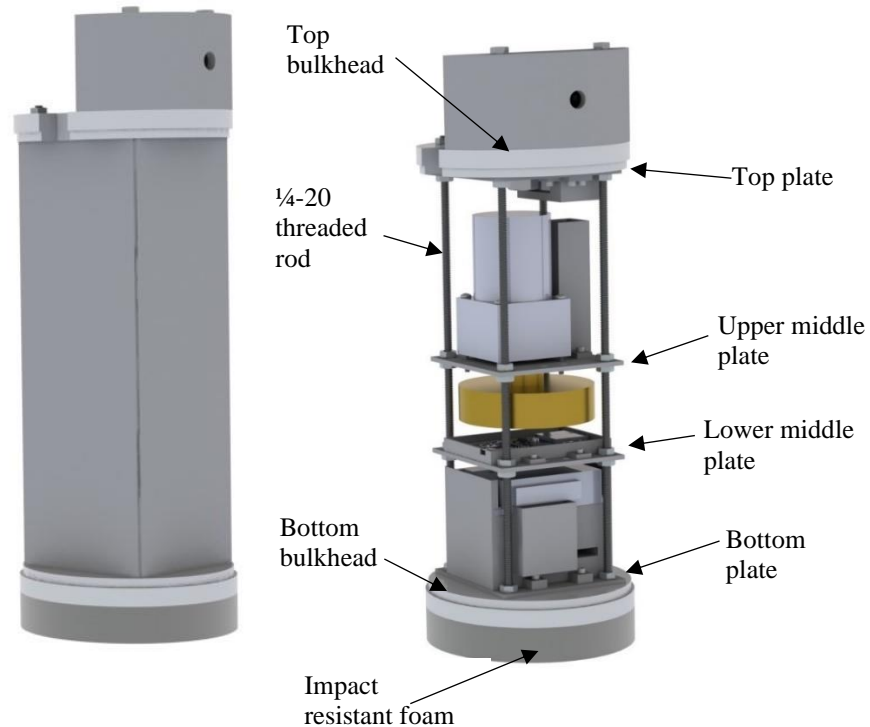
HEIGHT (INCH)	RADIUS (INCH)	LYY ABOUT C.O.M (LBM-IN <sup>2</sup> )	MASS (LBM)	LYY/MASS	RESULTANT MAX ANGULAR VELOCITY DISTURBANCE (DEG/S)
0.85	1.05	6.31	2.82	2.24	200.88
0.65	1.15	6.30	2.92	2.16	200.57

The final moment of inertia, taken at center of mass, of the reaction wheel was found to have a moment of inertia of 5.80 lbm-in<sup>2</sup>. The angular velocity output of the reaction wheel combined with the moment of inertia of the reaction wheel will allow for a theoretical maximum angular velocity disturbance of 200.88 deg/s, which will match the theoretical peak angular velocity disturbance and satisfy the requirement 4.3 of being able to mitigate disturbance to payload during deployment and descent. The maximum angular velocity disturbance the payload will be able to account for is calculated with the equation below:

$$\frac{I_{RW}\omega_{RW}}{I_{PL}} = \frac{(5.80 \text{ lbm in}^2)(150 \text{ RPM})}{28.27 \text{ lbm in}^2} = 200.88 \text{ deg/s} \quad (6)$$

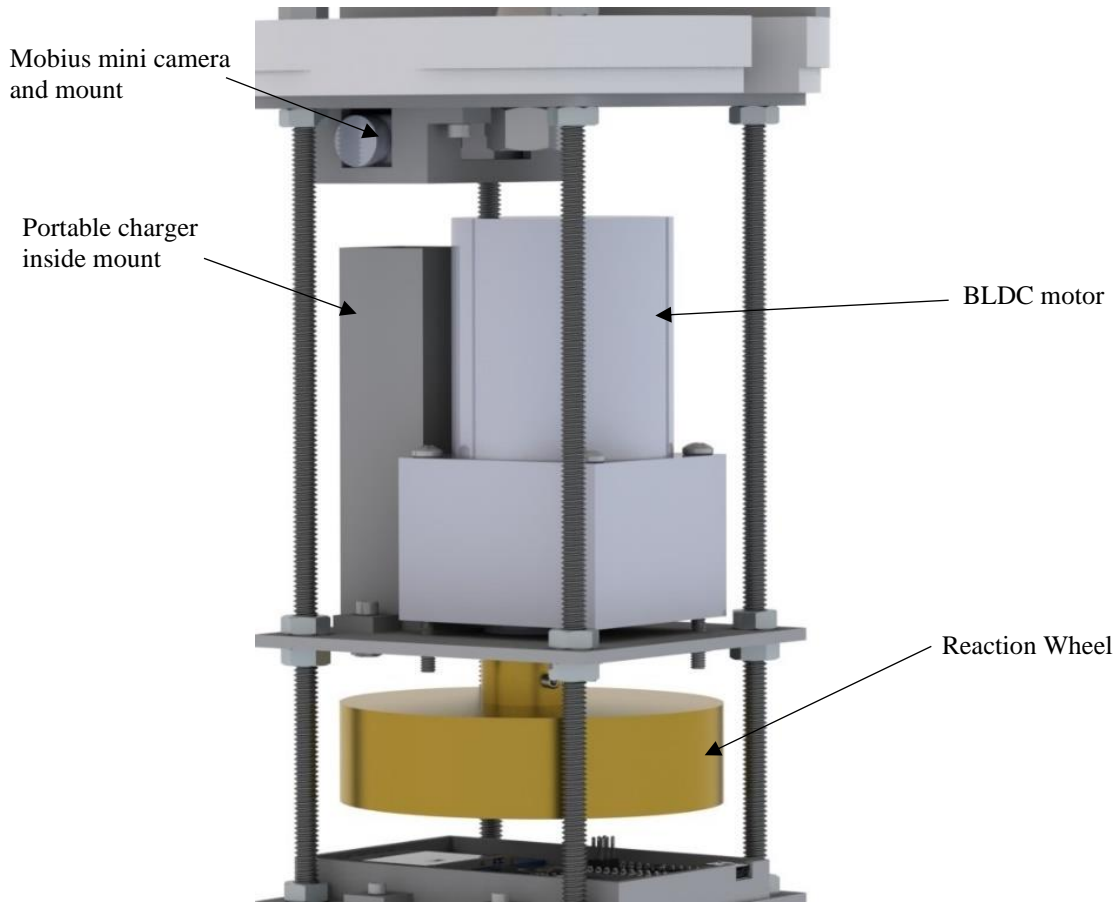
After the components of the system are obtained, an appropriate control scheme can be chosen. The payload is a linear time-invariant system assuming the control system is in operation only after it has been deployed from the launch vehicle. If the system is linear, the output of the system, the angular position, will vary linearly with the input, the reaction wheel speed. From equation 5, this can be seen to be true. The system is assumed to be time-invariant since during its operation, the conditions it operates in will not change besides its altitude which may affect air density, but this is assumed to be negligible. Based on this assumption, a simple PID controller is chosen to control the system. The gains for the proportional, integral, and derivative gains were obtained manually by running the control system on the payload and adjusting these gains until error between simulated disturbances were less than  $\pm 10^\circ$ .

The payload structure is composed of the interior CubeSat, which houses the payload components, and the adapter, which consists of PVC bulkheads on the top and bottom of the structure, with a 3/8 in. eyebolt and an avionics bay on the top bulkhead, and an inch long layer of impact resistant foam on the bottom bulkhead. The CubeSat structure consists of four 1/8-inch thick G10 fiberglass square plates, with a 4 in x 4 in cross-section to satisfy requirement 4.10. The CubeSat, bulkheads, avionics bay and foam are held together by four 1/4 inch steel threaded rods. The rods pass through the corners of all four of the CubeSat plates, and through the bulkheads and foam layer. Two rods also pass through the avionics bay and measure 18 inches, whereas the other two are 16 inches long, as seen in Fig. 28. The CubeSat is enclosed by fiberglass sealing panels that are 1/16 inch thick, held into the assembly by the PVC bulkheads. These serve the purpose of preventing ejection gases from the black powder from entering the CubeSat during deployment, as those gases could potentially fry the electronic components inside the CubeSat and would satisfy objective 4.4.



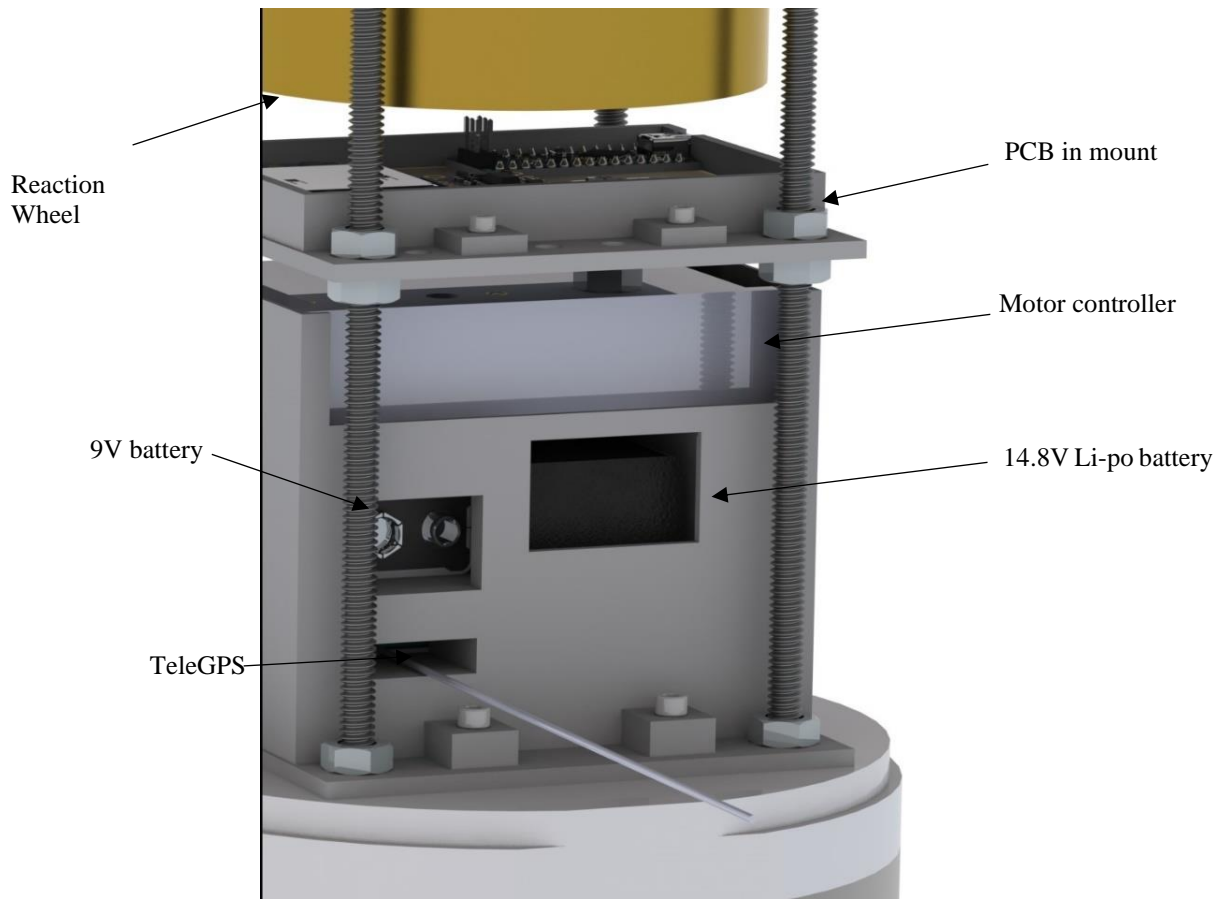
**Fig. 28 Views of payload with sealing panels, and with internal components visible**

Inside the CubeSat, a Mobius Mini camera is placed inside a 3D-printed mount and bolted into the bottom of the top CubeSat plate, with the screws used threaded into the top bulkhead. This camera is used to take video footage of the flight, payload deployment and roll control experiment. The portable charger used to keep the Mobius' battery running is found in a mount bolted to the plate below, the upper middle plate to satisfy requirement 4.3. The camera's USB cable is plugged into the portable charger from above. The upper middle plate also serves as the housing for the BLDC motor, which is bolted to it at the top. The brass reaction wheel used for the motor control experiment is then attached to the motor shaft below the plate via an 8-32 set screw. The reaction wheel placement allows for it to be as close to the center of gravity as possible, simplifying the control algorithm and satisfying requirement 4.8. The upper middle plate also contains holes for the motor's wires to pass through. The wires are additionally zip tied to the threaded rods to secure them and prevent them from interfering with the reaction wheel to satisfy requirement 4.12.



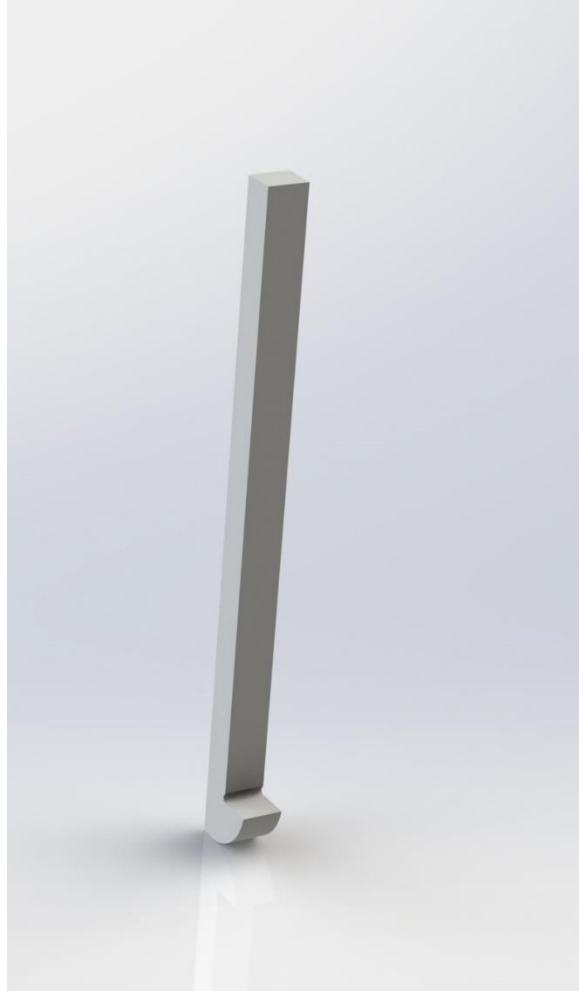
**Fig. 29 View of the top half of the payload.**

The lower middle plate contains a mount bolted to it which holds the PCB board right below the reaction wheel, which allows the IMU to be located at the center of mass, satisfying requirement 4.8. Additional holes for the motor wire to pass through are located on the back of the plate, and holes for the 9V battery wires to pass through from below and connect to the PCB's Teensy, satisfying requirement 4.12. Below it, in the bottom plate, a mount for the motor controller, batteries, and TeleGPS can be found. The motor controller is bolted to the top of the mount after the 9V battery lithium-ion battery, and TeleGPS are placed inside the mount, securing the batteries. The lithium-ion battery can thus connect to the motor controller from below, and the 9V battery connects to the PCB from below as previously mentioned. The battery for the TeleGPS is placed in a cavity at the bottom of the mount so that when placed inside the CubeSat, it is between the mount and the bottom plate and connects to the TeleGPS from behind it. The TeleGPS is placed as far as possible from the altimeter to prevent interference so that the altimeter can function properly.



**Fig. 30** View of bottom half of payload, with PCB mounted on the second plate from the bottom. Below it is the mount that contains the motor controller at its top, and 9V and 12 V batteries below it. The GPS can be seen with an exaggerated view of its antenna sticking out of the mount.

To retain the payload, the payload is slid into the airframe until it rests on two L-shaped rails with a rounded base, which are epoxied to the inner wall of the rocket's airframe. The top bulkhead of the payload has two square shaped cutouts across from each other for the long part of the rails to fit into, until it slides all the way down. The payload sits on the short part of the rails, preventing it from sliding further down the rocket and holding up the payload. The top of the payload rests on the nosecone, retaining the payload during flight and satisfying requirement 4.19. To mitigate tangling, slits are cut in the PVC bulkheads that allow the shock cord to pass through on the outside of the payload, without interfering with the payload or the guiders, satisfying requirement 4.19.



**Fig. 31 Guider rail used for assisting in installing the payload assembly.**

The structure has been rated using a drogue deployment force of 1114 N as calculated in the “Payload Recovery” section, which is the highest non-impact load could possibly resist in its flight, with all loaded components having a substantial amount of resistance to the deployment. The guiding rails have been rated for the deployment force of the main parachute. In terms of impact, the structure was rated via a drop test as described in appendix B. The table below shows the loads on the bulkhead, threaded rods, eyebolt, and payload rails, as well as the set screw, which was a major point of contention among the team, as the team was uncertain it would remain attached to the reaction wheel. This shows the structure satisfies requirement 4.2.



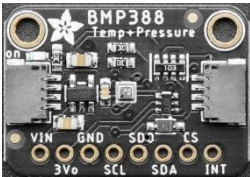


**TABLE XI**  
**COMPONENT STRESS RATINGS**

Component	Strength Rating [7]	Load Experienced	Factor of Safety
Bulkhead	3.45 MPa	0.21 MPa	16.75
Threaded Rod	861.80 MPa	35.37 MPa	24.37
Eyebolt	5783 N	1114 N	5.19
Set Screw	506.80 MPa	164.70 MPa	3.31
Rails	33.78 MPa	16.76 MPa	2.01

The objective for the payload electronics is to drive the RCS by employing a PID control mechanism in the flight software algorithm and collect inertial/environmental data of the payload. The payload is equipped with a camera, BLDC motor, power source, and flight computer. The flight computer is used to interface all the components to allow for fully programmable platform for operation. The flight computer records acceleration, orientation, magnetic field, pressure, and temperature to an external storage unit. Moreover, the flight computer can detect a change in the intensity of light via photoresistor, generate sound from a buzzer and emit light from an LED for debugging, and includes a programmable mechanical switch.

The purpose for payload telemetry is to relay real-time position data for recovery and mid-flight tracking. The module in the payload is equipped with a COTS GPS tracker which transmits RF signals to a three-directional antenna connected to a ground station laptop, a Raven flight computer, and SRAD flight computer. The SRAD flight computer can trigger ejection charges for parachute deployment. The key electrical components that make up the flight computer and telemetry module are listed in Table XII.

TABLE XII  
Payload Electronics Equipment

Device	Specification	Image
Teensy 4.1 Microcontroller	Arm Cortex-M7 at 600 MHz 8 Mb Flash Memory 2.4" × 0.7" × 0.2" 28.3 g / 0.4 oz	
Adafruit LSM9DS1 Inertial Measurement Unit	$\pm 2/\pm 4/\pm 6/\pm 8/\pm 16 g's$ $\pm 2/\pm 4/\pm 8/\pm 16 Gauss$ $\pm 245/\pm 500/\pm 2000 \text{ }^\circ/s$ 1.3" × 0.8" × 0.1" 2.5 g / 0.1 oz	
Adafruit BMP388 Precision Barometric Pressure Altimeter	$\pm 8 Pa$ $\pm 0.5 \text{ }^\circ C$ 1.0" × 0.7" × 0.1" 1.2 g / 0.1 oz	
Altus Metrum TeleGPS	16 mW Transmit Power 2 Mb Flash Memory 1.5" × 1.0" × 0.3" 12.3 g / 0.4 oz	
Altus Metrum TeleDongle	433 MHz Yagi Antenna 70 cm wavelength	

Mobius Mini V2

Max 2688×1212P  
30, 60, 120, 240 FPS  
27 g / 1.0 oz  
2.2" × 1.1" × 0.6"



BLDC Gear Motor

30W  
12V  
3000 RPM  
1.5 kg / 53.0 oz  
2.4" × 2.4" × 3.3"



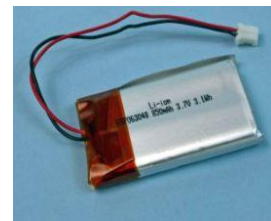
Ovonic 4s Lithium Polymer Battery

14.8V  
1550 mAh  
180 g / 6.7 oz  
2.8" × 1.4" × 1.3"



Lithium Polymer Battery

3.7V  
900 mAh  
24.1 g / 0.9 oz  
2.0" × 1.2" × 0.3"



Lithium Polymer Battery

3.7V  
2000 mAh  
40 g / 1.4 oz  
2.2" × 1.4" × 0.5"







---

Minor electrical equipment is not included in the table.

The Teensy 4.1 microcontroller acts as the central processing unit for the RCS. The justification for choosing this microcontroller was for its fast computing and relatively small size. A trade study of available microcontrollers was used to select the Teensy 4.1 and the decision matrix is depicted in Table XIII.



TABLE XIII  
Microcontroller Decision Matrix

Microcontroller			Teensy 4.1			Arduino Uno			Arduino Mega			Arduino Nano		
														
Objective	Weighting Factor	Parameter	Mag.	Score	Value	Mag.	Score	Value	Mag.	Score	Value	Mag.	Score	Value
Clock Speed	0.3	MHz	600	10	3.00	16	1	0.30	16	1	0.30	16	1	0.30
Mass	0.15	g	28.3	3.5	0.53	25	4	0.60	37	1	0.15	7	10	1.50
Area	0.3	in <sup>2</sup>	1.7	9	2.70	5.7	4	1.20	8.4	1	0.30	1.2	10	3.00
Cost	0.15	\$	\$26.85	7.5	1.13	\$24.20	8.5	1.28	\$42.40	1	0.15	\$21.80	10	1.50
RAM	0.1	kb	1024	10	1.00	2	1	0.10	8	1.1	0.11	2	1	0.10
<b>Overall Value</b>					<b>8.35</b>			<b>3.48</b>			<b>1.01</b>			<b>6.40</b>

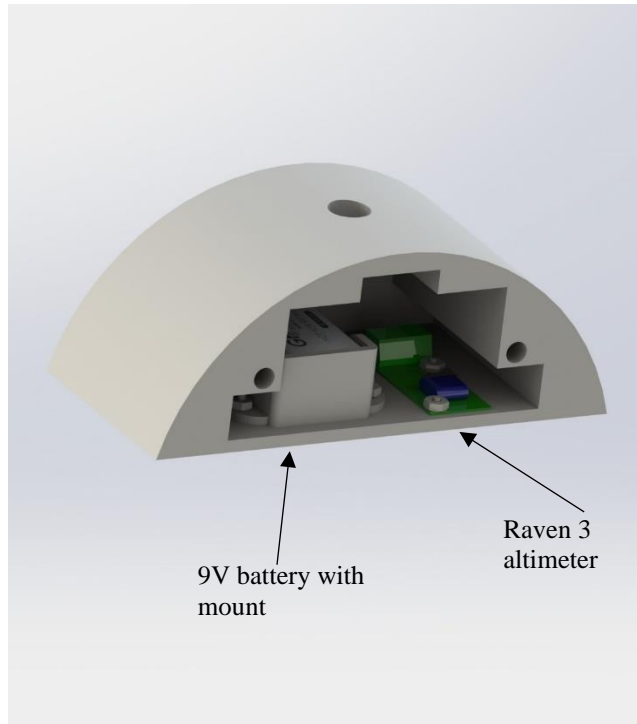
Each Arduino device housed the same CPU, the Atmega328P, which has a clock speed  $37.5\times$  slower than the Arm Cortex-M7 chip. The slim rectangular geometry of the Teensy 4.1 microcontroller was analogous to that of the Arduino Nano. However, the combination of the geometry and processing speed of the Arm Cortex-M7 chip made the Teensy 4.1 microcontroller the obvious choice for the RCS.

The telemetry module is housed in the same bay as the flight computer. The module consists of a COTS GPS tracker, the TeleGPS, which is the same one used for the launch vehicle. The TeleGPS transmits on a 70 cm band and requires a Ham Radio Technician License for operation which has been acquired by payload electronics lead. This transmission allows the operator to join an APRS network highly recommended by the IREC DTEG.

For operation of the telemetry module which includes the TeleGPS and TeleDongle, a ground station laptop is used. The laptop is loaded with AltusOS which is the proprietary software that comes with the COTS devices. The software allows for real-time tracking of the rocket via pre-loaded satellite maps and records the flight data to a spreadsheet for post-flight analysis.

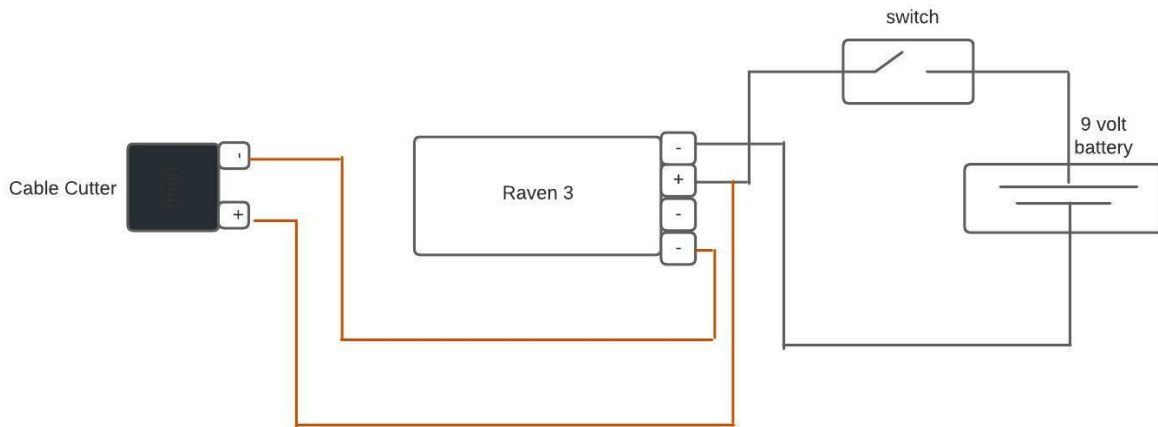
At apogee, the payload is ejected simultaneously with the nose cone. The parachute is packed with shock cord inside, with a Prairie Twister cable cutter zip attached to it by a zip tie that wraps around the parachute, retaining it during flight. The cable cutter is wired to the payload altimeter and flight computer to set off a contained black powder charge that will set break the zip tie, deploying the parachute to slow the payload's descent. Activating the e-charge soon after apogee was chosen because it prevents the reaction wheel from the sudden change of acceleration it would experience if the payload were to experience free fall and then deploy the parachute at a much lower elevation. This saves the reaction wheel from damage and ensures the roll control experiment runs smoothly. For redundancy purposes, a second ejection charge is located with the IMU in cases where the first one does not deploy the parachute.

The payload avionics bay consists of a 3D printed shell. It houses a 9V battery, which is placed into a mount that is bolted on the inside of the bay, and a Raven 3 altimeter, also bolted from the inside. To turn on the altimeter while it is inside the rocket's airframe, a switch is placed on the outside of the bay, which is connected to the altimeter and battery wires and can be pressed to turn on the altimeter, which satisfies requirement 3.20.



**Fig. 32 View of internal components in the avionics bay.**

The recovery events of the payload are controlled by a Raven 3 altimeter, which is connected to a 9V battery and is armed through a switch. The wiring configuration of the Raven 3 altimeter is shown in Fig. 33.



**Fig. 33 Wiring Diagram for the payload altimeter system using the Raven 3.**

The deployment force on the payload from its parachute is calculated using equations 3 and 4, applying the mass of the payload and its terminal velocity, which is the fastest velocity the payload would experience before the parachute deploys, in the event of a malfunction. The total deployment force from the payload parachute, which is the same as

the drogue parachute, is 1114 N. The maximum kinetic energy at landing, assuming the parachute never deploys, is calculated as follows:

$$KE = \frac{1}{2}mv^2 \quad (7)$$

Where v is the terminal velocity of the payload. The maximum kinetic energy that the payload could experience at impact is 1.516 kJ. The recovery components not directly related to the payload structure itself are rated below based on the forces previously calculated:

TABLE XIV  
PARACHUTE SYSTEM COMPONENT STRESS RATINGS

Component	Strength Rating	Load Experienced	Factor of Safety
Parachute	8896 N	1114 N	7.98
D-Link	4448 N	1114 N	3.5
Swivel	4448 N	1114 N	3.5

#### IV. Mission Concept of Operations Review

The complete operation of the launch vehicle is presented Fig. 34 and described by the phases below. Prior to loading the launch vehicle to the launch pad, the Payload and Flight Computer are powered on and left in a dormant state to reduce power draw and detect launch via a large impulse in acceleration. The mission concept of operations begins once the launch vehicle has been prepared by the RSO and brought to the launch rail to be prepared for launch. A complete table of nominal operations of each subsystem is presented in Table XV.

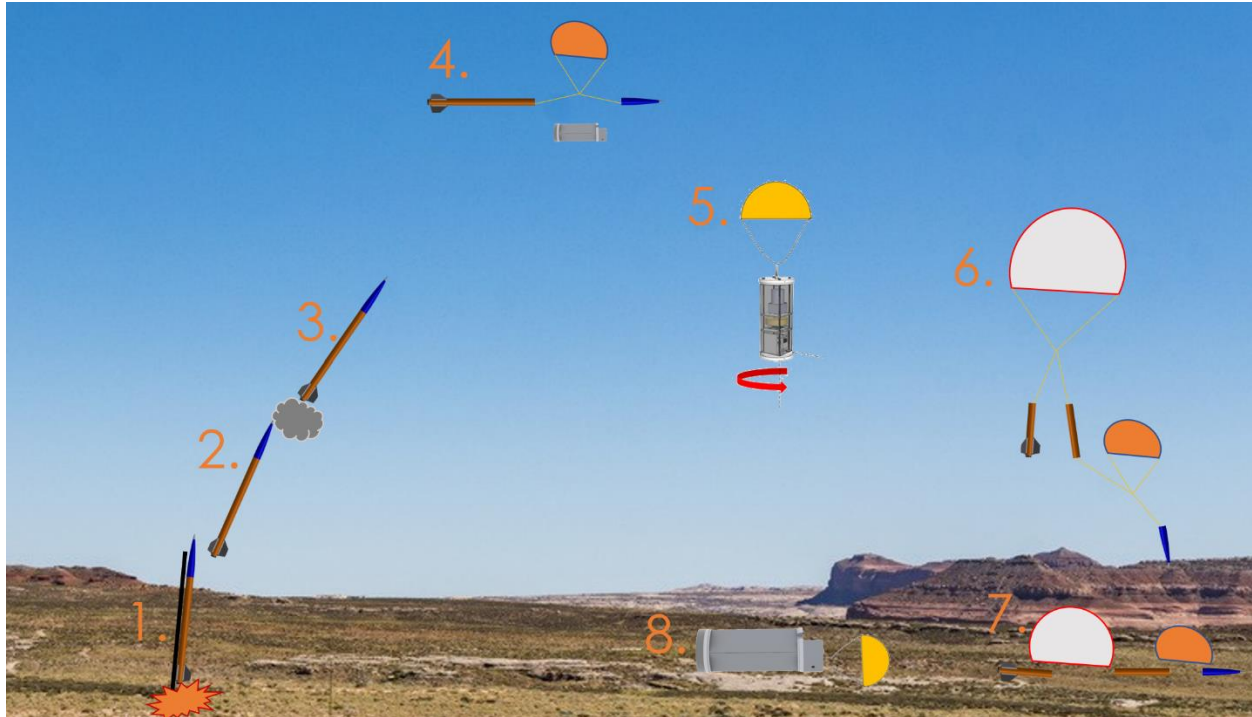


Fig. 34 Mission Concept of Operations diagram. Note, Phase 5 & 6 occur simultaneously.

**0. Preparation** – The phase is triggered by the approval for the team to prepare the launch vehicle by the RSO, and the team travels to the pad to prepare the launch vehicle for launch. The launch vehicle is loaded on the 1515 launch rail provided by ESRA by sliding its rail buttons into the launch rail. The altimeters for the launch vehicle and payload are then armed via the externally accessible switch for each altimeter and verified for flight readiness by the audible beeps prior to flight. The motor is prepared by inserting the igniter for the motor through the nozzle to the top of the motor and wiring the igniter to the ESRA provided ignition system. The payload remains in a deactivated state until ignition is detected by its accelerometer. Once continuity is met with the igniter system, the rocket is considered armed for launch, and the phase concludes with the team’s launch preparation team having left the launch pad to wait for launch.

**1. Ignition** – The phase is triggered by the ignition of the launch vehicle motor by the RSO using the ESRA provided ignition system. At the phase trigger, the motor is ignited by the high amp current passed through the igniter, igniting the propellant with a complete burn. The motor rapidly accelerates the launch vehicle and is restricted to propelling the launch vehicle vertically via the launch rail limiting the risk of an unstable flight path. The thrust ring will withstand the load of the motor ignition and transfer the thrust through the modular aft system into the airframe propelling the launch vehicle. The altimeters detect launch via a sudden increase in acceleration and air pressure, and use a Mach Inhibit mode set to the duration of the motors burn to prevent the premature deployment of the parachutes due to pressure variations caused by compressible effects near Mach 1. The payload remains in its deactivated state, with the payload adapter rails holding the payload subsystem in the up-right position against the loads of launch. This phase concludes once the launch vehicle’s bottom rail button has cleared the launch rail.

**2. Launch Rail Clearance** – This phase is triggered by the launch vehicle’s bottom rail button clearing the launch rail, allowing the launch vehicle to be free to translate in all axes. The fins will withstand the aerodynamic loads and redirect the launch vehicle along a stable flight path. The motor continues to accelerate the launch vehicle to the maximum flight velocity. The altimeters continue to monitor data in the Mach Inhibit mode, preventing the premature deployment of the parachutes. The Payload remains in its deactivated state with the rail system holding the payload against the loads of launch. The phase concludes once the motor has run out of propellant and no longer propels the launch vehicle.

**3. Motor Burnout** – This phase is triggered by the motor exhausting all its propellant and the launch vehicle continues to coast to apogee. The phase trigger marks the point of maximum velocity and aerodynamic loading of the launch vehicle. The airframe will withstand the loads of maximum dynamic pressure, and the fins will withstand the oscillatory modes of fin flutter. The altimeters are expected to deactivate the Mach Inhibit mode after the launch vehicle passes the point of maximum velocity and will remain activated for the duration of the coasting segment of flight to detect apogee and fire the ejection charge. The motor no longer powers the flight of the launch vehicle, and the launch vehicle continues to fly unpowered to apogee. The Payload remains in its deactivated state with the rail system holding the payload against the loads of coasting. The phase concludes once the launch vehicle has coasted to apogee.

**4. Apogee** – This phase is triggered by the launch vehicle reaching the apogee of its flight. The altimeters detect apogee via an increase in air pressure and fire the forward ejection charge. The sudden increase in pressure due to the ejection charge separates the forward airframe and nose cone by severing the shear pins which fasten them. The drogue parachute and payload are then ejected from the launch vehicle. Exposed to the air, the drogue parachute deploys steadying the descent of the launch vehicle. After a five second delay, the payload fires its cable cutter system, opening the payload parachute to slow its descent. The use of a delay for the deployment of the payload parachute limits the risk of the parachute tangling with the drogue parachute or deploying prematurely. At this point, both the payload and launch vehicle descend separately with their own parachutes. The photoresistor attached to the flight computer then detects a drop in resistance when exposed to sunlight, indicating the payload is outside of the launch vehicle. The phase is concluded when the payload’s flight computer initiates the experiment after a 15 second delay.

**5. Payload Experiment** – This phase begins when the payload’s flight computer initiates the roll control experiment, 15 seconds after payload deployment detection. At this phase trigger, both the launch vehicle and payload are descending on their own parachutes. The payload activates its experiment, allowing for the controller to begin the roll control experiment. The reaction wheel housed in the payload begins to reorient the CubeSat rotating it to the desired direction. The camera housed inside the payload records the descent to verify the successful operation of the payload. The payload continues the experiment throughout its descent until landing. The next phase begins once the launch vehicle reaches its main parachute deployment altitude of 1000 feet, however this phase continues simultaneously with the launch vehicle phases and concludes with phase 8.

**6. Main Parachute Deployment** – The phase is triggered once the launch vehicle reaches its main parachute deployment altitude of 1000 feet. The altimeters detect the altitude and fire the aft ejection charges. The aft section of the launch vehicle separates from the Avionics Bay and Forward airframe. The main parachute is then ejected from the aft section and the main parachute is exposed to the air and deploys. The avionics bay and the modular aft structures are expected to withstand the force of deployment transferred through the shock cord and recovery hardware. Once the main parachute is fully deployed, it slows the launch vehicle to a descent velocity less than 30 feet per second for landing. This phase is concluded once the launch vehicle has landed.

**7. Launch Vehicle Landing** – This phase is triggered once the launch vehicle has landed. All components of the aero-structure will withstand the force of landing without damage. In the case of damage to the fins, the modular aft system allows for the rapid replacement of the fins. The motor will remain in the aft of the launch vehicle, retained by the motor retainer. The recovery hardware and parachutes remain attached to the launch vehicle. The phase is concluded once the payload has landed.

**8. Payload Landing** – This phase is triggered once the payload lands. The payload structure and electronics will withstand the force of landing. The polyurethane foam on the bottom of the payload structure reduces the load on the structure reducing the risk of components inside being destroyed due to landing. To further minimize the damage to the electrical components from the impact of the landing, all powered electronics are deactivated five minutes after the payload experiment has been activated. All flight data is recorded continuously to an external SD card, reducing the risk of data loss due to damage from the impact of the payload landing. The mission is concluded after the payload has landed.

TABLE XV  
Mission Concept of Operations Summary

Device	Specification	Image	Device	Specification	Image	Device
0. Preparation	RSO approval for launch	Armed	Armed, Monitoring for launch	Armed	Armed, Monitoring for launch, Experiment Deactivated	Motor Ignition signal is fired
1. Lift off	RSO fires motor ignition signal	Burning	Altimeters collecting data, Mach Inhibit mode on	Armed	Altimeters collecting data, Mach Inhibit mode on, Experiment Deactivated	Bottom Rail button clears the launch rail
2. Launch Rail Clearance	Bottom Rail button clears the launch rail	Burning	Altimeters collecting data, Mach Inhibit mode on	Armed	Altimeters collecting data, Mach Inhibit mode on, Experiment Deactivated	Motor runs out of propellant to burn
3. Motor Burnout	Motor runs out of propellant to burn	Inactive	Altimeters collecting data, Mach Inhibit mode off	Armed	Altimeters collecting data, Mach Inhibit mode off, Experiment Deactivated	Launch Vehicle reaches apogee of the flight
4. Apogee	Launch vehicle reaches apogee of its flight	Inactive	Altimeter detects apogee, fires forward e-charge	Forward e-charge fired, Drogue parachute deployment	Payload ejected, Payload Parachute deploy after a 5 sec delay, Experiment Deactivated	Payload descends to altitude/delay of XXXX
5. Payload Experiment	A delay of 1-minute elapses	Inactive	Altimeters collecting data, monitoring for main deploy	Descent under Drogue Parachute	Payload experiment active, Descent under payload parachute	Launch vehicle descends to an altitude of 1000 feet
6. Main Parachute Deployment	Launch vehicle descends to an altitude of 1000 feet	Inactive	Altimeter detects 1000 feet, fires main e-charge	Aft e-charge is fired, Main Parachute is deployed	Payload experiment active, Descent under payload parachute	Launch vehicle reaches the ground

7. Launch Vehicle Landing	Launch vehicle reaches the ground	Inactive, Motor is retained in the aft section	Altimeters in post-flight mode	Drogue and Main Parachutes remain attached to the launch vehicle	Payload experiment active, Descent under payload parachute	Payload reaches the ground
8. Payload Landing	Payload lands on the ground	Inactive, Motor is retained in the aft section	Altimeters in post-flight mode	Parachutes remain attached to the launch vehicle	Payload is undamaged from landing, parachute is attached	Concludes Mission
10. Launch Rail Clearance	Bottom Rail button clears the launch rail	Burning	Altimeters collecting data, Mach Inhibit mode on	Armed	Altimeters collecting data, Mach Inhibit mode on, Experiment Deactivated	Motor runs out of propellant to burn
11. Motor Burnout	Motor runs out of propellant to burn	Inactive	Altimeters collecting data, Mach Inhibit mode off	Armed	Altimeters collecting data, Mach Inhibit mode off, Experiment Deactivated	Launch Vehicle reaches apogee of the flight

## V. Conclusion and Lessons Learned

The TropoGator launch vehicle and payload represents the culmination of team's prior knowledge of HPR developed through participation the NASA SLI with the research conducted by each of the subteams lead's experimental designs. Developing an SRAD flight simulator enabled the flight dynamics team to explore more complex designs with greater robustness in designing the launch vehicle to reach the target altitude. The carbon fiber airframe and fins and modular aft subsystem were a major leap in our design utilizing advanced engineering techniques. Keeping the avionics & recovery to a standard design allowed the team to reduce complexity in a discipline the team has had trouble with in the past. The payload design has been the first successful deployed payload in the teams history, and utilizes an experiment that combines each of the subteam leads education within mechanical and aerospace engineering. In these ways, the 2022 Spaceport America Cup has allowed each of the leads to engage with experimental design, leadership, and manufacturing by developing their own project, while pushing forward the capabilities of the team to develop more advanced subsystems.

Design-wise the biggest obstacle towards the completion of the launch vehicle and payload was the choice of an experiment that would require a deployed payload. Such a design increases the complexity of the recovery system significantly, and proved to be a roadblock in the design throughout the year. The advantages of a deployed payload include greater variety of experimentation, and a more stable descent for the launch vehicle due to the payload being removed. The cons include a lower stability than if the payload were stored in the nose cone, greater complexity of the recovery system, and a more involved design process to integrate the payload with the launch vehicle. The payload design developed this year has provided the team an example of a deployed payload configuration to expedite this process in future years. It is highly recommended to next year's team to define the payload design and mission concept of operations for it, in text, as early as possible in the year, so that the launch vehicle can be designed for it. In addition, the design can be adapted to develop a roll control experiment for the launch vehicle for roll stability. The carbon fiber airframe a modular aft has pointed the team in the right direction in terms of *level* of research and experimental design. The next steps are to utilize the same motivation in terms of developing a more reliable recovery configuration and extensive avionics bay design that maximizes accessibility.

In terms of operations, the team's major goal was to emphasize in-person meetings and utilize workshops in the mechanical design laboratory. The purpose of this goal was to increase the synergy and productivity of subteams after

working remotely due to the pandemic. For future iterations of the team, a standard for running subteam meetings across all subteams would help direct focus towards completing the project as fast as possible. An alternative to this format would be to operate exclusively in a workshop format, removing subteam meetings entirely. The subscale test flight proved to be a major success, both in terms of validating the payload deployment design, and engaging team members with the project by providing a hands-on project. Finally, budget cuts from the university's student government crippled the project's ability to continue. It is highly recommended to the next team to seek out external funding through sponsors or grants to secure the project and travel funding.



APPENDIX A: SYSTEM WEIGHTS, MEASURES AND PERFORMANCE DATA

## Appendix A: System Weights, Measures and Performance Data

Table XVI lists relevant launch vehicle and payload parameters. Table XVII lists relevant motor parameters. Table XVIII lists predicted mission performance parameters. Predicted flight data over time is displayed in Fig. 35. Tables XIX-XXI list important recovery parameters. An illustration of the flight profile is displayed in Fig. 36 and described in Table XXII.

TABLE XVI  
Launch Vehicle Information

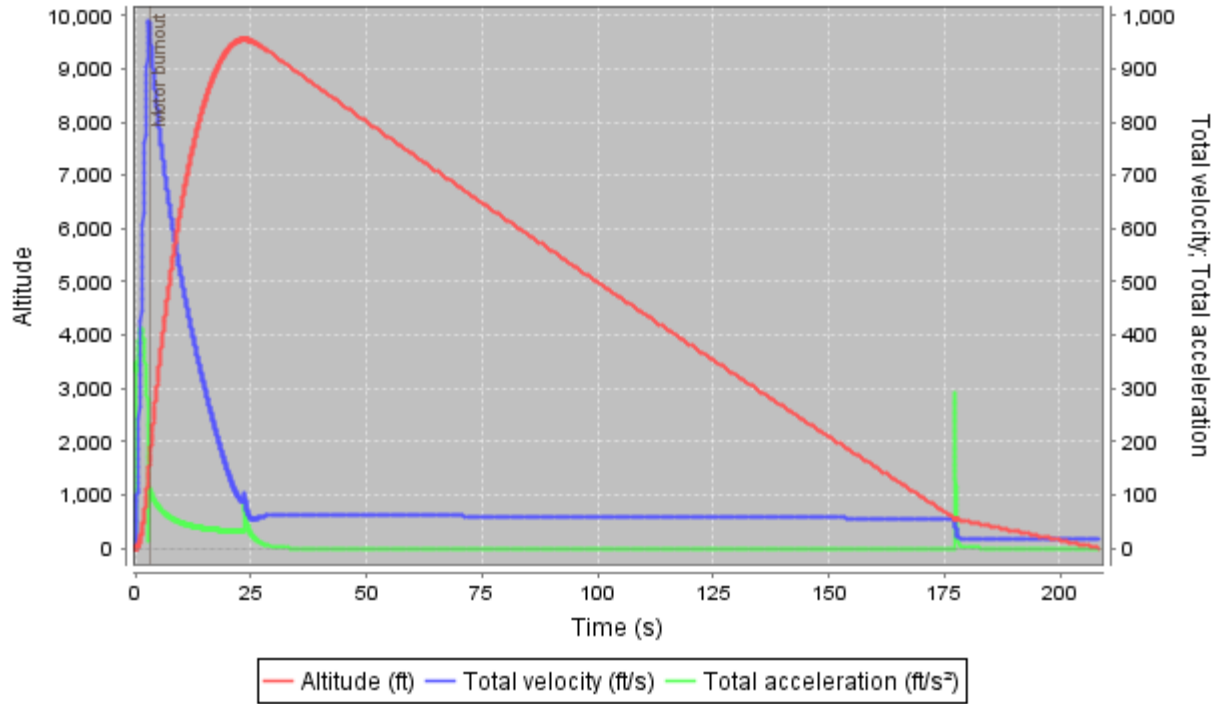
PARAMETER	VALUE
Number of Stages	1
Vehicle Length	128 in
Airframe Diameter	6.17 in
Number of Fins	3
Fin Semi-span	6.5 in
Vehicle Weight	24.4 lbf
Empty Motor Case Weight	6.25 lbf
Propellant Weight	7.56 lbf
Payload Weight	11.6 lbf
Liftoff Weight	49.7 lbf
Center of Pressure from Nose	94.0 in
Center of Gravity from Nose	82.5 in

TABLE XVII  
Propulsion Information

PARAMETER	VALUE
Motor Manufacturer Designation	Cesaroni M2505
Average Thrust	2,478 N
Total Impulse	7,396 N·s
Burn Time	2.98 s

TABLE XVIII  
Predicted Flight Data

PARAMETER	VALUE
Launch Rail	ESRA Provided
Rail Length	17 ft
Liftoff Thrust-Weight Ratio	11.2:1
Launch Rail Departure Velocity	108 ft/s
Minimum Static Stability Margin During Boost	1.93 cal
Maximum Acceleration	12.8 G
Maximum Velocity	988 ft/s
Target Apogee	10,000 ft
Predicted Apogee	9,553 ft



**Fig. 35 Mission performance prediction.**

**TABLE XIX**  
Recovery Information

PARAMETER	VALUE
COTS Altimeter	Raven 3
Redundant Altimeter	Stratologger SL100
Drogue Primary Deployment Charge	2.48 g
Drogue Backup Deployment Charge	3.0 g
Drogue Deployment Altitude	Apogee
Drogue Descent Rate	47.7 ft/s
Main Primary Deployment Charge	2.79 g
Main Backup Deployment Charge	3.25 g
Main Deployment Altitude	1000 ft
Main Descent Rate	15.8 ft/s

TABLE XX  
Shock Chords and Mechanical Links Strength and Dimensions

COMPONENT	DESCRIPTION	RATED STRENGTH*	FACTOR OF SAFETY
Eyebolt	3/8" Steel Eyebolt	5780 N	4.0
U-bolt	1/4" x 2-1/4" National Hardware U-bolt	1890 N	1.3
Threaded Rod	1/4" High-Strength Steel Threaded Rod	32800 N	22.8
Quick-Links	9/32" Thickness Steel Quick Link	4450 N	3.1
Swivel	RocketMan 3,000 lbf Stainless Steel Swivel	13400 N	9.3
Forward Shock Cord	RocketMan 1" Kevlar Shock Cord – 32 ft	24500 N	17.0
Aft Shock Cord	RocketMan 1" Kevlar Shock Cord – 32 ft	24500 N	17.0

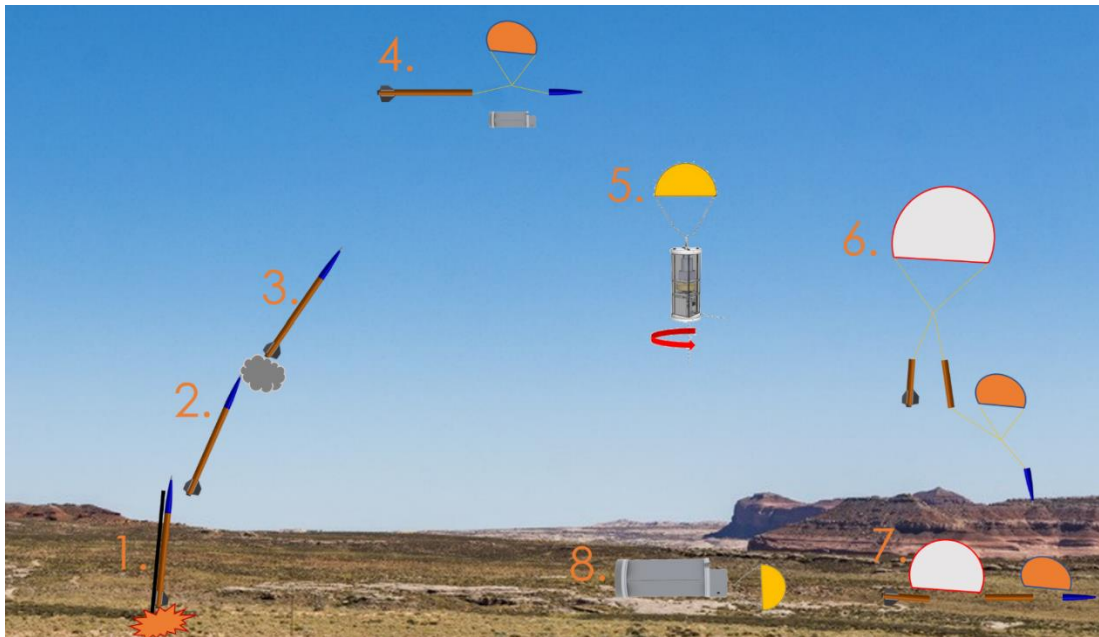
\* Values are converted from the manufactured provided units in lbf. to N.

TABLE XXI  
Shock Chords and Mechanical Link Connections

COMPONENT	DESCRIPTION	LOCATION	CONNECTS TO
Eyebolt	3/8" Steel Eyebolt	Nose Cone Bulkhead	Quick Link
Quick-Link	9/32" Thickness Steel Quick Link	Nose Cone Bulkhead	Eyebolt Swivel
Eyebolt Swivel	RocketMan 3,000 lbf Stainless Steel Swivel	Nose Cone Bulkhead	Shock Cord
Forward Shock Cord	RocketMan 1" Kevlar Shock Cord	Forward Airframe	Parachute Swivel
Parachute Swivel	RocketMan 3,000 lbf Stainless Steel Swivel	Forward Airframe	Shock Cord
Drogue Parachute	RocketMan 48" Standard Parachute	Forward Airframe	Parachute Swivel
Forward Shock Cord	RocketMan 1" Kevlar Shock Cord	Forward Airframe	Quick Link
Quick-Link	9/32" Thickness Steel Quick Link	Forward Avionics Bay Bulkhead	U-bolt
U-bolt	1/4" x 2-1/4" National Hardware U-bolt	Forward Avionics Bay Bulkhead	Threaded Rod*
Threaded Rod	1/4" High-Strength Steel Threaded Rod	Avionics Bay	U-bolt
U-bolt	1/4" x 2-1/4" National Hardware U-bolt	Aft Avionics Bay Bulkhead	Quick Link
Quick-Links	9/32" Thickness Steel Quick Link	Aft Avionics Bay Bulkhead	Shock Cord
Aft Shock Cord	RocketMan 1" Kevlar Shock Cord	Aft Airframe	Main Parachute
Main Parachute	Fruity Chutes IRIS Ultra 96" Parachute**	Aft Airframe	Aft Shock Cord
Aft Shock Cord	RocketMan 1" Kevlar Shock Cord	Aft Airframe	Eyebolt Swivel
Eyebolt Swivel	RocketMan 3,000 lbf Stainless Steel Swivel	Motor	Eyebolt
Eyebolt	3/8" Steel Eyebolt	Motor	Motor Casing

\* Threaded rod passes load through the avionics bay, connecting forward and aft section.

\*\* IRIS Ultra contains its own Parachute Swivel.



**Fig. 36 Flight profile graphic. Table XXII states events.**

**TABLE XXII**  
**Mission Events**

NUMBER	EVENT	DESCRIPTION
1	Ignition	Motor is ignited by RSO
2	Launch Rail Clearance	Launch Vehicle rail button clears Launch Rail
3	Motor Burn Out	Launch Vehicle is coasting
4	Apogee	Payload Ejection and Drogue Deployment
5	Payload Experiment	Payload activates its experiment after detecting its outside the airframe
6	Main Deploy	Main Deployment at 1000 feet
7	Launch Vehicle Landing	Motor Retained, Parachutes are attached
8	Payload Landing	Parachutes are attached, Experiment deactivates 5 minutes after phase 5

## APPENDIX B: PROJECT TEST REPORTS

## Appendix B: Project Test Reports

All tests conducted throughout the year for TropoGator have been consolidated in Table XXIII. The following pages describe successful tests in detail.

TABLE XXIII  
Load Testing of Airframes

SUBSYSTEM	DATE	TEST	OUTCOME
Payload	11/1/2021	Roll Rate Test	<b>Success</b>
Avionics & Recovery	3/19/2022	TeleGPS Flight Test	<b>Success</b>
Payload	3/19/2022	Subscale Test Flight	<b>Failure</b>
Structures	3/24/2022	Carbon Fiber Airframe Compression Testing	<b>Success</b>
Payload	3/31/2022	Payload Impact Test	<b>Success</b>
Payload	4/8/2020	Subscale Payload Cable Cutter Test	<b>Success</b>
Payload	4/16/2022	Subscale Test Flight	<b>Success</b>
Avionics & Recovery	4/28/2022	Altimeter Pressure Testing	<b>Success</b>
Avionics & Recovery	5/6/2022	Recovery System Testing	<b>Success</b>
Payload	5/12/2022	Flight Computer Ejection Charge Test	<b>Success</b>
Avionics & Recovery	5/12/2022	Flight Computer Inertial Measurement Unit Test	<b>Success</b>
Propulsion	-	SRAD Propulsion System Testing	<b>N/A</b>
Propulsion	-	SRAD Pressure Vessel Testing	<b>N/A</b>

\*Only successful tests are included in the report appendix.



## Roll Rate Test

**Date:** 11/19/2021, **Lead:** Tsz Pan Chu

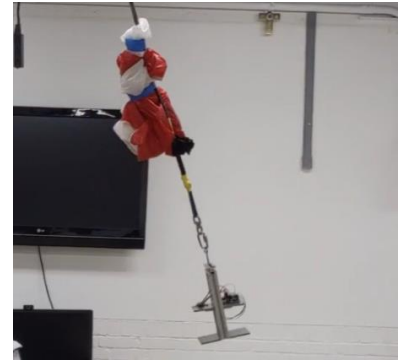
**Description:** A payload-mockup was built to determine its response to disturbances. The payload-mockup had a similar moment of inertia to the actual payload and attached to the recovery harness intended for the actual payload to replicate performance. The payload-mockup was subjected to different disturbances, and the angular velocity was recorded with a BNO055.

**Expected Outcomes:** Payload angular velocity is recorded.

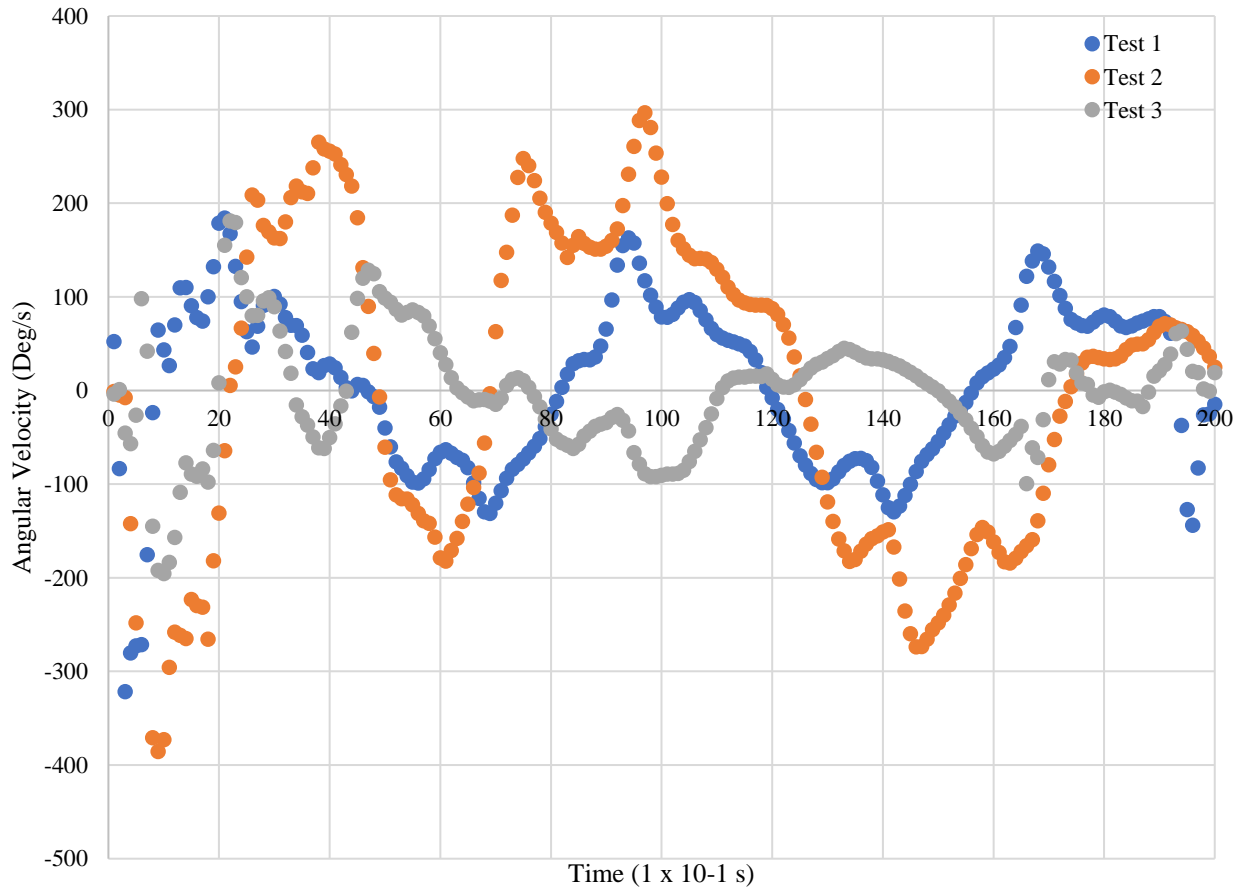
**Measured Variables:** Angular position, angular velocity, time.

### Results:

**Quantifiable** – Angular velocity of payload plotted against time.



**Fig. 37 Experiment Set up: Mock Payload is assembled with prototype IMU system recording angular rates and orientation.**



**Fig. 38 Test data from roll test. From the data, the design angular velocity was set at 200 deg /s.**

### Qualitative

- Payload angular velocity is dampened by friction on swivel.
- The system is linear. A larger input results in a larger peak, though dampening of swivel results in a similar second peak.

## TeleGPS Flight Test – Griffin Martin

**Date:** 3/19/21, **Lead:** Griffin Martin

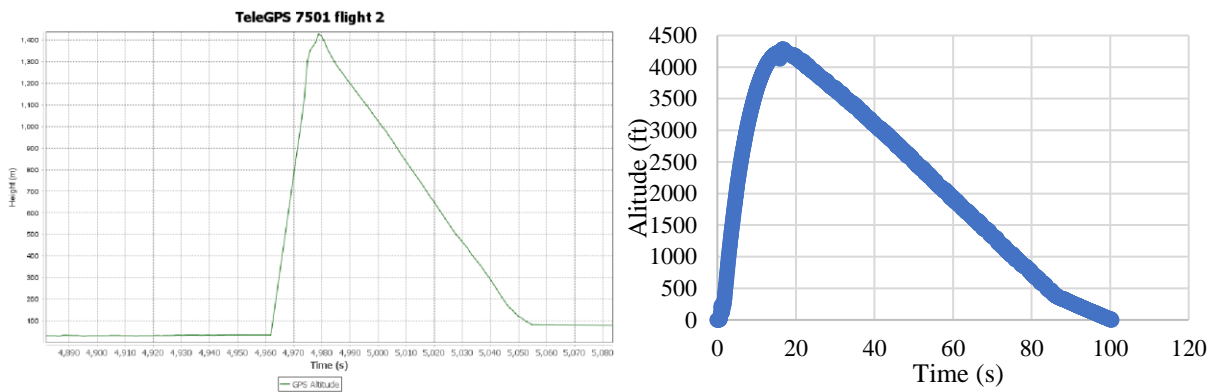
**Description:** Gavin Gamble’s L2 certification launch vehicle utilized the same telemetry module design that the TropoGator used, allowing for the functionality of both the TeleGPS and the mounting design to be tested when he performed his launch. While the fiberglass mounting ring was not included in his design and the inner ring was slightly different, this still allowed the integrity of the ring, epoxy, threaded inserts, screws, PETG components, and Velcro attachment to be tested. Additionally, the accuracy of the TeleGPS data vs the altimeter data, the connection strength between TeleGPS and TeleDongle at high altitudes, and the general efficacy of the TeleGPS system were tested.

**Expected Outcomes:** The TeleGPS would track the location of the launch vehicle and improve the team’s ability to recover it.

**Measured Variables:** TeleGPS altitude, altimeter altitude, TeleGPS coordinates

### Results:

**Quantifiable** - Altitude data from the TeleGPS, Altitude data from the altimeter



**Fig. 39** Altitude versus time of the flight from TeleGPS (left) and Stratologger SL100 (right)

### Qualitative

- The two graphs have similar shapes, and both register a change in altitude of ~4500 ft (1371m), confirming that the TeleGPS’s altitude functionality is reasonably accurate
- All visual contact by any observer was lost when the launch vehicle passed into a cloud, and visual contact was never reestablished as the vehicle and payload descended. Without the GPS data received, it is likely the vehicle and payload would not have been recovered, given the half-mile distance between the ground station and the final position of the vehicle. This made the test a success.

## Carbon Fiber Airframe Compression Testing

**Date:** 3/24/2022, **Lead:** Gavin Gamble

### Description:

The compressive strength of different airframe materials was tested using a 100 kN testing machine. The three materials tested were a SRAD 3-ply CFRP airframe, a SRAD 4-ply CFRP airframe, and COTS G12 airframe. All the airframes had an internal diameter of 6 inches. Each airframe type was tested in pure compression as well as being compressed through the thrust ring, which is the component that transfers the load from the motor to the airframe during flight. The purpose of including the thrust ring in the compression testing is to compare the failure mode of the airframes with and without the thrust ring and compare how the maximum loads were affected.

Pieces of airframe 6 inches in length were used for testing, to match the length to the diameter which prevents premature buckling and enforces a uniform stress distribution in the tube [XX]. The edges of each piece of airframe were cut with a rotary tool and grinding wheel to make the surface as flush as possible using the same manufacturing methods that will be used on the actual flight vehicle. The loads were applied to the body tubes using a flat plate on each end and the thrust ring cases were loaded with a disc the same diameter as the motor retainer that pushes on the thrust ring. All tests runs were displacement controlled at a rate of 0.05 inches per minute until the load on the airframe sample reached a peak.

### Expected Outcomes:

It was expected that the thrust ring would cause the samples to fail on a free surface and have a lower maximum load than the samples in pure compression.

### Measured Variables:

The force exerted on each airframe section was recorded during testing, as well as the dimensions of the tube so that the engineering stress could be calculated.



**Fig. 40** Left: 3-ply CFRP airframe being tested with the thrust ring. Right: COTS G12 airframe being tested in pure compression

### Results:

**Quantifiable** – Table IV

#### Qualitative

- All four CFRP samples did not fail catastrophically and stayed together during failure
- The COTS G12 sample loaded with the thrust ring fail catastrophically by splintering apart circumferentially.
- The COTS G12 sample loaded in pure compression was not able to be tested to failure because it reached the limits of the machine at 25,000 lbf.

## Payload Impact Test

**Date:** 03/31/2022, **Leads:** Cristian Edgar & Asher Siddiqui

**Description:** A drop test was conducted to see if the payload's structure could withstand the forces that would be faced due to landing without a parachute at terminal velocity. The payload structure was assembled, and to more accurately reflect the weight of the fully loaded payload that would be launched, "dummy" weights consisting of sandbags were fixed to the payload. Once the payload has a total of 11 pounds of sandbag weight added to the payload, the drop test could be conducted. The payload was taken to a parking garage where the top floor was around 80 feet above the ground. Once the payload is taken to the top floor, it was not to be thrown until the other person that is on the ground floor gave the "all clear" and immediately after that, the person on the ground floor was to clear the area. Once given the "all clear" and once the ground floor crew cleared the area, the person on the top story of the parking garage was to wait 10 seconds, check the drop zone, and then drop the payload. This procedure was to make sure that no one is injured while conducting the payload drop test. The payload was expected to strike the ground at terminal velocity. Once the payload was dropped and impacted the ground, it was inspected for any structural damage. To verify that the payload reached terminal velocity, a meter stick was set up next to where the payload would land. The footage was reviewed to see how many frames it took for the payload to descend the distance given by the meter stick, and the frames were converted to a time value. With this time value, the speed of the payload could be estimated.

**Expected Outcomes:** Payload structure survives crash with no damage

**Measured Variables:** Payload weight, terminal velocity

### Results:

#### Quantifiable

The velocity calculation upon reviewing footage showed that the payload reached a speed around that of the estimated terminal velocity of 79.08 ft/s.

#### Qualitative

When payload drop testing was conducted, it resulted in very minimal structural damage. Once dropped from the top of the parking garage the payload impacted the ground within seconds and the payload remained intact. This was repeated twice and neither test affected the payload structure.



**Fig. 41** Left: payload with bottom container filled with sand. The middle section was also filled for the drop test. Middle: ruler set up for speed measurements upon footage review. Right: Payload falling into dirt patch.

## Cable Cutter Test

**Date:** 4/8/2022, **Lead:** Oleksandr Dorotych



**Description:** The payload of the subscale launch vehicle utilized a 12-inch parachute that reduced the descend velocity below 30 ft/s. The parachute throughout the ascend and ejection is held closed by a zip tie. In-flight, this zip tie is broken five seconds after apogee by a black powder cable cutter. It is fired by an e-charge that is triggered using a Raven 3 altimeter. A reliable opening of the parachute is necessary for the safe recovery of the payload. To simulate the deployment of the parachute, the payload was set up in the launch configuration on the ground with separate wires running to the cable cutter. A 9-volt battery was used to trigger the cable cutter.

**Fig. 42 Experiment Set up: Payload is wired with cable cutter wrapped around parachute**

**Expected Outcomes:** The zip tie is broken by a cable cutter, and the parachute is free to deploy.

**Measured Variables:** Breaking of the zip tie, ease of parachute deployment.

### **Results:**

#### **Qualitative**

- The zip tie is broken - Success
- The Payload Parachute is free to deploy – Success

## Subscale Payload Demonstration Launch – Kilwin

**Date:** 4/16/2022, **Lead:** Bilal Hassan

**Description:** A subscale launch vehicle of TropoGator was built to demo the payload deployment scheme and fiberglass fins. The major concern with the payload deployment scheme was the risk of an ejection charge triggering the payload parachute due to the payload’s avionics bay being housed in the same section as the drogue deployment charge. A 3-inch diameter phenolic rocket with a 4 lbf. payload was designed in OpenRocket, modeled in SolidWorks, and built using a five-axis waterjet, and additive manufacturing. The payload uses a Raven 3 altimeter to fire a cable cutter, and deploy its parachute. The rocket was launched on an Aerotech J425 in a dual-deployment recovery configuration.

**Expected Outcome:** Payload is ejected at apogee, and can deploy its payload parachute, without tangling with other recovery.

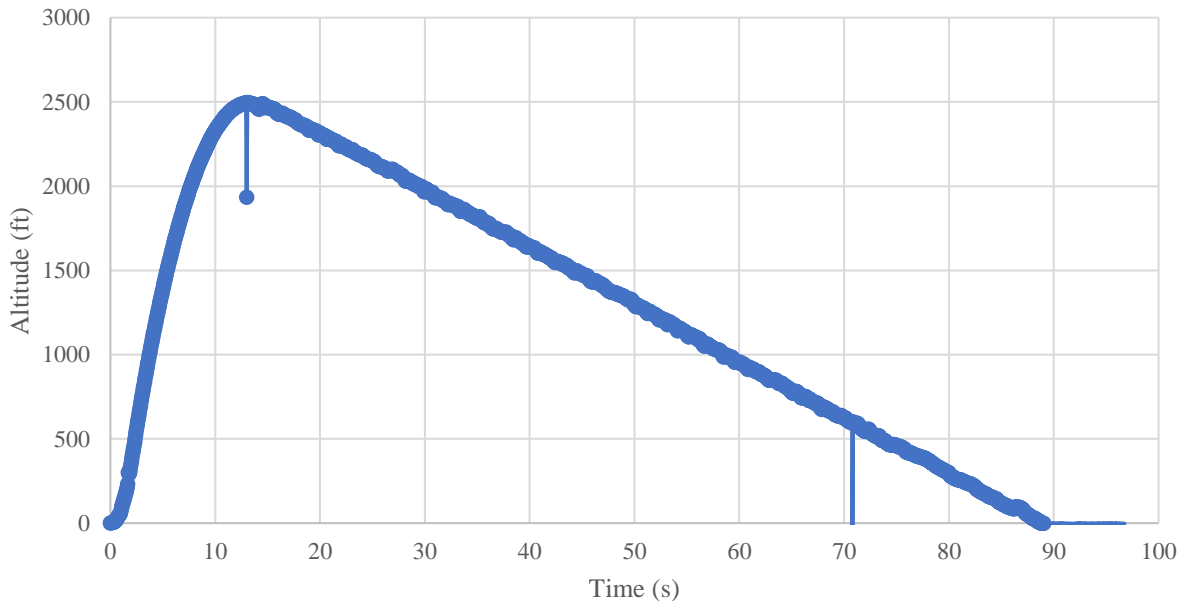
**Measured Variables:** Flight Data, Events of flight recovery.

**Results:**

**Quantifiable** – Test Flight Data from Raven 3 Payload Altimeter



**Fig. 43 Left: Kilwin on launch rail prior to launch, Right: Payload landed intact after flight**



**Fig. 44 Altimeter Data from the Raven 3 housed in Payload. Drops in altitude indicated pressure increase due to ejection gasses.**

**Qualitative**

- Drogue Parachute Deployment – Success
- Payload Ejection – Success
- Payload Parachute Deployment – Success

## Altimeter Pressure Testing

**Date:** 4/28/2022, **Lead:** Elizavetta Stetsenko



**Description:** To determine the reliability of the altimeters of setting off the ejection charges at the preprogrammed altitudes, testing was performed using a sealed jar, pressure pump, 9-volt battery and light bulbs. The two Raven 3 altimeters and the Stratologger SL100 were tested individually. The Raven3 altimeter needed to be shaken vertically to detect liftoff, since the altimeter detects lift-off through axial acceleration readings above 3 G's. In the place of ignitors, lightbulbs were attached to the apogee and main channels. The payload Raven 3 altimeter had the main channel programmed to be set off at 2 seconds after apogee. The Avionics Bay had the Raven 3 altimeter with the main channel set to 1000 feet and apogee set to apogee. The Stratologger SL100 had the main channel set to 1000 feet, and the drogue channel set to apogee. By decreasing pressure in the sealed jar by pumping out air using a vacuum pump, a launch was simulated. The pump was released after a pressure of 10 psi was reached, simulating descent.

**Fig. 45** Equipment laid out on table used in test.

**Expected Outcomes:** Light bulbs flash at expected pressures

**Measured Variables:** Flashing of lightbulbs, pressure change detection in flight data

**Results:**

**Qualitative:**

TABLE XXV  
Altimeter Pressure Testing Results

<b>Altimeter</b>	<b>Outcome</b>	<b>Results</b>
Payload Raven 3	Lightbulb went off at apogee with a two second delay	Success
Avionics Bay Raven 3	First lightbulb flashed at apogee, second lightbulb flashed at 1000 feet.	Success
Avionics Bay Stratologger SL100	First lightbulb flashed at apogee, second lightbulb flashed at 1000 feet.	Success

## Recovery System Testing

**Date:** 5/6/2022, **Lead:** Nurettin Kagan Aslan

**Description:** After being assembled, the avionics bay was tested to verify the function of the dual redundancy of the ejection charge sequence. Each altimeter was powered by an independent 9-volt battery and engaged by an independent key switch. The altimeters were then wired to an ejection charge via the XT60 connector soldered and heat shrunk to an e-match. Each altimeter controls a main and drogue event, with the secondary set to a delay of 2 seconds after the primary altimeter. Both altimeters were then connected to two separate computers for a flight to be simulated. This test ensures that in the case main altimeter fails, there is a secondary altimeter to ensure the ejection charge is still fired. Two different altimeters are used to reduce the chance of a singular failure point causing a failure in both.

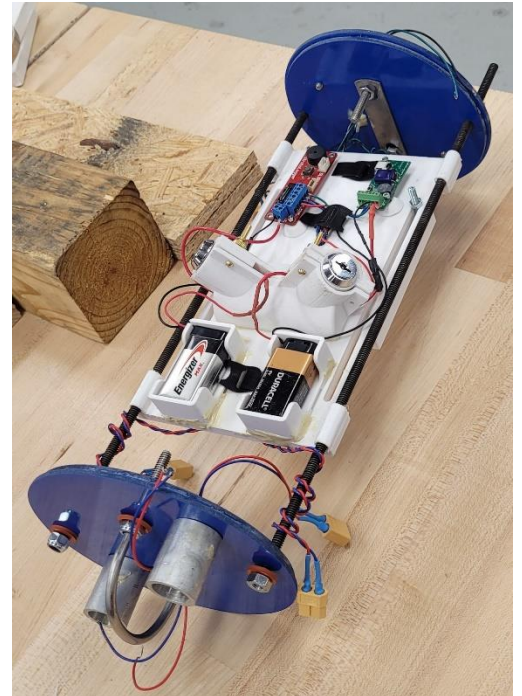
**Expected Outcomes:** E-match is fired at the set times based on flight simulation.

**Measured Variables:** Observation of e-match.

**Results:**

**Quantifiable:**

**Qualitative:** All four e-matches fired at the prescribed times based on the flight simulation. Dual redundancy of the recovery system is verified.



**Fig. 46** Wired Avionics Bay post assembly prepared for testing



## Flight Computer Ejection Charge Test

Date: 5/12/2022, Lead: Wiler Sanchez



Fig. 47 Flight Computer final design with e-match wired to it.

**Description:** After the flight computer was assembled with all the key and minor components on the printed circuit board, the ejection charge setup was tested. For the microcontroller to output a high enough current for the ejection charges to detect, a transistor is utilized. The software was programmed to send the voltage signal. A picture was captured the ejection setting off from the flight computer.

**Expected Outcomes:** The ejection charge is set off.

**Measured Variables:** Current [*Amp*]

**Results:**

**Quantifiable** – ~50 mA triggered the ejection.

**Qualitative** - Ejection charge has been successfully ignited.

## Flight Computer Inertial Measurement Unit Test

**Date:** 5/12/2022, **Lead:** Wiler Sanchez

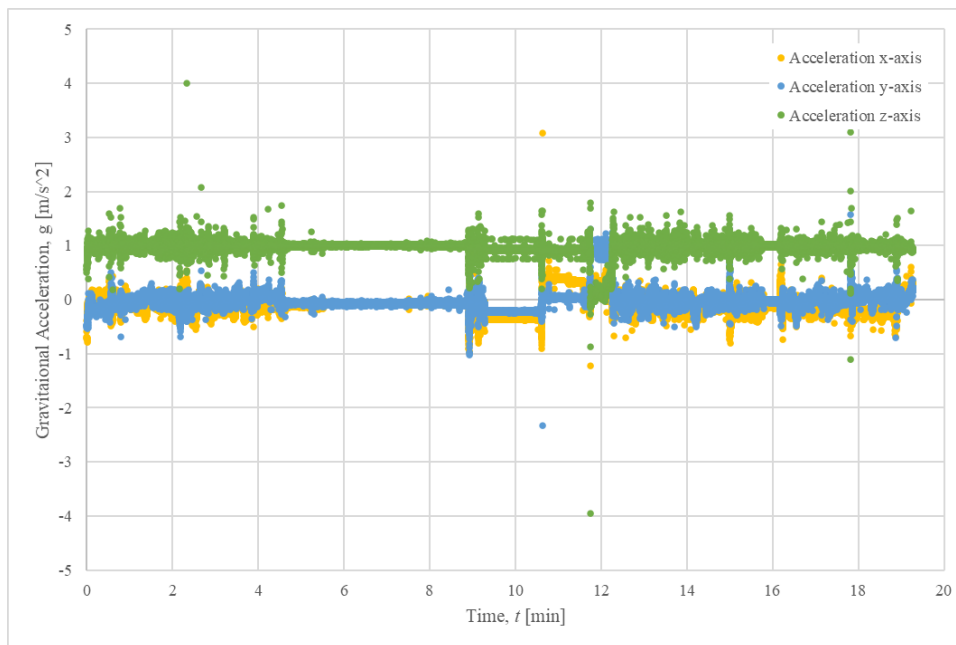
**Description:** After the flight computer was assembled with all the key and minor components on the printed circuit board, testing of the on-board inertial measurement unit was conducted. The flight computer was powered, and the sensor was actively collecting raw data. The computer was then placed in a vehicle and the vehicle was driven to the highway. On the highway, the driver accelerated the vehicle quick enough for the inertial measurement unit to detect large changes in acceleration. After the vehicle reached its destination, all raw data was recorded and loaded into MATLAB for analysis. The trajectory of the vehicle was mapped on a graph and the acceleration data on all three axes was put on a plot. The measurements in acceleration are compared to the changes in velocity the vehicle's speedometer read during the period where the vehicle was on the highway. This confirms the functionality of the inertial measurement unit. The mapping of the trajectory of the vehicle confirms the accuracy of the gyroscope and acceleration measurements.

**Expected Outcomes:** The inertial measurement unit will detect the changes in acceleration with large amounts of noise. The mapping of the trajectory extracted from the gyroscope and accelerometer data will be nearly unreadable.

**Measured Variables:** Acceleration [ $m/s^2$ ],

### Results:

**Quantifiable** – Accelerometer data acquired from LSM9DS1 inertial measurement unit.



**Fig. 48 Acceleration Data from flight computer after the test**

**Qualitative** – Acceleration detection - Success

## **SRAD Propulsion System Testing**

THIS PAGE INTENTIONALLY LEFT BLANK

## **SRAD Pressure Vessel Testing**

**THIS PAGE INTENTIONALLY LEFT BLANK**

## APPENDIX C: HAZARD ANALYSIS

## Appendix C: Hazard Analysis

A personnel hazard analysis was conducted to identify potential hazards to the health and well-being of team members and any other people in the vicinity of the launch vehicle’s manufacturing and testing. The Risk Assessment Code (RAC) was used to evaluate the likelihood and impact of each individual hazard so that the appropriate mitigation strategies could be put in place (Table XXVI). The table of personnel-related hazards was divided into three subsections: Launch Hazards, Testing Hazards, and Manufacturing Hazards. Launch Hazards deals with launch site and flight-related risks. Testing Hazards deals with risks posed by component testing procedures. Manufacturing Hazards deals with any risks posed by tools or machinery used to create and assemble the launch vehicle. These subsections are represented by separate tables, but each are evaluated using the RAC table.

TABLE XXVI  
Risk Assessment Code

Impact (I)		Likelihood (L)
1	No effect on flight/no injury obtained/no risk of mission loss	Extremely Unlikely
2	Slight impact on flight or launch vehicle /very minor injury/mission obstructed	Unlikely/low probability
3		
4	Moderate impact on flight/significant effect on launch vehicle /minor injury	Likely
5		
6	Severe flight impact/extensive repair/partial mission loss or entire mission at risk/moderate injury risk	Highly likely/high probability
7		
8		
9	Total loss of vehicle function/moderate to severe injury	
10	Complete loss of vehicle/major injury or death of personnel	Extremely likely/almost certain

### A. Launch Hazards

TABLE XXVII  
Launch Hazards

Hazard	Cause	Effect	I	L	Mitigation
Motor ignites near person	People close to launchpad during ignition	Hearing damage or burns	8	1	Abide by NAR minimum distance code
	Ignition during motor loading	Hearing damage or burns	8	2	Ground motor loading area, no member in fire-line of energetic
	Delayed motor ignition after failed launch attempt	Hearing damage or burns	8	1	RSO removes safety interlock switch, team waits 60 seconds to approach launch vehicle on launchpad
Falling debris	Parachutes come untied	Impact injury or skin laceration	7	3	Verify correct knots used to tie parachutes (Test 7) Maintain proper stand-off distance Aim launch vehicle away from crowds/personnel
	Shock cord fails	Impact injury or skin laceration	7	2	Examine cords used for frayed portions Maintain proper stand-off distance Aim launch vehicle away from crowds/personnel
	Main parachute does not deploy	Impact injury or skin laceration	7	4	Redundant altimeters and blast charges (Tests 2/7) Maintain proper stand-off distance

Falling debris	Drogue chute does not deploy	Impact injury or skin laceration	7	4	Aim launch vehicle away from crowds/personnel Redundant altimeters and blast charges (Tests 2/7) Maintain proper stand-off distance Aim launch vehicle away from crowds/personnel
	Spectator attempts to catch descending launch vehicle	Impact injury or skin laceration	6	2	Maintain proper stand-off distance Aim launch vehicle away from crowds/personnel
	Fins break off launch vehicle body during flight	Impact injury or skin laceration	6	2	Multiple points of contact for adhesive and sufficiently strong fin material selected (Tests 1/4) Maintain proper stand-off distance Aim launch vehicle away from crowds/personnel
	Main Parachute does not open after deploying	Impact injury or skin laceration	7	4	Verify no interference between shroud lines and parachute protector
	Drogue chute does not open after deploying	Impact injury or skin laceration	7	4	Verify no interference between shroud lines and parachute protector
	No separation events after apogee	Severe impact injury or death	10	3	Redundant altimeters and ejection charges, test E-charges (Test 2) Maintain proper stand-off distance Aim launch vehicle away from crowds/personnel
	Launch vehicle changes trajectory mid-flight	Severe impact injury	9	4	Verify launch vehicle design is sufficiently stable before launch Maintain proper stand-off distance Aim launch vehicle away from crowds/personnel
Ballistic launch vehicle hits person	Launch vehicle exits too slowly off launch rail	Severe impact injury	9	2	Verify safe exit velocity achievable with motor and provided launch rail length Maintain proper stand-off distance Aim launch vehicle away from crowds/personnel
	Ignition during motor loading	Severe impact injury	10	2	Launch vehicle pointed away from spectators, members do not stand behind fuselage Maintain proper stand-off distance Aim launch vehicle away from crowds/personnel
	Black powder ignites near person	Static electricity ignites black powder	7	3	Members handling black powder ground themselves
Electrical shock/thermal burns from component wiring	Live wire from electrical component exposed	Burns and minor electrocution	4	2	All component wiring complete before applying power supply

## C.2 Testing Hazards

TABLE XXVIII  
Testing Hazards

Hazard	Cause	Effect	I	L	Mitigation
Premature charge ejection test	Black powder ignites during loading	Burns and skin lacerations	6	3	Members handling black powder will ground themselves to a surface
Falling debris during drop test	People standing in drop test area during test	Impact injury	4	1	Area cleared before test and proper warning given

### C.3 Manufacturing Hazards

TABLE XXIX  
Manufacturing Hazards

Hazard	Cause	Effect	I	L	Mitigation
<b>Bandsaw blade touches person</b>	Hand in blade path while cutting material	Skin laceration	9	1	Keeping hands out of blade plane
	Small workpiece limits space between hands and blade	Skin laceration	9	2	Using a piece of material as a buffer when cutting small workpiece
<b>Spinning lathe chuck touches member</b>	Hands move too close to spinning jaws	Skin laceration	8	2	Keep hands 6 inches away from cutting zone while machining
	Face too close to spinning chuck jaws	Skin laceration and physical trauma	8	2	Measurements or adjustments never made with machine turned on
<b>Chuck key flies out of lathe chuck</b>	Lathe turned on with chuck key in	Severe physical trauma, possible mortality	10	1	Constant lathe supervision, hand stays on chuck key while in chuck
<b>Spinning drill touches member</b>	Hand brought too close to cut zone	Skin laceration	9	1	Keep hands 6 inches away while machining
<b>Sharp tool cuts person</b>	Holding sharp tool with bare hand	Skin laceration	6	5	Use a rag to carry sharp tools
<b>Hands sucked into drill press cutting zone</b>	Wearing safety gloves while machining	Skin laceration	9	1	No gloves on when machining
<b>Workpiece flies out of cutting zone and hits person</b>	Workpiece not properly clamped in drill press vise	Skin laceration or impact injury	6	3	At least two clamps used on workpiece when mounting to drill press
<b>Harmful fiberglass debris</b>	Dust and fumes from sanded fiberglass	Skin irritation and inhalation hazard	6	4	Use facemask with air filter while cutting, perform cutting in well-ventilated area and alert other personnel of operation
<b>Spray paint gets on person</b>	Proper protection equipment not used	Skin irritation and inhalation hazard	6	4	Use of face masks and gloves, proper ventilation of application area (outside)
<b>Vise pinches person</b>	Hands not kept out of work area	Pinching or skin laceration	4	1	Keep hands out of work zone when operating machinery
<b>Soldering injury</b>	Exposure to melted solder or hot soldering iron	Skin irritation or burns	5	2	Proper use of equipment, space between soldering zone and body parts
<b>Hammer injury</b>	Hammer impacts person's body	Pinching, contusion, or skin laceration	5	2	Body parts clear of hammer work area, no excessive force used
<b>Exposure to battery acid</b>	Batteries dropped or abused	Chemical hazard or skin irritation	6	2	Proper battery storage, safe handling
<b>Loud manufacturing process</b>	Long duration of operation	Hearing damage	4	8	Wear ear protection
<b>Sudden and excessively loud operation</b>	Person startled by operation while in proximity to sharp tools	Skin lacerations or physical trauma	4	2	Verbal warning before any loud and sudden operation is performed
<b>Material debris in workspace</b>	Cutting material causes chips or dust	Eye irritation or skin laceration	3	10	Wear safety glasses always, debris cleared with air or rag
<b>Epoxy on person's body</b>	Epoxy drips off part or tool	Skin irritation	2	5	Wear nitrile gloves when using adhesive



## APPENDIX D: RISK ANALYSIS

## Appendix D: Risk Analysis

Failure Modes and Effects Analyses were conducted to evaluate the potential risks that could impact the flight of the launch vehicle. A separate FMEA was conducted for each distinct subsystem of the launch vehicle. The RAC Table was applied to the FMEA tables (Table XX-XXIV).

### A. Propulsion Hazard Analysis

TABLE XXX  
Propulsion FMEA

Component	Function	Failure Mode	Failure Cause	Failure Effects			I	L	Mitigation
				Local Effects	Next Higher Level	System Effects			
<b>Motor Nozzle</b>	Generate thrust vector	Deformation	Physical impact to nozzle	Ignited propellant cannot escape	Motor pressure rupture	Damage to aft section of vehicle	9	2	Handle motor nozzle carefully at all times
<b>Motor Nozzle</b>	Generate thrust vector	Deformation	Physical impact to nozzle	Ignited propellant released in an undesirable direction	Motor propels vehicle at undesirable thrust vector direction	Vehicle trajectory altered	4	3	Handle motor nozzle carefully at all times
<b>Propellant</b>	Fuel for vehicle	Wetting	Improper storage of propellant	Propellant does not ignite	Motor cannot propel vehicle	Vehicle does not take off	9	2	Store propellant in a dry location
<b>Motor Casing</b>	Protect vehicle body from ignited propellant	Breach of casing wall	Physical impact to casing	Ignited propellant escapes from casing	Modular aft damaged	Structural integrity of aft section compromised	7	2	Handle motor casing carefully at all times
<b>Motor Forward Closure</b>	Protect vehicle body from ignited propellant	Breach in closure	Physical impact to closure	Ignited propellant escapes from closure	Damage to forward vehicle components	Loss of vehicle integrity/function	8	1	Handle motor forward closure carefully at all times
<b>Motor Retainer</b>	Restrict motor from moving axially	Detachment from thrust plate	Screws unthread during flight due to vibration	Retainer falls off during flight	Motor falls out during flight	Launch vehicle is overstable due to sudden change in CG	5	2	Use a COTS approved motor retainer; fasten screws securely
<b>Thrust Plate</b>	Transfer thrust force to airframe	Detachment from modular aft	Screws unthread during flight due to vibration	Thrust plate and retainer fall off during flight	Motor falls out during flight	Launch vehicle is overstable due to sudden change in CG	5	2	Fasten screws securely

### B. Structures Hazard Analysis

TABLE XXXI  
Structure FMEA

Component	Function	Failure Mode	Failure Cause	Failure Effects			I	L	Mitigation
				Local Effects	Next Higher Level	System Effects			
<b>Fin</b>	Provide stability to the	Harmonic Flutter	High aerodynamic forces	Fin breaks off	Launch vehicle loses stability	Launch vehicle goes spinning out of control	10	3	Design fin and launch vehicle to be below fin flutter velocity

	launch vehicle								
<b>Fin</b>	Provide stability to the launch vehicle	Breaks upon impact with ground	High impact forces causing bending moment	Fin breaks off	Launch vehicle loses stability	Launch vehicle is not capable of flying again	4	4	Have spare parts for replacement
<b>Airframe</b>	Transfer thrust of motor through vehicle	Fractures during motor firing	Imperfections in layup cause stress concentration	Force is not transferred through the airframe	Motor pushes through flight vehicle	Rocket does not leave the pad	10	1	Ensure there are no major defects in the airframe after manufacturing
<b>Sealing Disk</b>	Contain Ejection Gasses in Aft Airframe	Breaks under high pressure	Ignition forces are too high	Gasses leak past sealing disk	Pressure does not build up in aft rocket section	Separation event does not occur and parachute is not deployed	7	1	Proper ejection testing and charge sizing
<b>Rail Guides</b>	Retain the Payload during ascent	Adhesion Failure	Poor adhesion due to set up or heat	Bracket holding payload falls off	Payload is no longer retained or guided during deployment	Drogue and payload fail to deploy at apogee	8	2	Proper epoxy techniques used, keep rocket under canopy during assembly
<b>Rail Guides</b>	Retain the Payload during ascent	Rail Guide bracket shear	Bracket fails under loads of ascent	Bracket holding payload snaps in two	Payload is no longer retained or guided during deployment	Drogue and payload fail to deploy at apogee	8	2	Maximize strength of 3D printed part
<b>Centering Rings</b>	Transfer load between the fin brackets	Heat Expansion	Excessive expansion of the motor casing during firing causes plastic deformation	Material yields	Fin structure is weakened	Likelihood of fins breaking off is increased			Size centering rings so that they cannot be affected by thermal expansion
<b>Centering Rings</b>	Transfer load between the fin brackets	Mechanical Failure	Screws unthread during flight due to vibration	The motor is no longer fixed and aligned	The direction of thrust is not stable	The flight path is unpredictable	10	1	Ensure that the centering rings are aligned and assembled securely
<b>Bulkheads</b>	Hold Eyebolt	Mechanical failure	Eyebolt strips off and shears bulkhead due to deployment forces	The launch vehicle separates in multiple parts	The launch vehicle cannot be recovered in one piece	Parts of the launch vehicle can potentially be lost	8	2	Proper rating of bulkhead and proper fastening of eyebolt
<b>Fin Bracket</b>	Fasten fins to airframe	Mechanical Failure	Screws unthread during flight due to vibration	Fin Bracket detaches during flight	Fin is no longer secured and detaches	Launch vehicle is unstable	10	3	Fasten screws securely, design to use multiple screws to reduce risk

### C. Avionics & Recovery Hazard Analysis

TABLE XXXII  
Avionics & Recovery FMEA

Component	Function	Failure Mode	Failure Cause	Failure Effects			I	L	Mitigation
				Local Effects	Next Higher Level	System Effects			
<b>Kevlar Recovery Harness</b>	Connects airframe segments to each other and to parachutes	Zippering	Excessive speed upon parachute deployment.	Wear on recovery harness	Airframe is damaged	Launch vehicle cannot be relaunched until airframe is repaired or replaced	5	2	Add cushioning to the segment of shock cord that will contact the edge of the body tube. Test for zippering during flight test
<b>Altimeter</b>	Measures altitude and ignites parachute deployment charges	Battery disconnects	Faulty wiring, disconnect due to flight forces, or dead battery	Altimeter does not measure altitude or ignite charge wells	Parachute is not deployed	High velocity impact with ground and total destruction of launch vehicle	9	2	Check battery voltage and wiring prior to flight. Conduct "Tug Test" on all altimeter connections
<b>Altimeter</b>	Measures altitude and ignites parachute deployment charges	Faulty measurement of altitude	Sudden pressure changes in avionics bay due to wind	Premature ignition of ejection charges	Parachutes are deployed early	Launch vehicle will need to be re-prepared (if on pad) or will endure extreme flight forces	5	2	Drill air venting holes to altimeter manufacturer specifications, Test altimeter using pressure chamber
<b>Altimeter</b>	Measures altitude and ignites parachute deployment charges	Wiring ejection charges in reverse (drogue ejection connected to main terminal)	Inaccurate labelling of terminals or improper altimeter programming	Main parachute is deployed at apogee instead of drogue	Main parachute is deployed at apogee	The launch vehicle drifts excessive amount, potentially causing the launch vehicle to be lost	5	3	Accurate labelling of ejection charges
<b>Altimeter</b>	Measures altitude and ignites parachute deployment charges	Ejection charges detonate when the altimeter is armed, altimeter is damaged	Polarity of battery wiring reversed	Ejection charges detonate on launch pad	Potential injury for person arming altimeter	Unable to launch	3	6	Test the wiring of the altimeters before placing them in rocket and adding ejection charges
<b>Main Parachute</b>	Slows final launch vehicle descent	Tangling	Improper packing of shroud lines	Parachute deployment may be partially obstructed	Faster and less stable launch vehicle descent	Launch vehicle impacts ground at a higher velocity	7	4	Fold shroud lines prior to packing into launch vehicle. Visually inspect shroud lines for tangles
<b>Main Parachute</b>	Slows final launch vehicle descent	Partial or non-deployment	Not enough Black powder used in ejection charge	Parachute does not deploy or deploys late	Launch vehicle impacts the ground at a high velocity	Damage to launch vehicle airframe and/or payload	9	3	Conduct ground testing of all ejection systems prior to launch

<b>Drogue Parachute</b>	Slows descent before main deployment	Tangling	Improper packing of shroud lines	Parachute deployment may be partially obstructed	High velocity deployment of main parachute	Potential zippering of airframe upon main parachute deployment	5	4	Fold shroud lines prior to packing into launch vehicle. Visually inspect shroud lines for tangles
<b>Drogue Parachute</b>	Slows launch vehicle descent before main deployment	Partial or non-deployment	Not enough Black powder used in ejection charge	Parachute does not deploy or deploys late	High velocity deployment of main parachute	Potential zippering of airframe upon main parachute deployment	3	3	Conduct ground testing of all ejection systems prior to launch (Tests 2/7)
<b>TeleGPS</b>	Tracks launch vehicle location for recovery	Battery dies	Improper charging, leaving battery plugged in	TeleGPS does not have necessary voltage to broadcast data to TeleDongle	Rocketeers on ground do not receive GPS data	Potential failure to recover launch vehicle	3	3	Only plug in TeleGPS within 1 hour of launch
<b>TeleGPS</b>	Tracks launch vehicle location for recovery	O-ring seal fails	Improper O-ring connection	Ejection gases enter the nosecone	The TeleGPS electronics are damaged	Loss of GPS signal, potential irreparable destruction of TeleGPS	5	1	Ensure o-ring is sitting well in slot before attaching mount to nosecone
<b>TeleGPS</b>	Tracks launch vehicle location for recovery	No satellites in solution	Fails to lock on to enough satellites – possibly influenced by weather	TeleGPS does not obtain GPS data	Rocketeers on ground do not receive GPS data	Potential failure to recover launch vehicle	3	2	Ensure GPS signal is acquired before attaching mount to nosecone
<b>Electronics mount</b>	Holds TeleGPS and battery	Fracture	PETG fractures during flight, likely at landing	TeleGPS is free to move about interior of nosecone	Potential for battery connection to fail or TeleGPS to sustain damage	Potential loss of GPS signal, potential irreparable destruction of TeleGPS	4	1	Use 100% infill when manufacturing mount
<b>Electronics mount</b>	Holds TeleGPS and battery	Comes loose from mounting ring	Improper tightening of screws	Telemetry module is free to move about interior of nosecone	Potential for battery connection to fail or TeleGPS to sustain damage, nosecone is no longer attached to rest of recovery system	Potential loss of GPS signal, potential irreparable destruction of TeleGPS, loss of nosecone	6	2	Ensure screws are properly torqued when attaching mount to nosecone
<b>Mounting ring</b>	Holds electronics mount to nose cone	Epoxy failure	Epoxy connection between mounting ring and nosecone fails	Telemetry module is free to move about interior of nosecone	Potential for battery connection to fail or TeleGPS to sustain damage, nosecone is no longer attached to rest of recovery system	Potential loss of GPS signal, potential irreparable destruction of TeleGPS, loss of nosecone	6	2	Use proper procedures when applying epoxy

## D. Payload Hazard Analysis

TABLE XXXIII  
Payload FMEA

Component	Function	Failure Mode	Failure Cause	Failure Effects			I	L	Mitigation
				Local Effects	Next Higher Level	System Effects			
<b>Kevlar Recovery Harness</b>	Connects airframe segments to each other and to parachutes	Zippering	Excessive speed upon parachute deployment.	Wear on recovery harness	Airframe is damaged	Launch vehicle cannot be relaunched until airframe is repaired or replaced	5	2	Add cushioning to the segment of shock cord that will contact the edge of the body tube. Test for zippering during flight test
<b>PCB</b>	House the electronic components that allow experiment to function	Impact	Impact force at landing causes electronic components to fail due to impact even if structure is unaffected	One or more electric components lose functionality	Components cannot communicate with flight computer	Roll control experiment can no longer run after flight	5	4	Add layer of impact resistant foam below bulkhead.
<b>PCB</b>	House the electronic components that allow experiment to function	Exposure to ejection gas	Black powder charges interact with PCB components, frying them	One or more electric components lose functionality	Components cannot communicate with flight computer	Roll control experiment can no longer run during descent	6	5	Sealing plates around cube sat to prevent ejection gases from passing through
<b>PCB</b>	House the electronic components that allow experiment to function	Shock	Deceleration from parachute deployment results in disconnection of wires or damage to the electronics	One or more electric components lose functionality	Components cannot communicate with flight computer	Roll control experiment can no longer run	6	5	Ensure that all the wires are securely connected using the "tug" test.
<b>PCB</b>	House the electronic components that allow experiment to function	Obstruction	Residue from black powder obstructs the photoresistor	Photoresistor does not detect the change in lighting	The flight computer cannot discern that the payload is outside the airframe	The parachute does not deploy, and the roll control experiment can no longer run	8	2	Ensure that the surface of the payload is clean and sufficiently sealed
<b>PCB</b>	House the electronic components that allow experiment to function	Software Error	An unaccounted component in the software causes a system error	The electronics reboot or stop functioning	One or more parts of electronic systems stop functioning.	Roll control experiment can no longer run	5	2	Extensive prior testing is conducted to identify potential errors
<b>IMU</b>	Controls payload's RCS	Miscalibration	Experimental data does not sufficiently account for	RCS does not sufficiently counteract the rotation	The payload rotates throughout the descend	The camera footage is not stable	2	5	Ensure that extensive testing and

			the moment of the payload	of the payload				calibration is done	
<b>Cable Cutter</b>	Release parachute during deployment	Premature Ignition	Incorrect pressure readings in the altimeter cause the cable cutter to ignite within the airframe	Payload deploys parachute within airframe	Launch Vehicle recovery deployment is interrupted	Launch Vehicle separates nose cone but without drogue parachute	9	3	Altimeter placed in tight container to block out pressures from inside the airframe
<b>Cable Cutter</b>	Release parachute once deployment occurs	No ignition	Cable Cutter e-charge does not release	Payload parachute does not release	Payload lands at excessive impact, leading to damaged components	Roll Control experiment fails, payload may need to be repaired and rebuilt. Payload descends ballistic and could damage bystanders	9	2	Utilize redundant recovery system in case first one does not go off
<b>Drogue Parachute</b>	Slows descent before main deployment	Tangling	Improper packing of shroud lines	Parachute deployment may be partially obstructed	High velocity deployment of main parachute	Potential zippering of airframe upon main parachute deployment	5	3	Slits in payload bulkhead to allow shock cord to pass through
<b>Swivel</b>	Allows Parachute to rotate on Shock Cord without Tangling	Jammed	Material from ejection enters gaps of swivel	Swivel no longer rotates	Parachute may tangle its shroud line	Payload fails to slow down during descent	8	2	Ensure swivel turns before preparing recovery
<b>Flight Computer Battery</b>	Power the flight computer	Loss of power	Dead or partially charged batteries are used	Battery outputs insufficient power	Flight computers do not function properly	Payload redundant charge does not fire. Payload is reliant on one altimeter for deployment	8	4	Ensure that new and fully charged batteries are used
<b>Reaction Wheel Battery</b>	Power the reaction wheel	Loss of power	Dead or partially charged batteries are used	Battery outputs insufficient power	The reaction wheel does not function	Roll control experiment can no longer run	5	4	Ensure that new and fully charged batteries are used
<b>Camera Battery</b>	Power the camera	Loss of power	Dead or partially charged batteries are used	Battery outputs insufficient power	The camera does not function	No footage is recovered	2	4	Ensure that new and fully charged batteries are used
<b>Power Wiring</b>	Connects the power to various electronic systems	Poor connection	Connection between the components is temporary or permanently lost	One or more electronic systems lose power	One or more components do not function	Roll control experiment can no longer run. Payload is reliant on one altimeter for deployment	8	5	Ensure that all the wires are securely connected using the "tug" test

<b>Data Wiring</b>	Connects various electronic systems	Poor connection	Connection between the components is temporary or permanently lost	One or more electronic systems do not communicate with the rest of the systems	One or more components do not function	Roll control experiment can no longer run. Payload redundant charge does not fire. Payload is reliant on one altimeter for deployment	8	5	Ensure that all the wires are securely connected using the "tug" test
<b>GPS</b>	Tracks the location of the payload	Interference	The electronics or the reaction wheel interfere with the transmission of the GPS	GPS signal is not or partially transmitted	GPS tracking data is inconsistent or absent	The location of the payload cannot be accurately discerned	7	2	Bring Binoculars, Test system before hand to ensure stability of GPS connection.
<b>Structure</b>	Protects and houses the inner components of the payload	Fracture	Parachute deployment causes excessive stress	Eyebolt tears off bulkhead.	The payload detaches from parachute	The payload is in free fall.	10	1	Ensure that the payload bulkhead is rated for deployment forces
<b>Structure</b>	Protects and houses the inner components of the payload	Fracture	Landing causes excessive stress	The payload component that hits the ground first is fractured	The structural integrity of the payload is compromised	The payload and internal components break during landing	5	1	Use foam padding to soften fall Make sure the parachute is sufficiently sized

### E. Environmental Hazard Analysis

An analysis was conducted to evaluate the hazards the environment posed to the launch vehicle and vice versa. The launch vehicle will have the most exposure to the environment at launch sites, so those locations were specifically evaluated for potential concerns. The RAC table was used to evaluate the hazards in the table (Table XXV).

TABLE XXXIV  
Environmental Effects on Launch Vehicle Analysis

Hazard	Cause	Effect	I	L	Mitigation
<b>Precipitation soaks launch vehicle</b>	Weather change at launch site	Ruined electronics	7	2	Bring canopy for prep area and waterproof storage for electronics
	Weather change at launch site	Warped airframe shape	7	2	Bring canopy for prep area and waterproof storage for electronics
<b>Descent into body of water</b>	Launch vehicle drifts too far	Ruined electronics	7	1	Minimize drift with drogue, angle launch rail into wind
	Launch vehicle drifts too far	Warped airframe shape	8	1	Minimize drift with drogue, angle launch rail into wind
<b>Launch vehicle caught in tree or power line</b>	Launch vehicle drifts too far	Difficulty retrieving	6	1	Verify launch site is away from obstacles
<b>Launch vehicle flies into cloud</b>	Liftoff occurs without waiting for clear sky	Launch vehicle collision with unseen aircraft	9	2	Delay launch until sky is clear Verify that present cloud cover is not located below expected apogee
<b>High winds</b>	Launch vehicle drifts during descent	Difficulty retrieving	5	6	Angle launch rail into wind
	Launch vehicle changes flight trajectory	Ballistic launch vehicle crashes at high speed	9	3	Launch does not occur in high wind, verify launch vehicle is not over stable



<b>Dryness</b>	Brittle adhesive (JB Weld) at critical joint locations	Fins, centering rings, or bulkheads come loose or break off	7	3	JB Weld with longer curing time used at design critical joints for improved resistance to environment
<b>Humidity</b>	Moisture affects electrical components	Recovery system or payload malfunction	5	4	Altimeter performance tested on site to verify functionality
<b>High Temperatures</b>	Electrical components overheat	Recovery system or payload malfunction	5	8	Canopy brought to launch site to keep launch prep area out of sunlight, quick retrieval after launch vehicle landing, bring lots of water, utilize PETG to reduce heats impact on components, paint rocket light colors
<b>Fog/Low Visibility</b>	Launch vehicle descent out of view	Launch vehicle retrieval after descent difficult	7	2	Launch delayed until visibility improves or launch canceled
<b>Sand/Dirt in Structural Components</b>	Wind blowing sand/dirt during assembly	Increased friction may prevent separation	8	4	Ensure parts are able to smoothly slide in and out before launch
<b>Sand/Dirt in Electrical Components</b>	Wind blowing sand/dirt during assembly	Altimeters fail to fire deployment charge	8	3	Ensure avionics bays are sealed and shielded from winds.

TABLE XXXV  
Launch Vehicle Effects on Environmental Analysis

<b>Hazard</b>	<b>Cause</b>	<b>Effect</b>	<b>I</b>	<b>L</b>	<b>Mitigation</b>
<b>Fire around launchpad</b>	Motor ignition sets grass on fire	Fire damage to launch site	7	1	NAR minimum distance code, remove dry grass and equipment from launch pad area
<b>Fire at launch prep site</b>	Black powder spilled and ignited	Fire damage to private property	8	3	Pour water on black powder to reduce likelihood of ignition. Bring Fire extinguisher in case of any fires.
<b>Litter</b>	Components or trash left behind	Pollution of land	3	4	Post-launch clean-up enforced by RSO
<b>Chemical leaks</b>	Battery acid from ruptured battery case	Harms vegetation or wildlife	5	2	Batteries with quality casing selected, proper disposal into designated waste bins
<b>Launch vehicle Debris</b>	Ballistic launch vehicle impact scatters debris	Pollution of land	5	2	Redundancies used in recovery system to prevent ballistic descent

### Personal Protective Equipment

A variety of personal protective equipment items are currently available for team members to use. This equipment allows mitigation strategies to be employed to prevent personal injury from hazardous materials or processes. The safety officer and safety stewards observe work performed by team members and prevent any work being done without applying the appropriate PPE.

- **Safety Glasses:** Must always be worn when working in the Student Design Center or Student Design Shop. They protect eyes from material debris, projectiles, and air contaminants such as dust or smoke.
- **Heavy duty Safety Gloves:** Must be worn when handling metal material that has not been deburred using a file. Safety gloves protect the user's hands from sharp edges that could otherwise cause lacerations. Safety gloves, or gloves of any kind, cannot be worn when operating powered machinery, due to the risk of the gloves catching on a moving edge.
- **Rags:** Rags are heavy duty materials that protect the user's hands from sharp workpiece or tool edges. Rags are used when a team member must operate powered machinery, therefore eliminating the ability to wear safety gloves, and must change tools or adjust a workpiece.
- **Nitrile Gloves:** Nitrile gloves are flexible skin-tight gloves worn when a team member must handle a potentially hazardous material that does not pose a risk of skin laceration, meaning no sharp edges. Specific instances of nitrile glove use include working with adhesive such as epoxy and handling components with motor or black powder residue.
- **Ear Plugs:** Ear plugs are available for long machining operations that are also distracting or hazardously loud.

- **Earmuffs:** Earmuffs perform an identical function to ear plugs, except earmuffs provide more hearing protection. Members are required to wear earmuffs during machining operations that take a long time and are loud enough to cause hearing damage.
- **Face masks:** Face masks prevent air contaminants from being breathed in by the user via the mouth or nose. Team members must wear face masks when an operation produces toxic fumes or a material debris fine enough to be inhaled.
- **Respirators:** Respirators perform the same function as face masks; however, they are capable of catching much finer material debris and filtering it out of the air inhaled by the user. Respirators are required for use during the sanding of any composite materials, which for this project means fiberglass, because composite dust is too fine to be blocked by regular face masks.
- **Rounded Polypropylene Spatula:** A rounded polypropylene spatula is a non-static, non-sparking utensil. Its purpose is to handle black powder when creating ejection charges without causing premature combustion due to heat from static or sparks.

APPENDIX E: ASSEMBLY, PREFLIGHT, LAUNCH, AND RECOVERY CHECKLISTS APPENDIX

## Assembly

### Payload

- Battery mount:
  1. Place the TeleGPS and the 9V battery inside their specified slits.
  2. Afterwards, place battery for motor controller into the mount in its specified space.
  3. Screw in the motor controller into its space at the top of the mount.
  4. Place TeleGPS battery at bottom of the mount, ensuring that its wire sticks out of its specified slit. Then gently place mount on fiberglass plate and screw the mount into the plate and bulkhead.
- PCB mount
  1. Attach Lithium-Ion battery to the PCB.
  2. Tape Velcro at bottom of PCB.
  3. Place PCB inside the mount and pass the Velcro through specified slits, then wrap it around the bottom of the mount.
  4. Bolt the mount into its specified plate.
  5. Perform calibration sequence.
  6. LED and sound generated by buzzer on PCB will notify operator the computer is ready for flight.
- Portable charger mount
  1. Slide charger into mount, then bolt mount into specified plate.
- Motor-reaction wheel assembly
  1. Bolt Motor into specified plate.
  2. Slide reaction wheel up shaft and then tighten set screw into its hole using 5/64 Allen Wrench.
- Camera mount
  1. Place camera in mount and ensure that usb cable can slide out of its specified slit, then bolt into the top plate.
- Eyebolt
  1. Bolt eyebolt through top bulkhead and top plate and then
- Avionics bay
  1. Perform calibration sequence (**Procedure for Calibrating Raven3**)
  2. Connect Lithium-Ion battery to flight computer.
  3. Place Flight computer on adjustable sled.
  4. Place four screws on rounded slots with nuts attached on opposite to desired position.
  5. Place 9V battery in its mount and fasten it using Velcro.
  6. Install red switch into its specified hole.
  7. Bolt the 9V battery in its mount and the altimeter into the bay from the inside.
  8. Connect the 9V battery to the altimeter and to the switch.
  9. LED and sound generated by buzzer on PCB will notify operator the computer is ready for flight.
- Positioning components
  1. With the battery mount, bottom plate, and bottom bulkhead attached, position polyurethane layer below the bottom bulkhead, then slide the four threaded rods through their specified holes and secure them with lock nuts. Secure the top of the bottom plate with four regular 1/4-20 nuts.
  2. Install the middle plates at the specified distance from the bottom plate. Do this by position nuts to hold the plates at the top and having nuts at the top to secure the plates.
  3. Slide the eyebolt-top bulkhead-top plate assembly through the rods until reaching a specified distance marked by nuts resting on the bottom of the top plate. On the shorter rods, slide lock on the top of the rods so that they rest on the top bulkhead.
  4. Slide the avionics bay through the longer rods and then slide lock nuts through the rods so that they rest on top of the bay.
- Wiring
  1. Connect the USB wire from the camera to the portable charger below, and secure by zip tying to the nearest threaded rod as well as taping to the mount.
  2. Pass the wires from the 9V battery through the plate with the PCB and then connect to the Teensy.
  3. Pass wires from the Li-ion battery through slit and connect to motor controller right above it.

4. Pass wire for TeleGPS battery from the slit at the back of the mount and connect it to the TeleGPS from behind.
5. Pass wires from BLDC motor through the specified holes in the middle two plates and zip tie near the top plate and below the plate with the PCB, then connect to the motor controller at the specified spots.
6. Install the sealing plates so that the CubeSat is completely sealed.

### **Procedure for Calibrating Raven3**

1. Plug altimeter into computer with MicroUSB and turn altimeter on with button.
2. Make sure altimeters are programmed correctly.
  - a. Check that Altitude for deployment is 1000 feet.
  - b. Calibrate pressure to launch site.
  - c. Attach LEDs to the ejection charge terminals and run flight simulation.
3. Prepare the ejection charge with the black powder.
4. Replace the LEDs with ejection charges
5. Perform tug tests and ensure there is continuity in wiring.
6. After checking altimeter is programmed correctly, turn altimeter on and off.
7. Make sure the correct beeping sequence is emitted (outlined below).
8. Check that there is enough storage in the altimeter.
9. Turn off the altimeter with the switch.

### **Procedure for Calibrating StratoLogger SL100**

1. Connect the data cable to the altimeter and connect to the microUSB.
2. Plug altimeter into computer using the microUSB, and turn altimeter on with switch.
3. Make sure the altimeter is programmed correctly.
  - a. Check that Altitude for main deployment is 1000 feet.
  - b. Calibrate pressure to launch site.
  - c. Attach LEDs to the ejection charge terminals and run flight simulation.
4. Prepare the ejection charge with the black powder.
5. Replace the LEDs with ejection charges.
6. Perform tug tests and ensure there is continuity in wiring.
7. After checking altimeter is programmed correctly, turn altimeter on and off .
8. Make sure the correct beeping sequence is emitted (outlined below).
9. Check that there is enough storage in the altimeter.
10. Turn off the altimeter with the switch.

### **Telemetry Assembly**

1. Turn on AltOS & connect dongle.
2. Plug in GPS.
3. Ensure GPS is communicating with computer.
4. Secure GPS to mount.
5. Secure battery to mount.
6. Gently put mount into nosecone.
7. Screw down mount screws.
8. Keep antenna pointed at rocket during launch.

### **Avionics Bay Assembly**

1. Ensure altimeters have been calibrated to launch site (Procedure for Calibrating Raven 3 & Stratologger SL100)
2. Install new batteries into Electronics Sled
3. Secure Batteries using Velcro zip ties
4. Install altimeters by wiring altimeters to batteries and switch
5. Conduct Tug Test on all wiring
6. Slide threaded rod through electronics sled, and secure with nuts
7. Fasten threaded rod assembly to bottom bulkhead with nuts.

8. Slide assembly into coupler  
ATTENTION: Ensure key switches are aligned with externally accessible key hole locations.
9. Fasten top bulkhead to threaded rod assembly.
10. Connect e-matches to XT-60 Connectors located on top and bottom bulkhead.
11. Pack e-charge wells with black powder.
12. Seal e-charge wells.

**Modular Aft Assembly:**

1. For each fin, attach to fin brackets using 5 fasteners.
2. Insert forward-most centering ring into the aft airframe and hold in place with fasteners.
3. Attach fin brackets to forward centering ring.
4. Repeat step three for all centering rings.
5. Mount rail button to airframe.
6. Attach thrust ring to aft centering ring.
7. Ensure all fasteners are secure.

**Motor Assembly**

1. Use manufacturer provided procedures for preparing motor.

**Pre-Launch Procedure**

1. Pack folded payload parachute, payload, folded drogue parachute, shock cord and fire-resistant wadding into forward airframe.  
CAUTION: Ensure shroud lines and shock cord do not tangle inside the airframe.  
CAUTION: Ensure payload rests on rail guides without shock cord tangling  
CAUTION: Ensure shock cord passes payload
2. Slide forward airframe onto the forward end of the avionics bay and fasten with rivets  
CAUTION: Ensure fire-resistant wadding is nearest component to the floating ejection charge
3. Pack folded main parachute, shock cord and fire-resistant wadding into aft airframe.  
CAUTION: Ensure fire-resistant wadding is nearest component to the floating ejection charge
4. Slide modular aft onto aft end of avionics bay and fasten with shear pins.  
CAUTION: Ensure fire-resistant wadding is nearest component to the floating ejection charge
5. Slide Nose Cone onto forward airframe and fasten with shear pins
6. Weigh the launch vehicle without the motor using the large electronic scale and document result.
7. Load assembled motor into aft airframe through the nozzle end.
8. Attach the motor retention ring.
9. Weigh launch vehicle with the motor using the large electronic scale and document result.  
CAUTION: No members should be directly in front or behind loaded launch vehicle.  
CAUTION: Point the launch vehicle away from personnel in case of premature ignition.
10. Use the loaded motor weight to run an OpenRocket Simulation and document predicted altitude, Static Stability Margin, and Rail Exit Velocity

**Launch Pad**

1. Have the Range Safety Officer inspect the launch vehicle and give approval for launch
2. Carry the launch vehicle out to the launch pad  
CAUTION: Make sure the launch vehicle is pointed away from personnel  
At least 2 people must carry the vehicle to keep it stably pointed away from personnel
3. Bring the altimeter arming keys, a small ladder, igniter, and tape
4. Carefully lift launch vehicle and slide the lower rail button into the slot in the rail.
5. Move the launch vehicle down until the second rail button is in place on the rail.  
CAUTION: Ensure the airframe is not in direct contact with the rail while sliding  
Scraping the rail while loading the vehicle can damage the rail buttons

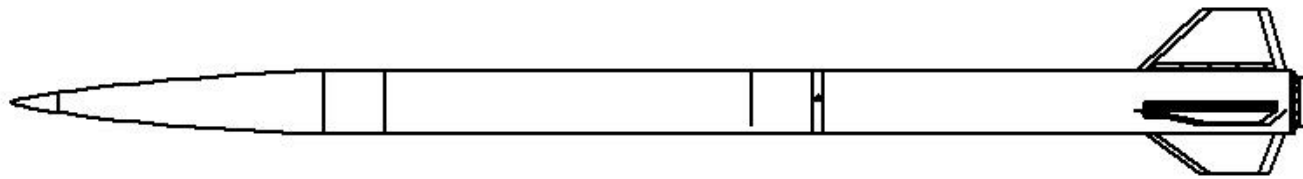
6. Slide the launch vehicle all the way to the stopper on the rail.
7. Readjust the launch rail according to the wind direction and the location of spectators  
CAUTION: If the wind speed exceeds 20 mph, launch cannot commence until it reduces
8. Use a small ladder brought to the launch pad to reach the main altimeter arming switch keyhole
9. Insert the altimeter arming key into the keyhole and twist until audible beeps from the altimeter are heard, indicating it has been powered on
10. Wait and listen while the altimeter goes through a sequence of beeps representing its start-up process  
CAUTION: Remain silent while the altimeter starts up  
The beeps will be more difficult to hear through the airframe material
11. Once the altimeter is issuing a sequence of three quick beeps periodically, the altimeter is armed
12. Repeat steps 8-11 for the secondary altimeter and Payload altimeter
13. Ignitor wire leads are in contact with each other when ignitor is brought out to launch pad.  
CAUTION: All personnel except propulsion lead, team mentor, and safety officer move to a minimum safe distance.  
CAUTION: Clearance in case of premature ignition of ignitor.
14. Insert ignitor into motor via nozzle throat as far up as possible.
15. Tape ignitor to the stand to keep it inside of the motor.
16. Disconnect ignitor leads from each other and reconnect them to the ignitor terminals by the launch pad.  
CAUTION: Do not allow ignitor leads to contact any metal except the terminals to prevent static electricity from causing ignition.
17. Verify electrical continuity across the ignitor and vacate the launch pad area.  
NAR High Power Rocket Safety Code Minimum Personnel Distance: 300 feet.

#### **Recovery**

1. Wait for approval by RSO to search field for launch vehicles
2. Locate position of launch vehicle using TeleGPS
3. Use Binoculars to search for parachutes
4. Walk/Drive to launch vehicle
5. Take photos of landing prior to touching any components
6. Disarm altimeters using arming key
7. Ensure motor is retained and parachutes are attached
8. Recover all sections of launch vehicle
9. Repeat steps 2-8 for Payload.

APPENDIX F: ENGINEERING DRAWINGS APPENDIX





TOLERANCE UNLESS NOTED				TITLE:	
OPERATION	PLACES IN DIMENSION			Tropogator Assembly	
	0.0	0.00	0.000	DRAWN	GRIFFIN MARTIN
MACHINING	0.050	0.020	0.005	DESIGNED	SIMAMP LAUNCH I REC
CUT OFF (SAW, BURN, SHEAR)	0.1	0.060	//	SIZE	DWG. NO.
WELDING	0.1	0.060		<b>A</b>	
ANGULAR DIMS	5	2	0.5	SCALE: 1:15	SHEET 2 OF 2

5

1

4

1

3

1

2

1

1



TITLE: Tropogator Assembly

DRAWN: GRIFFIN MARTIN

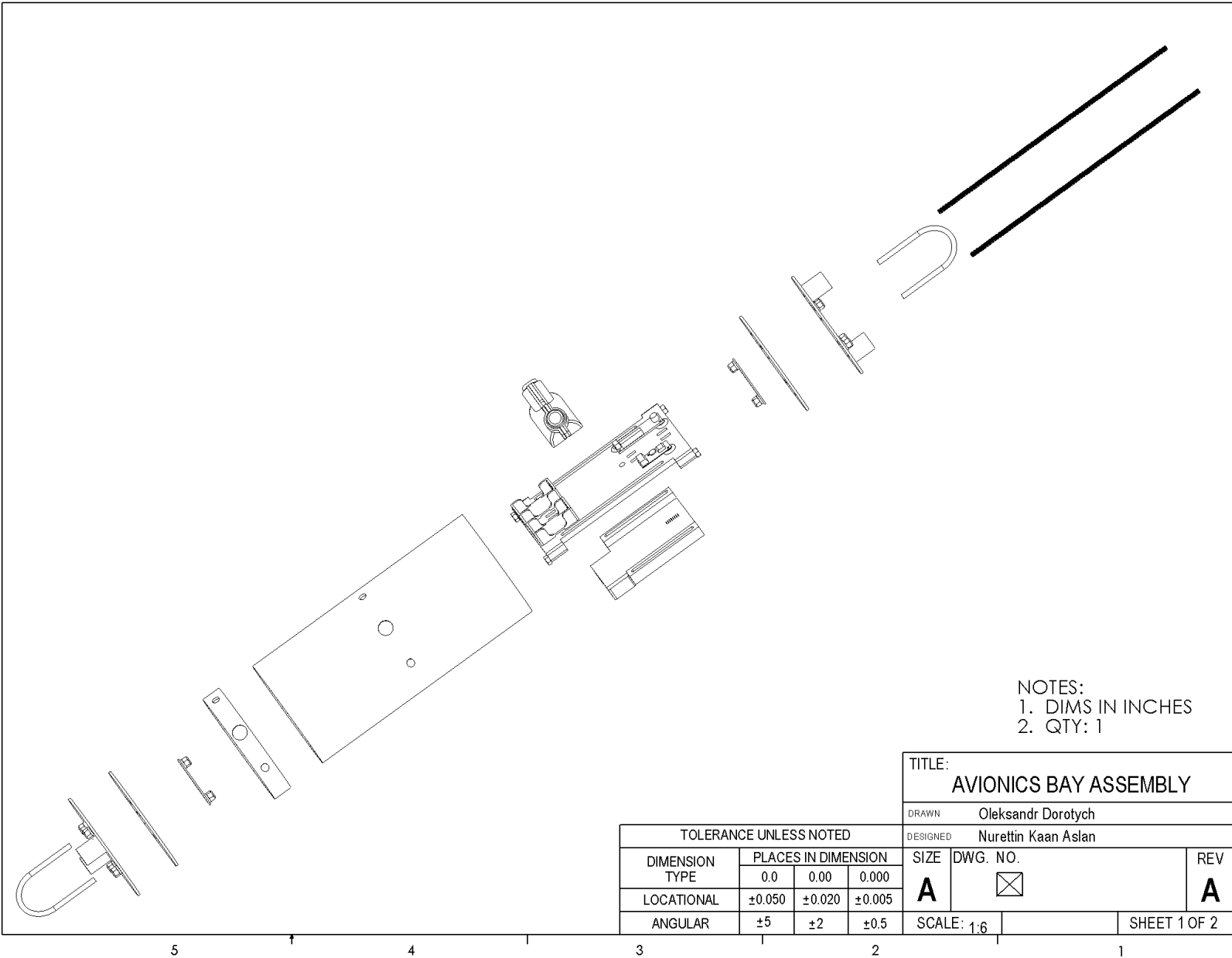
DESIGNED: SIWAMP LAUNCH IREC

TOLERANCE UNLESS NOTED			
DIMENSION TYPE	PLACES IN DIMENSION		
	0.0	0.00	0.000
LOCATIONAL	0.050	0.020	0.005
ANGULAR	5	2	0.5

SIZE	DWG. NO.	REV
<b>A</b>		<b>A</b>

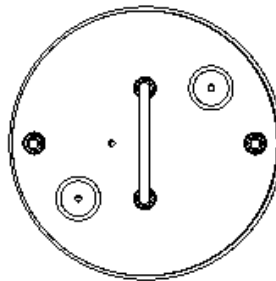
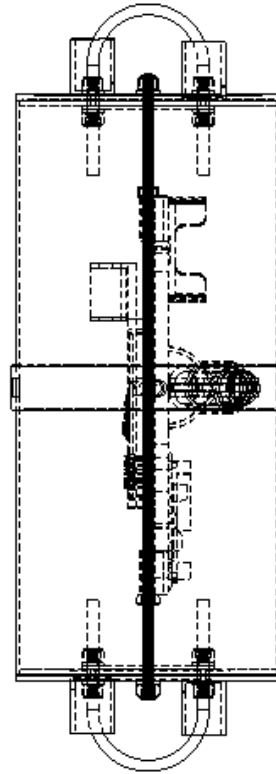
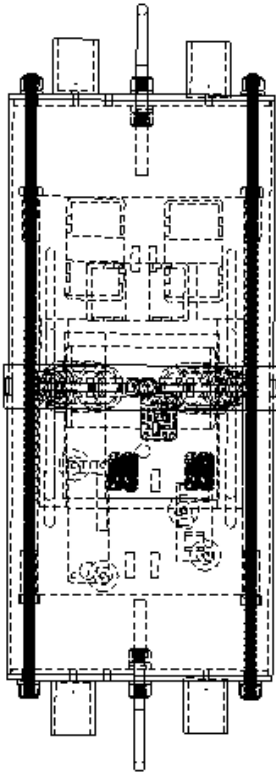
SCALE: 1:30 SHEET 1 OF 2

5 4 3 2 1



NOTES:  
 1. DIMS IN INCHES  
 2. QTY: 1

TITLE:		AVIONICS BAY ASSEMBLY	
DRAWN:		Oleksandr Dorotych	
DESIGNED:		Nurettin Kaan Aslan	
DIMENSION TYPE	PLACES IN DIMENSION	SIZE	DWG. NO.
	0.0 0.00 0.000	<b>A</b>	☒
LOCATIONAL	±0.050 ±0.020 ±0.005		<b>A</b>
ANGULAR	±5 ±2 ±0.5	SCALE: 1:6	SHEET 1 OF 2

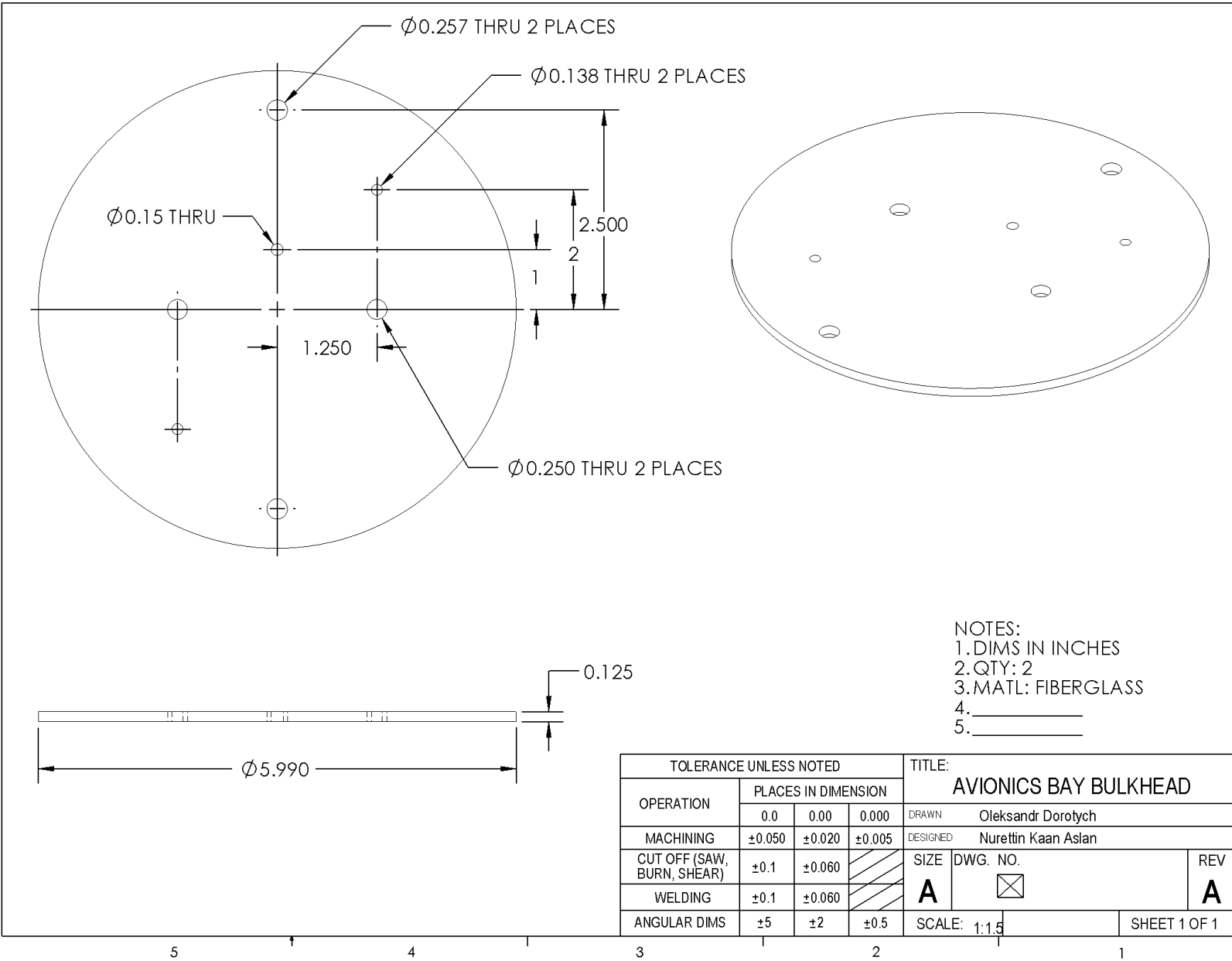


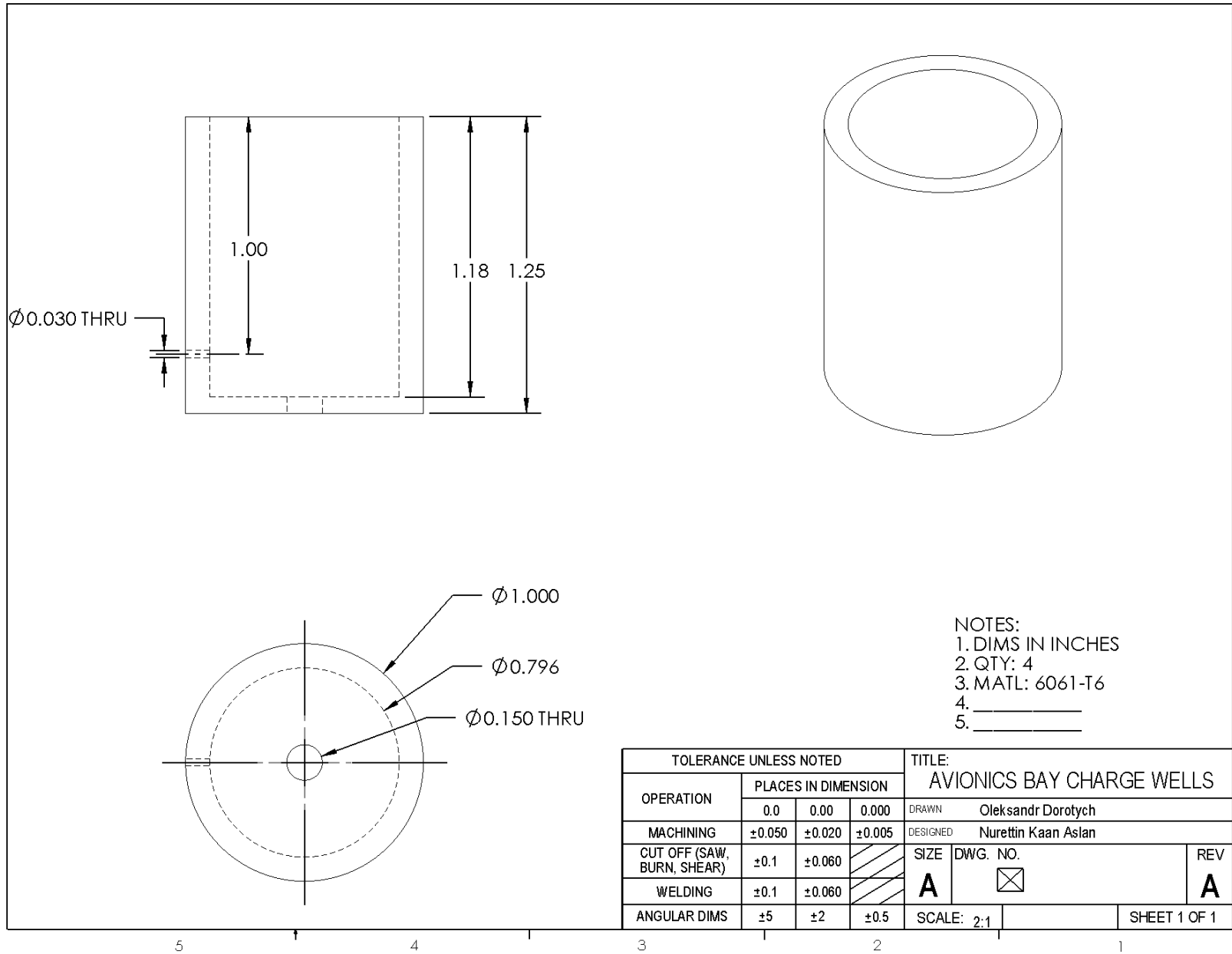
NOTES:  
 1. DIMS IN INCHES  
 2. QTY: 1

TITLE:		AVIONICS BAY ASSEMBLY	
DRAWN	Oleksandr Dorotych		
DESIGNED	Nurettin Kaan Aslan		
SIZE	DWG. NO.	REV	
<b>A</b>		<b>A</b>	
SCALE: 1:3,5			SHEET 2 OF 2

DIMENSION TYPE	PLACES IN DIMENSION		
	0.0	0.00	0.000
LOCATIONAL	±0.050	±0.020	±0.005
ANGULAR	±5	±2	±0.5

5 4 3 2 1

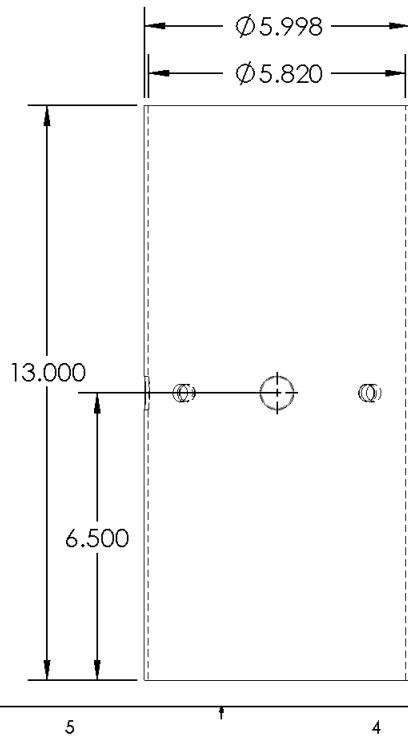
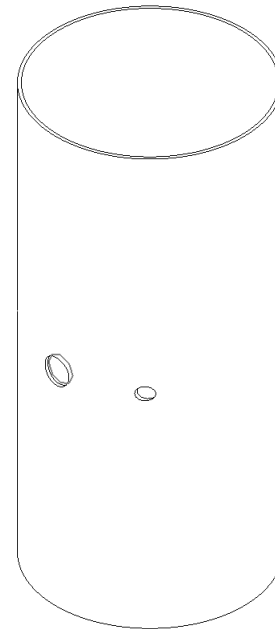
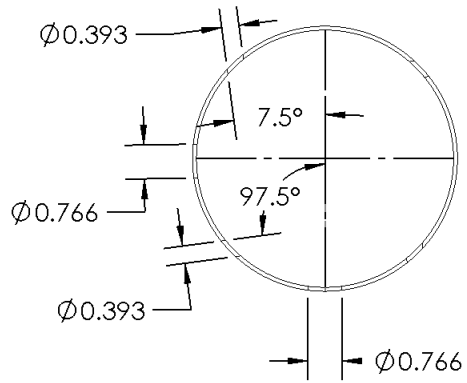




NOTES:  
 1. DIMS IN INCHES  
 2. QTY: 4  
 3. MATL: 6061-T6  
 4. \_\_\_\_\_  
 5. \_\_\_\_\_

TOLERANCE UNLESS NOTED				TITLE: AVIONICS BAY CHARGE WELLS	
OPERATION	PLACES IN DIMENSION			DRAWN	Oleksandr Dorotych
		0.0	0.00	0.000	DESIGNED
MACHINING	±0.050	±0.020	±0.005	SIZE	DWG. NO.
CUT OFF (SAW, BURN, SHEAR)	±0.1	±0.060		<b>A</b>	<input checked="" type="checkbox"/>
WELDING	±0.1	±0.060		SCALE: 2:1	REV <b>A</b>
ANGULAR DIMS	±5	±2	±0.5	SHEET 1 OF 1	

5 4 3 2 1

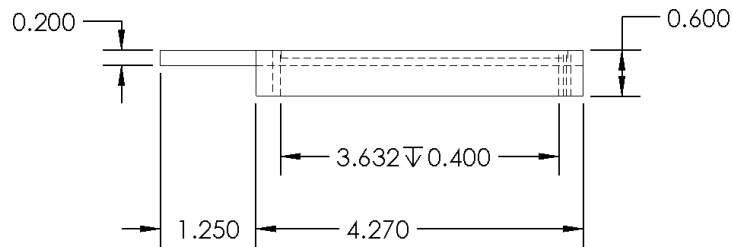
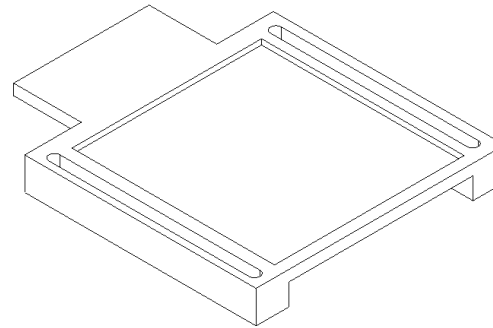
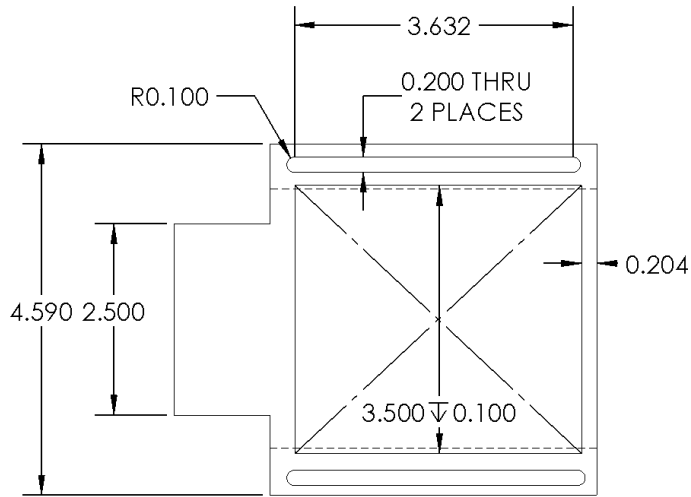


- NOTES:  
 1. DIMS IN INCHES  
 2. QTY: 1  
 3. MATL: G12 FIBERGLASS  
 4. \_\_\_\_\_  
 5. \_\_\_\_\_

TOLERANCE UNLESS NOTED				TITLE:	
OPERATION	PLACES IN DIMENSION			AVIONICS BAY COUPLER	
		0.0	0.00	0.000	DRAWN
MACHINING	±0.050	±0.020	±0.005	DESIGNED	Nurettin Kaan Aslan
CUT OFF (SAW, BURN, SHEAR)	±0.1	±0.060		SIZE	DWG. NO.
WELDING	±0.1	±0.060		<b>A</b>	<b>A</b>
ANGULAR DIMS	±5	±2	±0.5	SCALE: 1:3.5	SHEET 1 OF 1







- NOTES:  
 1. DMS IN INCHES  
 2. QTY: 1  
 3. MATL: PET  
 4. \_\_\_\_\_  
 5. \_\_\_\_\_

TOLERANCE UNLESS NOTED				TITLE:	
OPERATION	PLACES IN DIMENSION			AVIONICS BAY IMU MOUNTING BOARD	
	0.0	0.00	0.000	DRAWN	Oleksandr Dorotych
MACHINING	±0.050	±0.020	±0.005	DESIGNED	Nurettin Kaan Aslan
CUT OFF (SAW, BURN, SHEAR)	±0.1	±0.060		SIZE	DWG. NO.
WELDING	±0.1	±0.060		<b>A</b>	
ANGULAR DIMS	±5	±2	±0.5	SCALE: 1:2	SHEET 1 OF 1

5

4

3

2

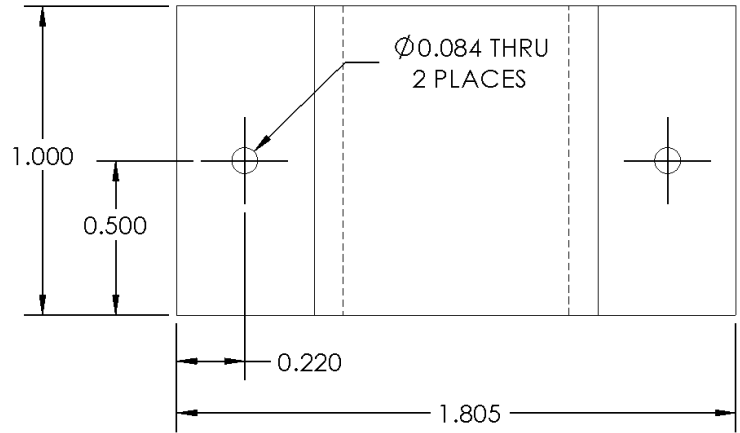
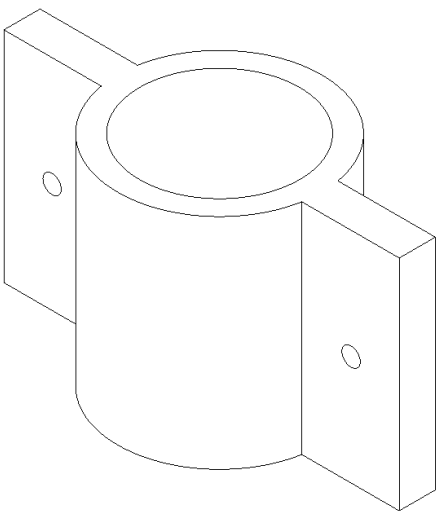
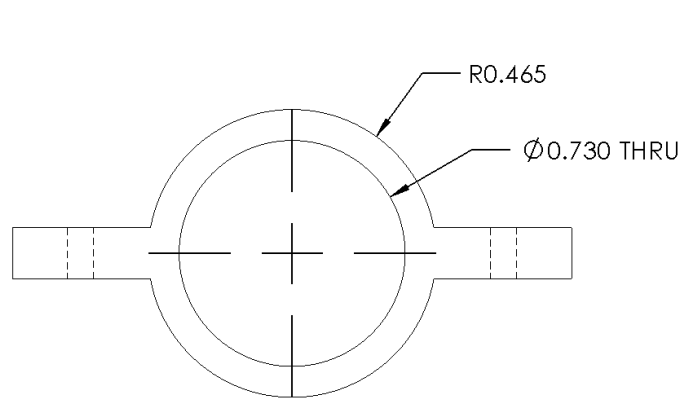
1

**Dimensions:**  
 Front View: 3.156 (total length), 0.180 (top thickness),  $\text{Ø}1.836$  (outer diameter), R0.1 (fillet).  
 Angled View: 1.754, 1.627, 1.500, 1.374, 0.500, 0.190,  $\text{Ø}0.933 \nabla 1.550$ ,  $\text{Ø}0.116$  THRU 2 PLACES, 45.0°.

**Notes:**  
 1. DIMS IN INCHES  
 2. QTY: 1  
 3. MATL: PET  
 4. \_\_\_\_\_  
 5. \_\_\_\_\_

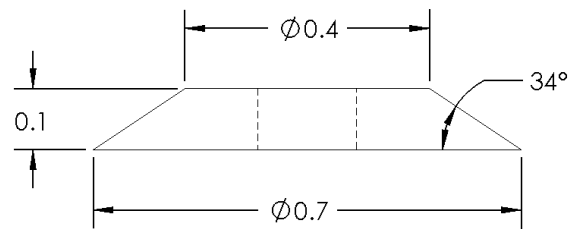
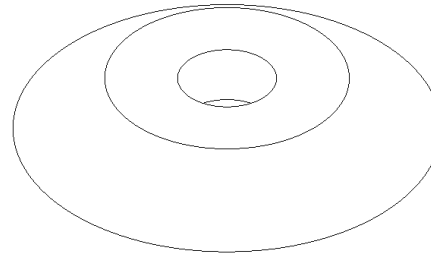
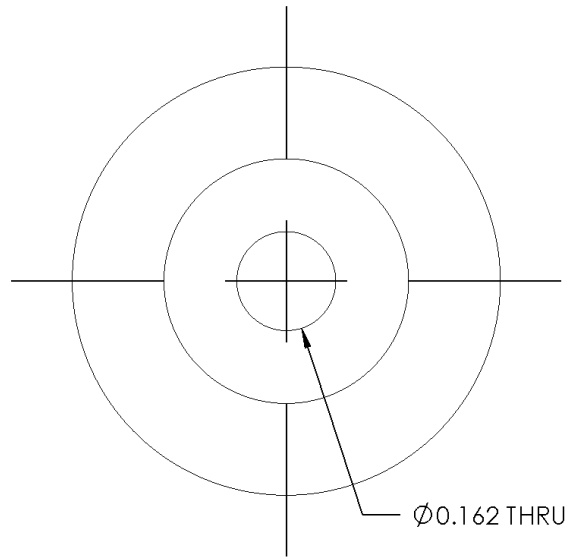
OPERATION	TOLERANCE UNLESS NOTED			TITLE:	
	PLACES IN DIMENSION			AVIONICS BAY KEY SWITCH HOLDER	
	0.0	0.00	0.000	DRAWN	Oleksandr Dorotych
MACHINING	±0.050	±0.020	±0.005	DESIGNED	Nurettin Kaan Aslan
CUT OFF (SAW, BURN, SHEAR)	±0.1	±0.060		SIZE	DWG. NO. <span style="border: 1px solid black; padding: 2px;"> </span>
WELDING	±0.1	±0.060		<b>A</b>	<b>A</b>
ANGULAR DIMS	±5	±2	±0.5	SCALE: 1:1.25	

SHEET 1 OF 1



- NOTES:  
1. DIMS IN INCHES  
2. QTY: 2  
3. MATL: PET  
4. \_\_\_\_\_  
5. \_\_\_\_\_

TOLERANCE UNLESS NOTED			TITLE:		
OPERATION	PLACES IN DIMENSION			AVIONICS BAY KEY SWITCH MOUNT	
	0.0	0.00	0.000	DRAWN	DRAWER'S NAME
MACHINING	±0.050	±0.020	±0.005	DESIGNED	DESIGNER'S NAME
CUT OFF (SAW, BURN, SHEAR)	±0.1	±0.060		SIZE	DWG. NO. <span style="float: right;">REV</span>
WELDING	±0.1	±0.060		<b>A</b>	<input checked="" type="checkbox"/> <b>A</b>
ANGULAR DIMS	±5	±2	±0.5	SCALE: 2:1	SHEET 1 OF 1



- NOTES:  
 1. DIMS IN INCHES  
 2. QTY: 4  
 3. MATL: PET  
 4. \_\_\_\_\_  
 5. \_\_\_\_\_

TOLERANCE UNLESS NOTED				TITLE:	
OPERATION	PLACES IN DIMENSION			AVIONICS BAY STRATOLOGGER RAISER	
	0.0	0.00	0.000	DRAWN	Oleksandr Dorotych
MACHINING	±0.050	±0.020	±0.005	DESIGNED	Nurettin Kaan Aslan
CUT OFF (SAW, BURN, SHEAR)	±0.1	±0.060		SIZE	DWG. NO.
WELDING	±0.1	±0.060		<b>A</b>	<input checked="" type="checkbox"/>
ANGULAR DIMS	±5	±2	±0.5	SCALE: 4:1	SHEET 1 OF 1

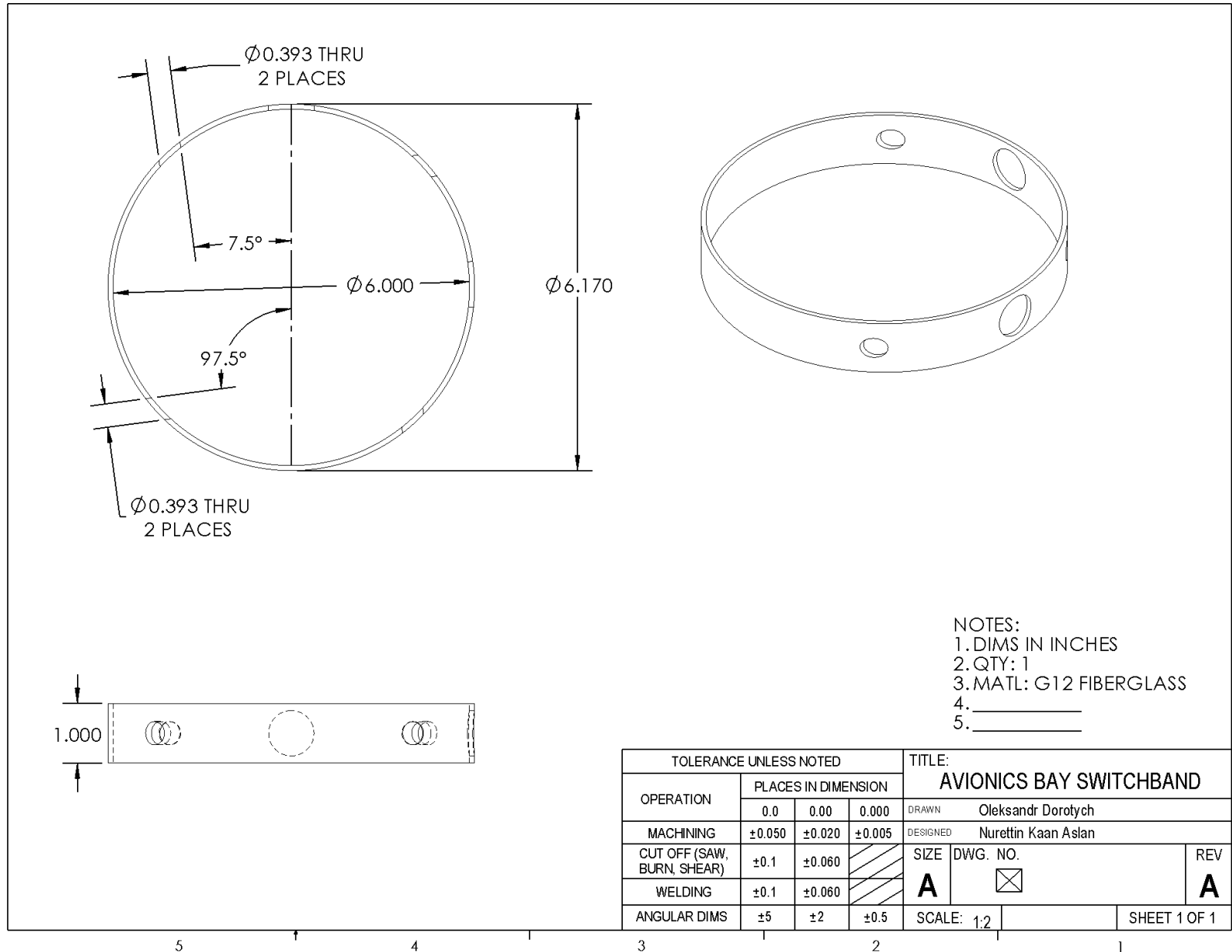
5

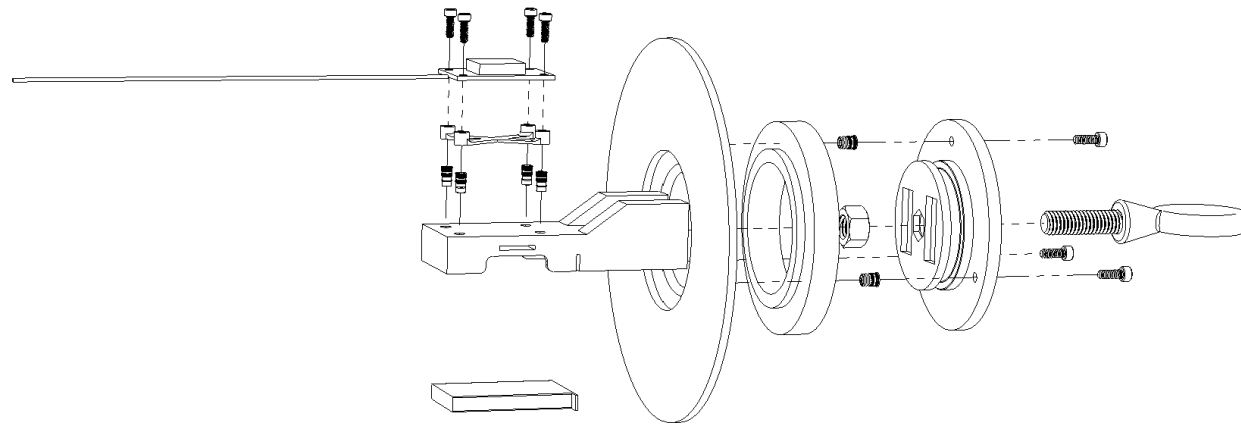
4

3

2

1





TITLE:  
TeleGPS nose cone mount assembly

DRAWN Griffin Martin

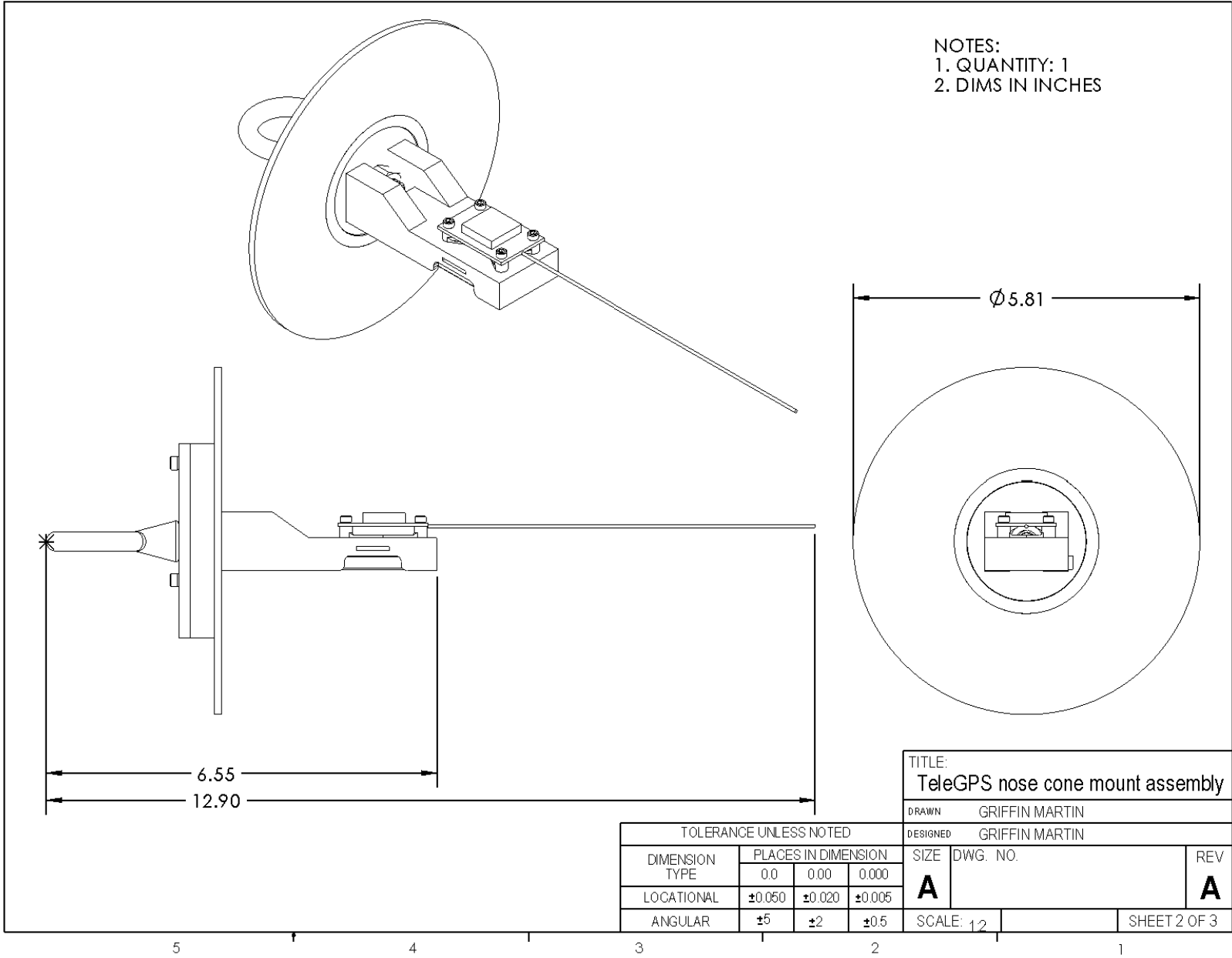
DESIGNED Griffin Martin

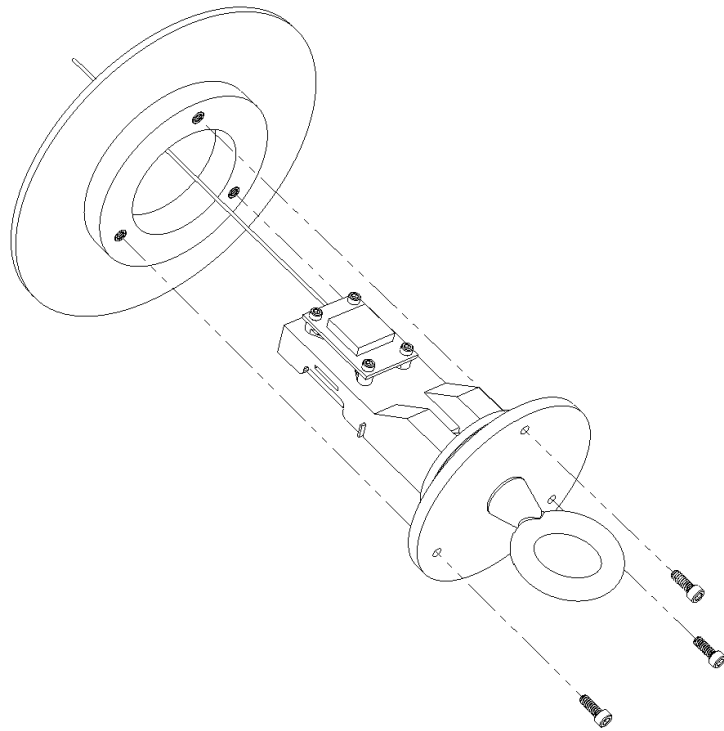
TOLERANCE UNLESS NOTED				SIZE	DWG. NO.	REV
DIMENSION TYPE	0.0	0.00	0.000			
LOCATIONAL	±0.050	±0.020	±0.005	<b>A</b>		<b>A</b>
ANGULAR	±5	±2	±0.5			

SCALE: 1:2

SHEET 1 OF 3

5 4 3 2 1





TOLERANCE UNLESS NOTED				TITLE:	
OPERATION	PLACES IN DIMENSION			TeleGPS nose cone mount assembly	
	0.0	0.00	0.000	DRAWN	GRIFFIN MARTIN
MACHINING	±0.050	±0.020	±0.005	DESIGNED	GRIFFIN MARTIN
CUT OFF (SAW, BURN, SHEAR)	±0.1	±0.060		SIZE	DWG. NO.
WELDING	±0.1	±0.060		<b>A</b>	<b>A</b>
ANGULAR DIMS	±5	±2	±0.5	SCALE: 1:2	SHEET 3 OF 3

5

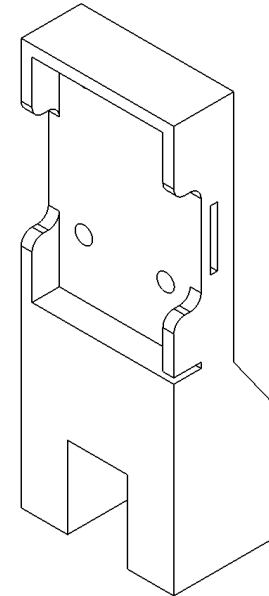
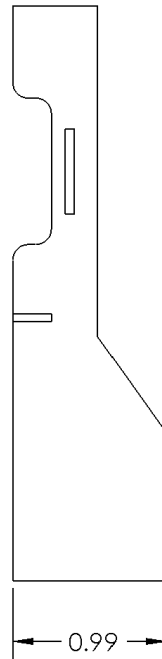
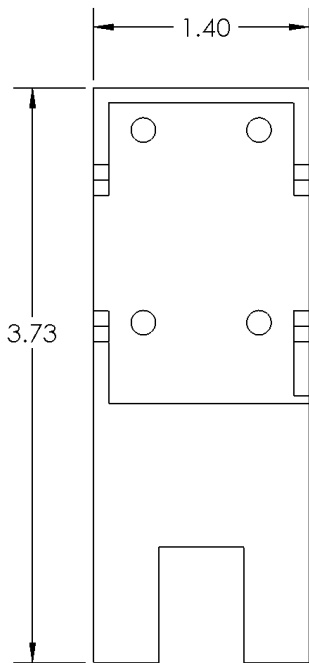
4

3

2

1





NOTES:  
 1. QUANTITY: 1  
 2. MAT'L: PETG  
 3. ALL DIMS IN INCHES

TOLERANCE UNLESS NOTED				TITLE: Electronics Mount	
OPERATION	PLACES IN DIMENSION			DRAWN: GRIFFIN MARTIN	
		0.0	0.00	0.000	DESIGNED: GAVIN GAMBLE
MACHINING	±0.050	±0.020	±0.005	SIZE DWG. NO.	
CUT OFF (SAW, BURN, SHEAR)	±0.1	±0.060	//	<b>A</b>	REV <b>A</b>
WELDING	±0.1	±0.060	//		
ANGULAR DIMS	±5	±2	±0.5	SCALE: 1:1	

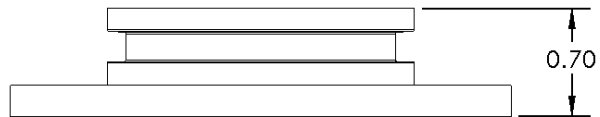
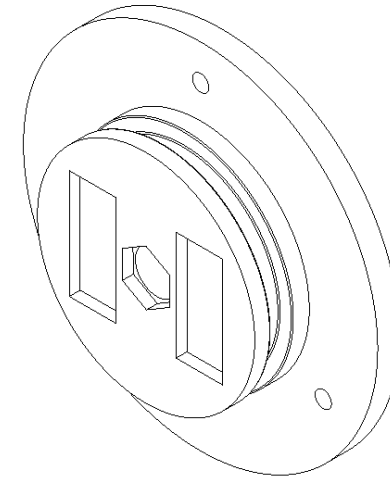
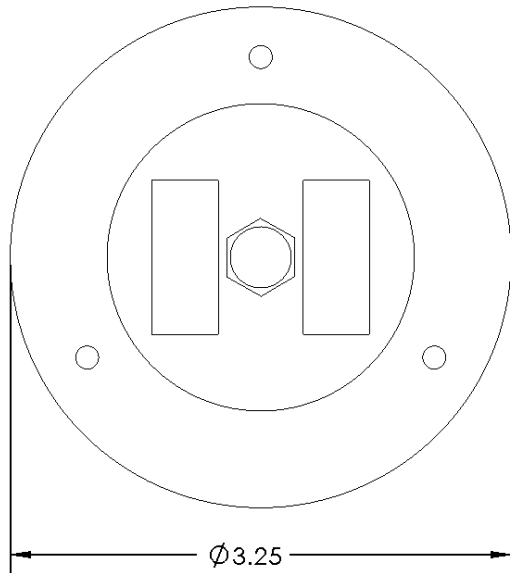
5

4

3

2

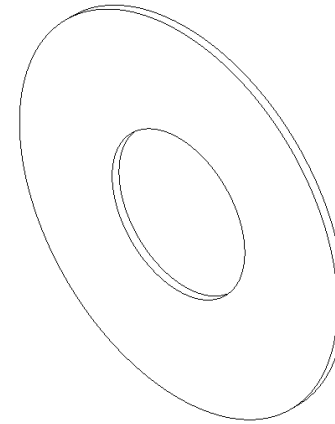
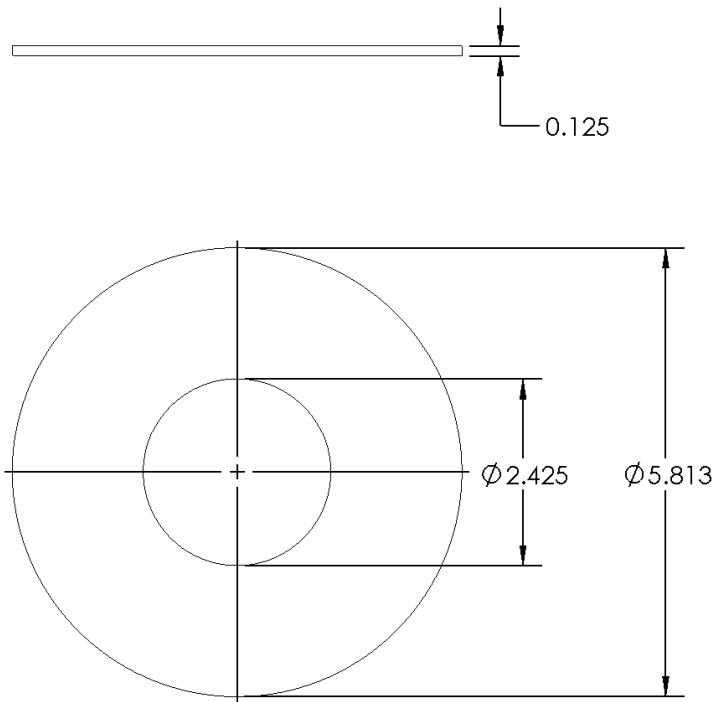
1



NOTES:  
 1. QUANTITY: 1  
 2. MAT'L: PETG  
 3. ALL DIMS IN INCHES

TOLERANCE UNLESS NOTED				TITLE:	
OPERATION	PLACES IN DIMENSION			Nosecone Bulkhead	
	0.0	0.00	0.000	DRAWN	GRIFFIN MARTIN
MACHINING	±0.050	±0.020	±0.005	DESIGNED	GAVIN GAMBLE
CUT OFF (SAW, BURN, SHEAR)	±0.1	±0.060		SIZE	DWG. NO.
WELDING	±0.1	±0.060		<b>A</b>	<b>A</b>
ANGULAR DIMS	±5	±2	±0.5	SCALE: 1:1	SHEET 1 OF 1

5 4 3 2 1



- NOTES:  
 1. QUANTITY: 1  
 2. MAT'L: FIBERGLASS  
 3. ALL DIMS IN INCHES

TOLERANCE UNLESS NOTED				TITLE:	
OPERATION	PLACES IN DIMENSION			Nosecone Mounting Ring	
	0.0	0.00	0.000	DRAWN	GRIFFIN MARTIN
MACHINING	±0.050	±0.020	±0.005	DESIGNED	GRIFFIN MARTIN
CUT OFF (SAW, BURN, SHEAR)	±0.1	±0.060		SIZE	DWG. NO.
WELDING	±0.1	±0.060		<b>A</b>	<b>A</b>
ANGULAR DIMS	±5	±2	±0.5	SCALE: 1:2	SHEET 1 OF 1

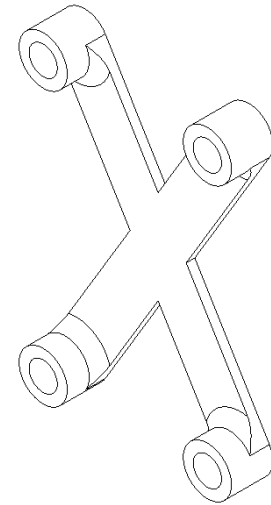
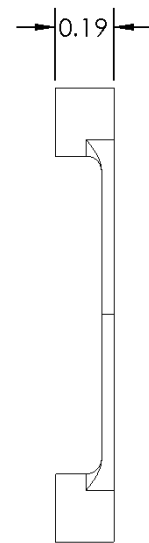
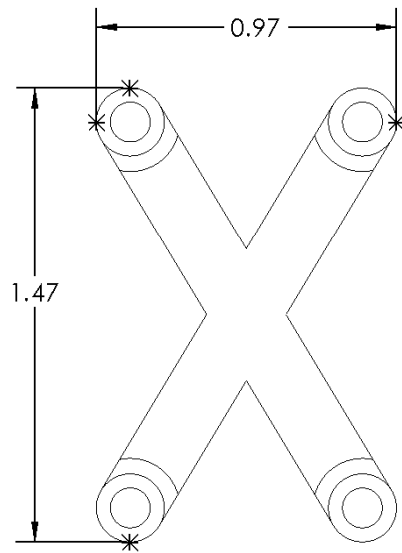
5

4

3

2

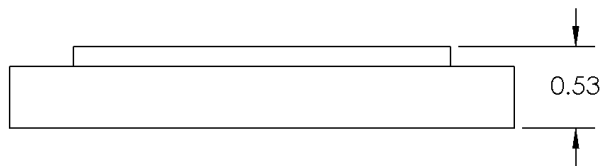
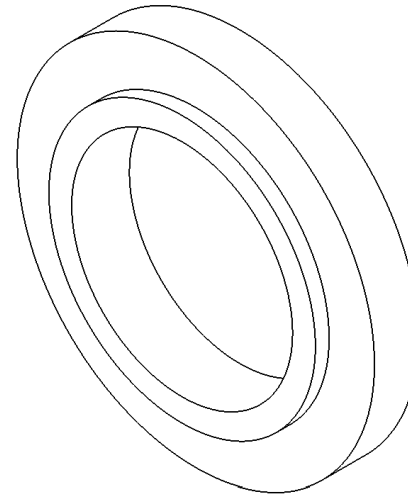
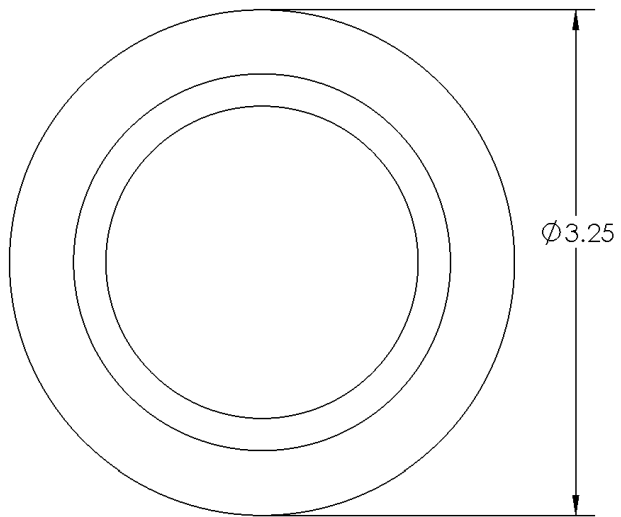
1



NOTES:  
 1. QUANTITY: 1  
 2. MAT'L: PETG  
 3. ALL DIMS IN INCHES

TOLERANCE UNLESS NOTED				TITLE: TeleGPS standoff	
OPERATION	PLACES IN DIMENSION			DRAWN	GRIFFIN MARTIN
	MACHINING	±0.050	±0.020	±0.005	DESIGNED
CUT OFF (SAW, BURN, SHEAR)	±0.1	±0.060		SIZE	DWG. NO.
WELDING	±0.1	±0.060		<b>A</b>	<b>A</b>
ANGULAR DIMS	±5	±2	±0.5	SCALE: 2:1	SHEET 1 OF 1

5 4 3 2 1



- NOTES:  
 1. QUANTITY: 1  
 2. MAT'L: PETG  
 3. ALL DIMS IN INCHES

TOLERANCE UNLESS NOTED				TITLE:	
OPERATION	PLACES IN DIMENSION			Inner Mounting Ring	
	0.0	0.00	0.000	DRAWN	GRIFFIN MARTIN
MACHINING	±0.050	±0.020	±0.005	DESIGNED	GRIFFIN MARTIN
CUT OFF (SAW, BURN, SHEAR)	±0.1	±0.060		SIZE	DWG. NO.
WELDING	±0.1	±0.060		<b>A</b>	<b>A</b>
ANGULAR DIMS	±5	±2	±0.5	SCALE: 1:1	SHEET 1 OF 1

5

↑

4

↑

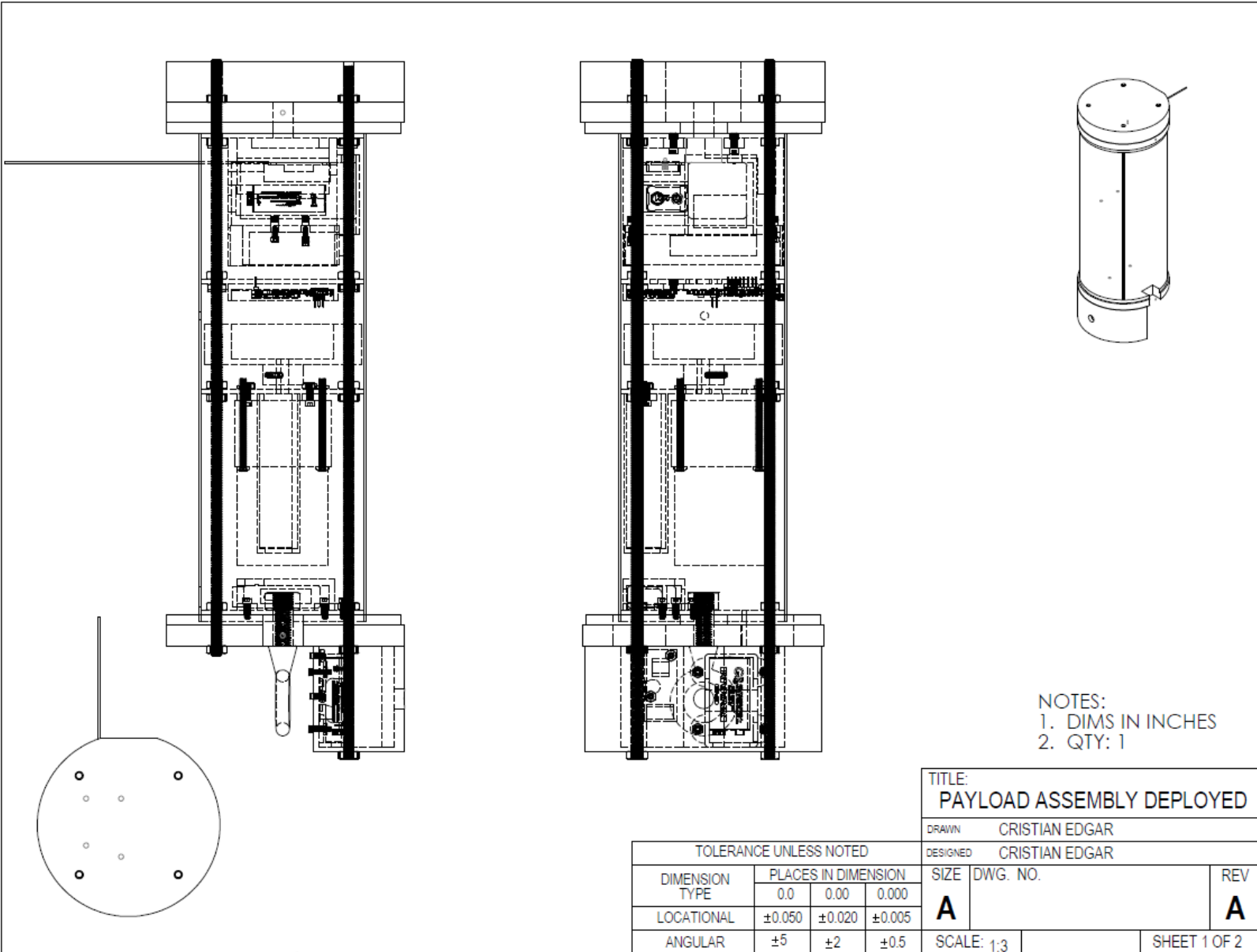
3

↑

2

↑

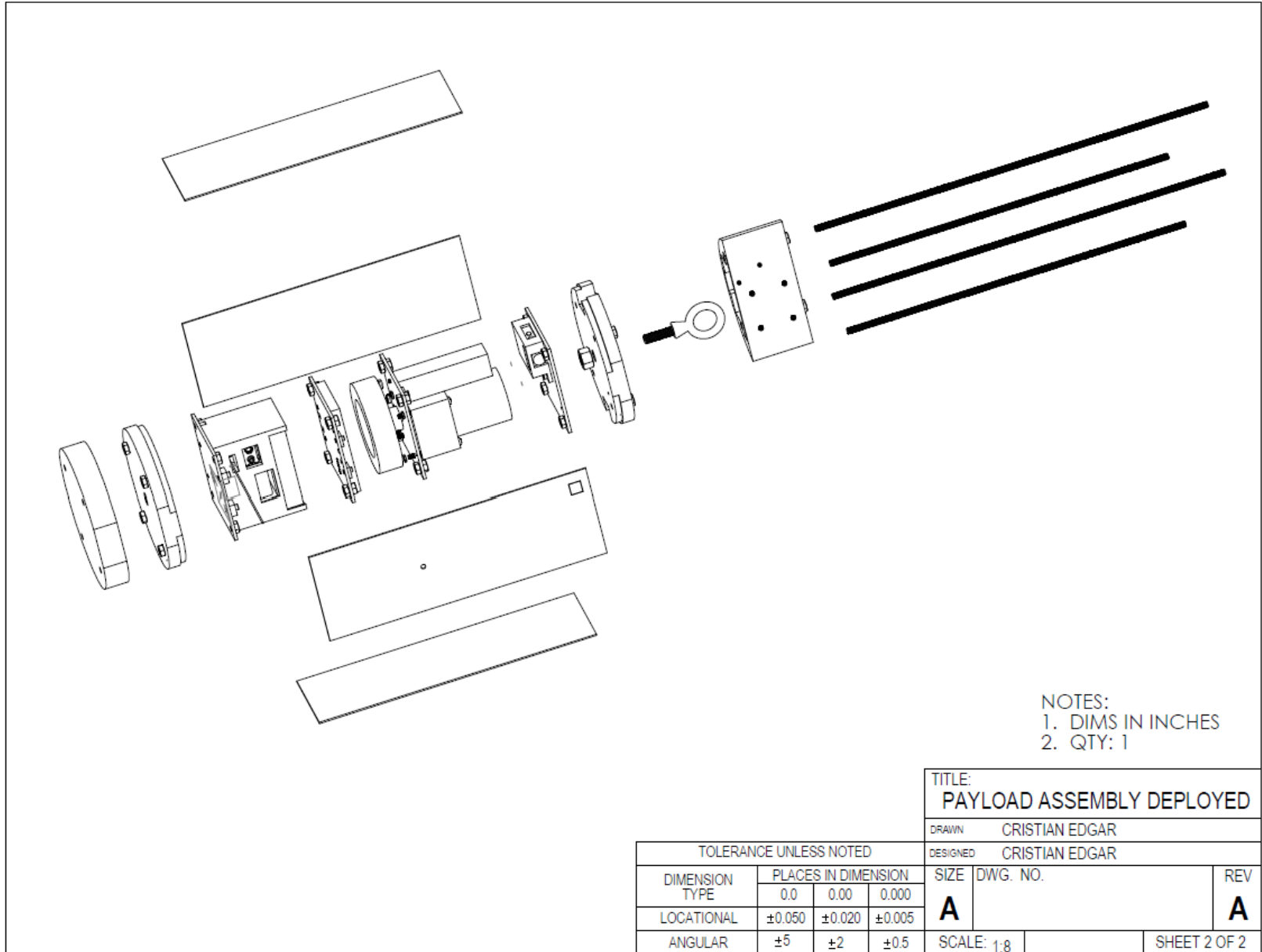
1



NOTES:  
 1. DIMS IN INCHES  
 2. QTY: 1

TITLE: <b>PAYLOAD ASSEMBLY DEPLOYED</b>			
DRAWN		CRISTIAN EDGAR	
DESIGNED		CRISTIAN EDGAR	
DIMENSION TYPE	PLACES IN DIMENSION	SIZE	DWG. NO.
	0.0 0.00 0.000	<b>A</b>	
LOCATIONAL	±0.050 ±0.020 ±0.005		
ANGULAR	±5 ±2 ±0.5	SCALE: 1:3	REV <b>A</b>
			SHEET 1 OF 2

SOLIDWORKS Educational Product. For Instructional Use Only.



NOTES:  
 1. DIMS IN INCHES  
 2. QTY: 1

TITLE:  
**PAYLOAD ASSEMBLY DEPLOYED**

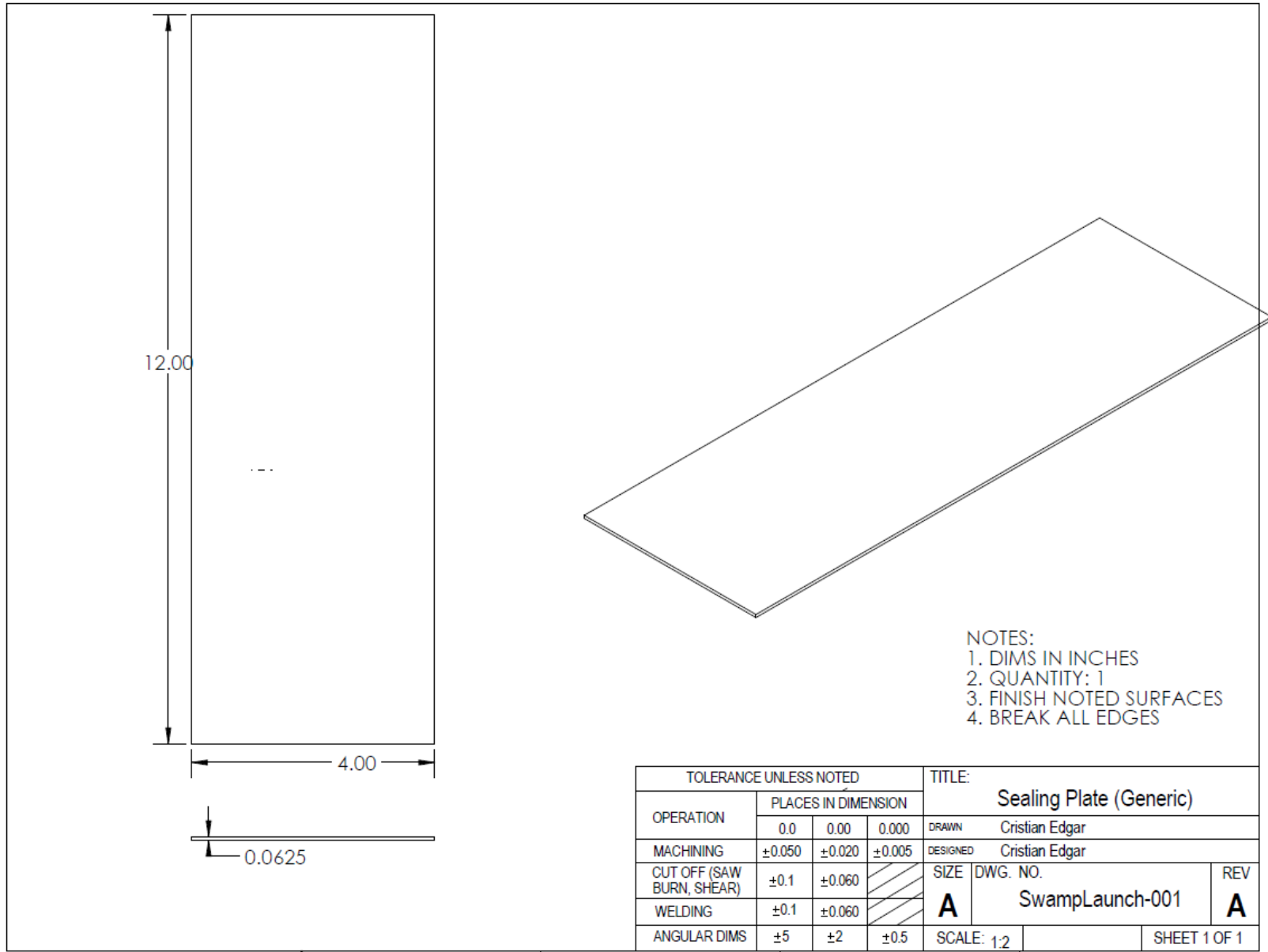
DRAWN CRISTIAN EDGAR

DESIGNED CRISTIAN EDGAR

TOLERANCE UNLESS NOTED			
DIMENSION TYPE	PLACES IN DIMENSION		
	0.0	0.00	0.000
LOCATIONAL	±0.050	±0.020	±0.005
ANGULAR	±5	±2	±0.5

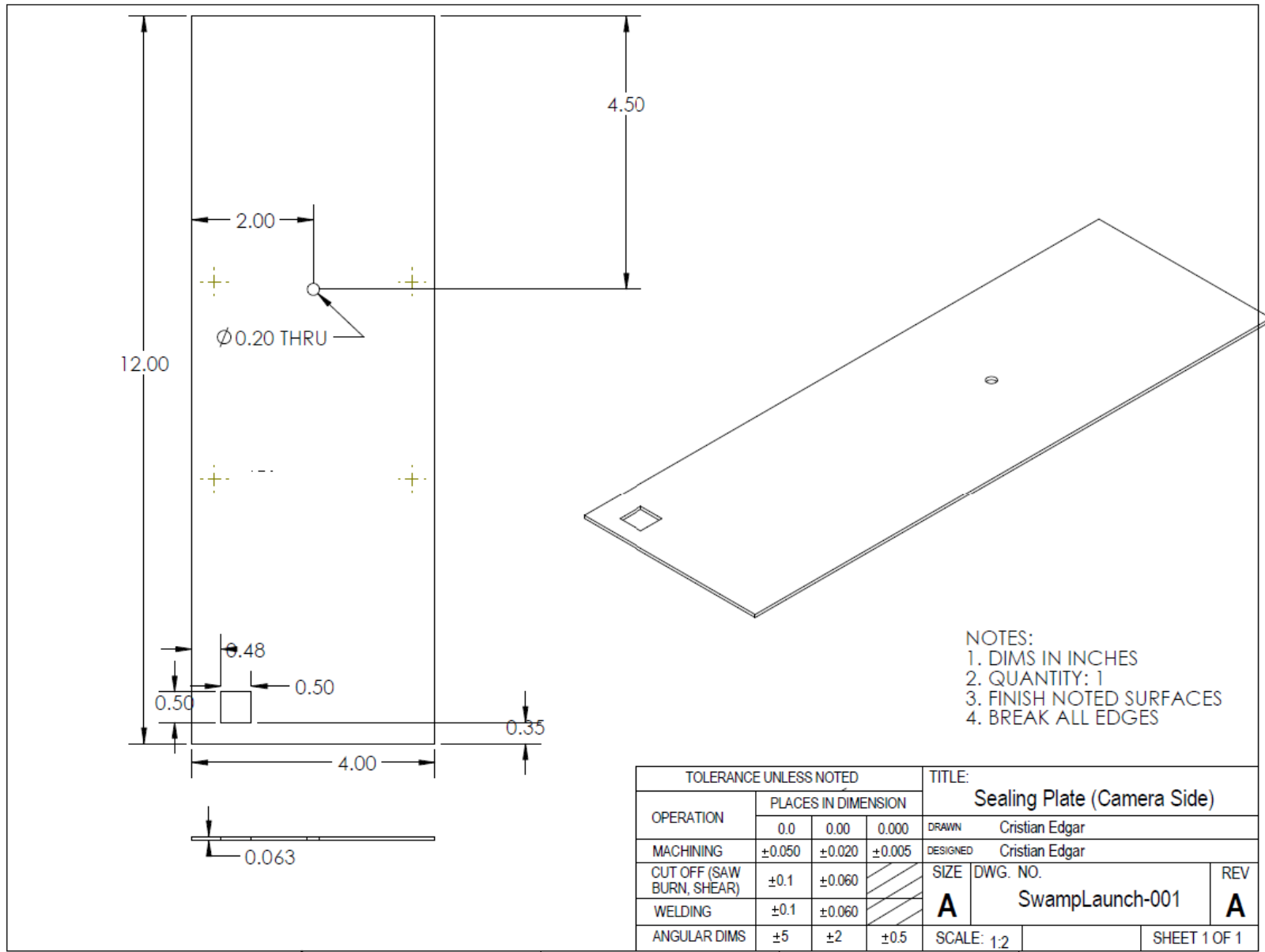
SIZE	DWG. NO.	REV
<b>A</b>		<b>A</b>

SCALE: 1:8 SHEET 2 OF 2



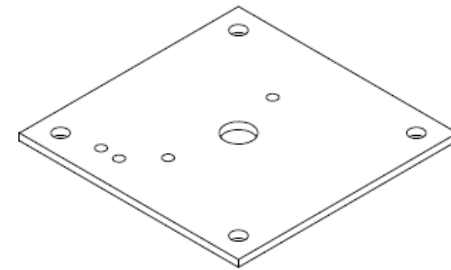
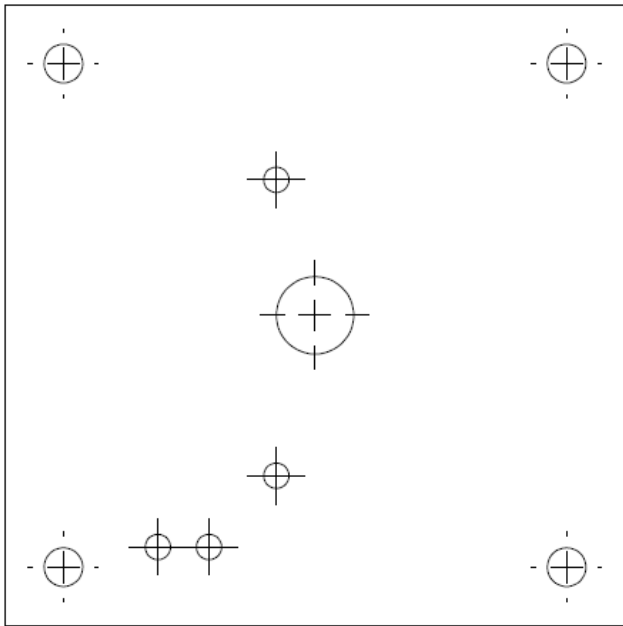
SOLIDWORKS Educational Product. For Instructional Use Only.





TOLERANCE UNLESS NOTED				TITLE:	
OPERATION	PLACES IN DIMENSION			Sealing Plate (Camera Side)	
	0.0	0.00	0.000	DRAWN	Cristian Edgar
MACHINING	±0.050	±0.020	±0.005	DESIGNED	Cristian Edgar
CUT OFF (SAW BURN, SHEAR)	±0.1	±0.060		SIZE	DWG. NO.
WELDING	±0.1	±0.060		<b>A</b>	SwampLaunch-001
ANGULAR DIMS	±5	±2	±0.5	SCALE: 1:2	SHEET 1 OF 1

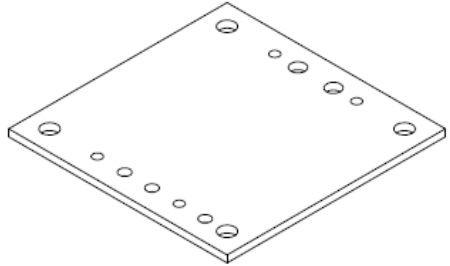
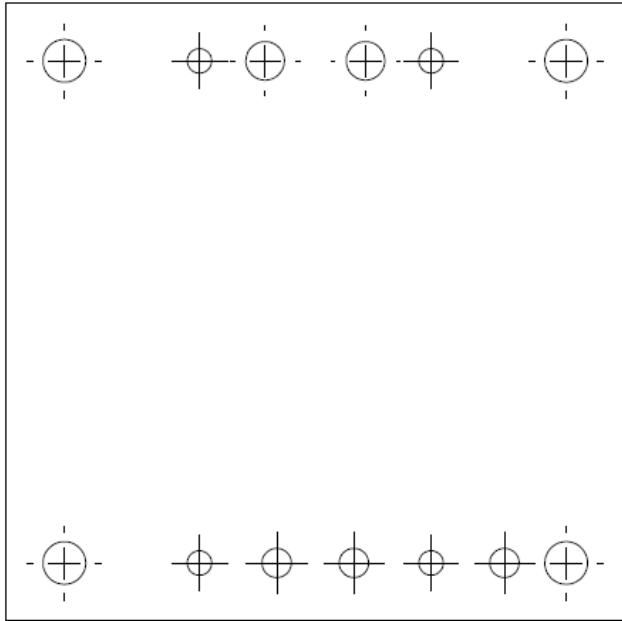
SOLIDWORKS Educational Product. For Instructional Use Only.



ALL PLANAR GEOMETRY CUT  
USING ABRASIVE WATERJET

- NOTES:  
 1. DIMS IN INCHES  
 2. MATL: FRP  
 3. QTY: 1  
 4. BREAK ALL EDGES

TOLERANCE UNLESS NOTED				TITLE:	
OPERATION	PLACES IN DIMENSION			PAYLOAD TOP PLATE	
	0.0	0.00	0.000	DRAWN	JOSHUA CARSON
MACHINING	±0.050	±0.020	±0.005	DESIGNED	CRISTIAN EDGAR
CUT OFF (SAW, BURN, SHEAR)	±0.1	±0.060		SIZE	DWG. NO.
WELDING	±0.1	±0.060		<b>A</b>	<b>A</b>
ANGULAR DIMS	±5	±2	±0.5	SCALE: 1:1	SHEET 1 OF 1

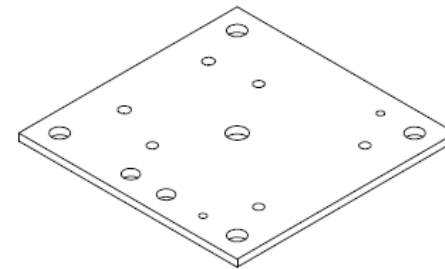
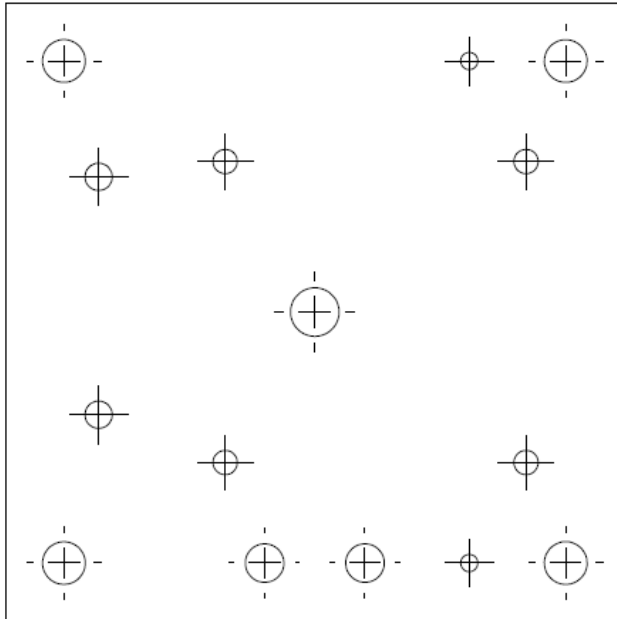


ALL PLANAR GEOMETRY CUT  
USING ABRASIVE WATERJET

- NOTES:  
 1. DIMS IN INCHES  
 2. QTY: 1  
 3. MATL: FRP  
 4. BREAK ALL EDGES

TOLERANCE UNLESS NOTED				TITLE:	
OPERATION	PLACES IN DIMENSION			PAYLOAD MIDDLE PLATE LOWER	
	0.0	0.00	0.000	DRAWN	JOSHUA CARSON
MACHINING	±0.050	±0.020	±0.005	DESIGNED	CRISTIAN EDGAR
CUT OFF (SAW, BURN, SHEAR)	±0.1	±0.060		SIZE	DWG. NO.
WELDING	±0.1	±0.060		<b>A</b>	<b>A</b>
ANGULAR DIMS	±5	±2	±0.5	SCALE: 1:1	SHEET 1 OF 1

SOLIDWORKS Educational Product. For Instructional Use Only.

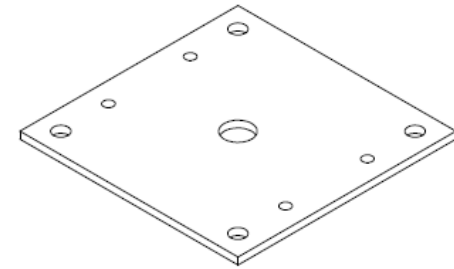
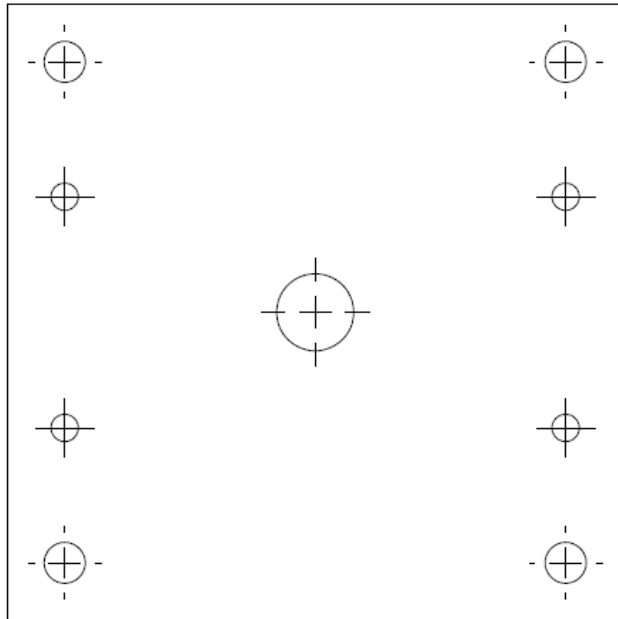


ALL PLANAR GEOMETRY CUT  
USING ABRASIVE WATERJET

- NOTES:  
 1. DIMS IN INCHES  
 2. MATL: FRP  
 3. QTY: 1  
 4. BREAK ALL EDGES

TOLERANCE UNLESS NOTED				TITLE: PAYLOAD MIDDLE PLATE UPPER		
OPERATION	PLACES IN DIMENSION			DRAWN	JOSHUA CARSON	
	0.0	0.00	0.000			
MACHINING	±0.050	±0.020	±0.005	DESIGNED	CRISTIAN EDGAR	
CUT OFF (SAW, BURN, SHEAR)	±0.1	±0.060		SIZE	DWG. NO.	REV
WELDING	±0.1	±0.060		<b>A</b>		<b>A</b>
ANGULAR DIMS	±5	±2	±0.5	SCALE: 1:1		SHEET 1 OF 1

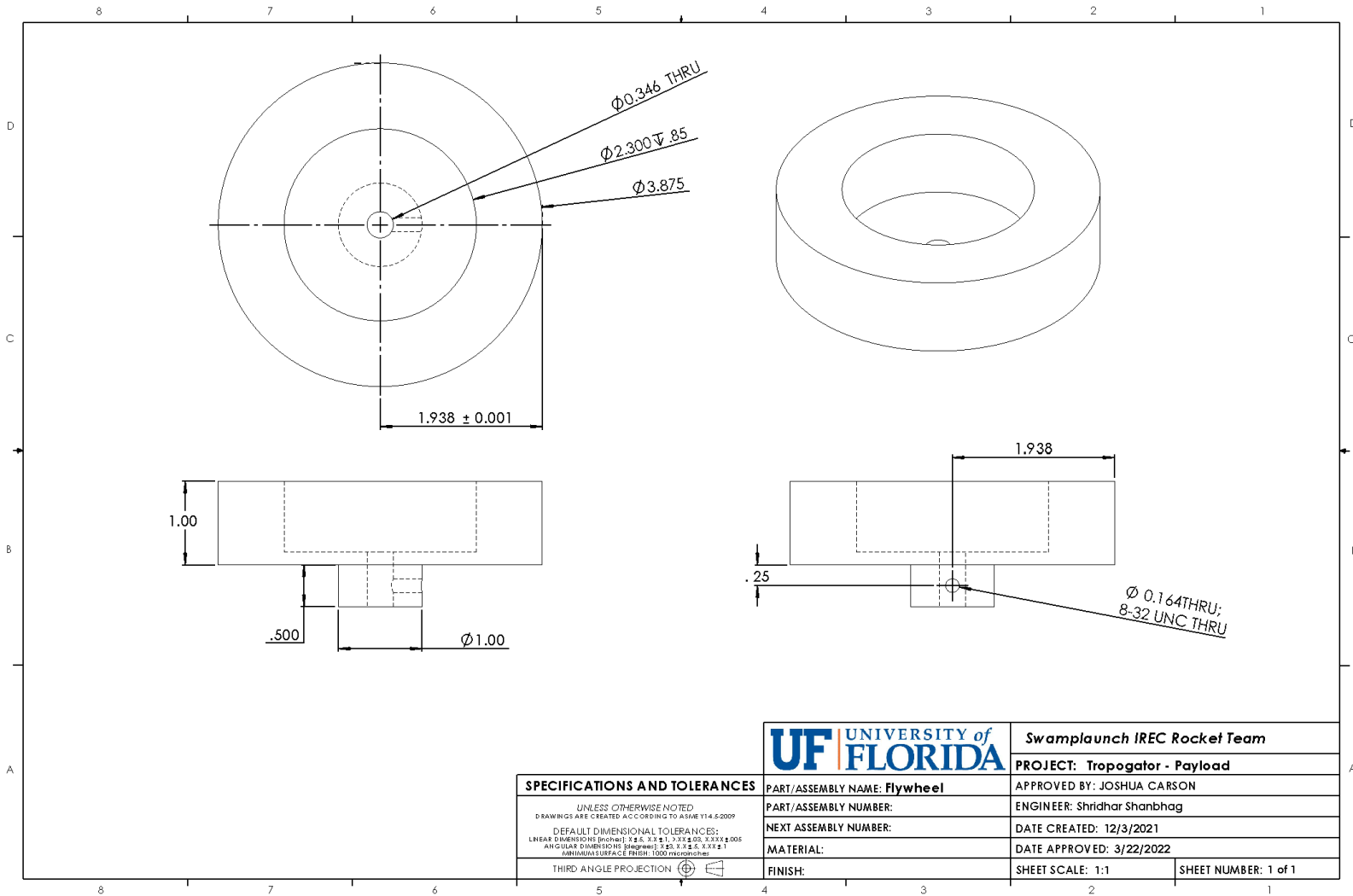
SOLIDWORKS Educational Product. For Instructional Use Only.



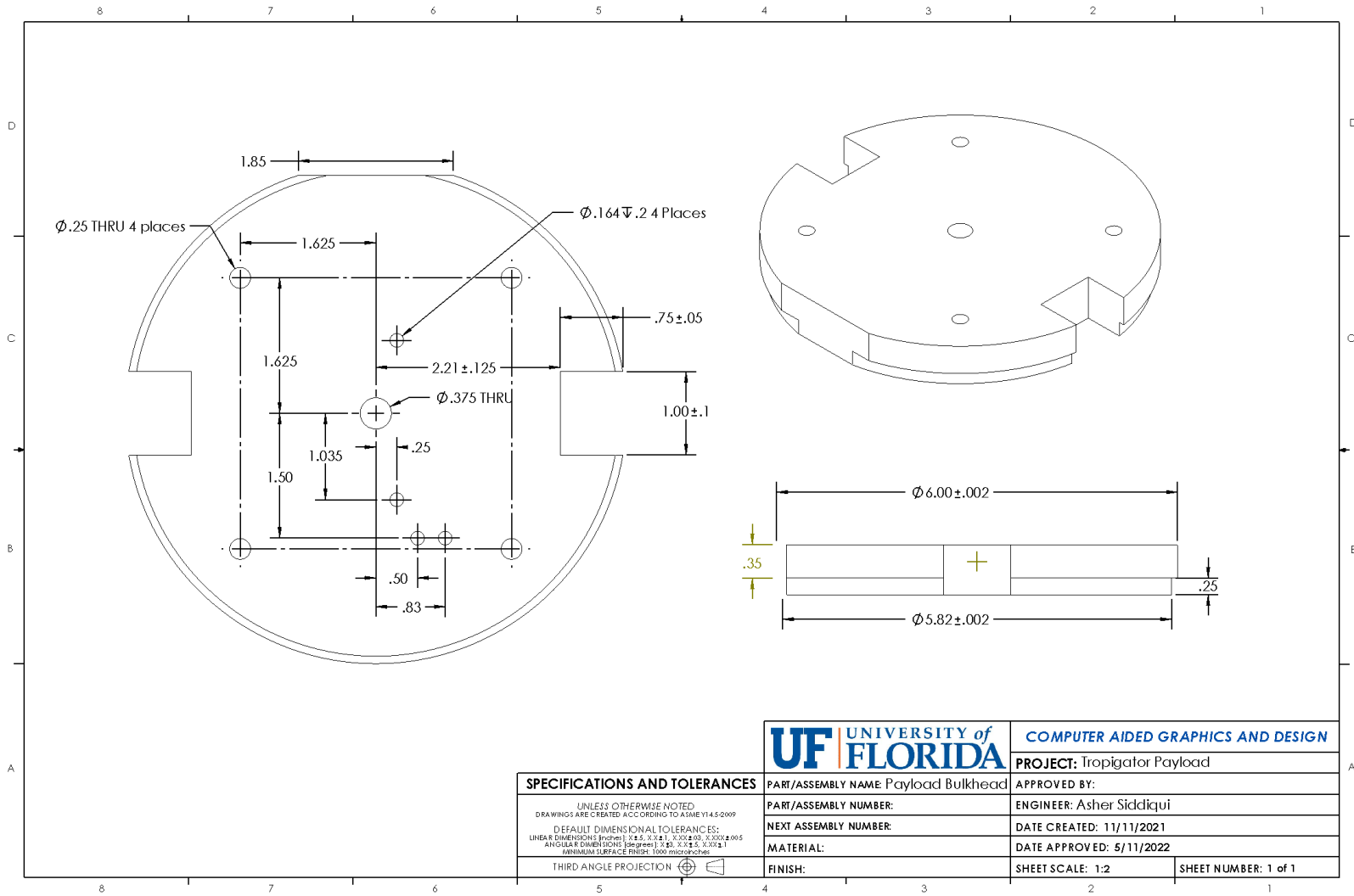
ALL PLANAR FEATURES CUT  
USING ABRASIVE WATERJET

- NOTES:  
 1. DIMS IN INCHES  
 2. MATL: FRP  
 3. QTY: 1  
 4. BREAK ALL EDGES

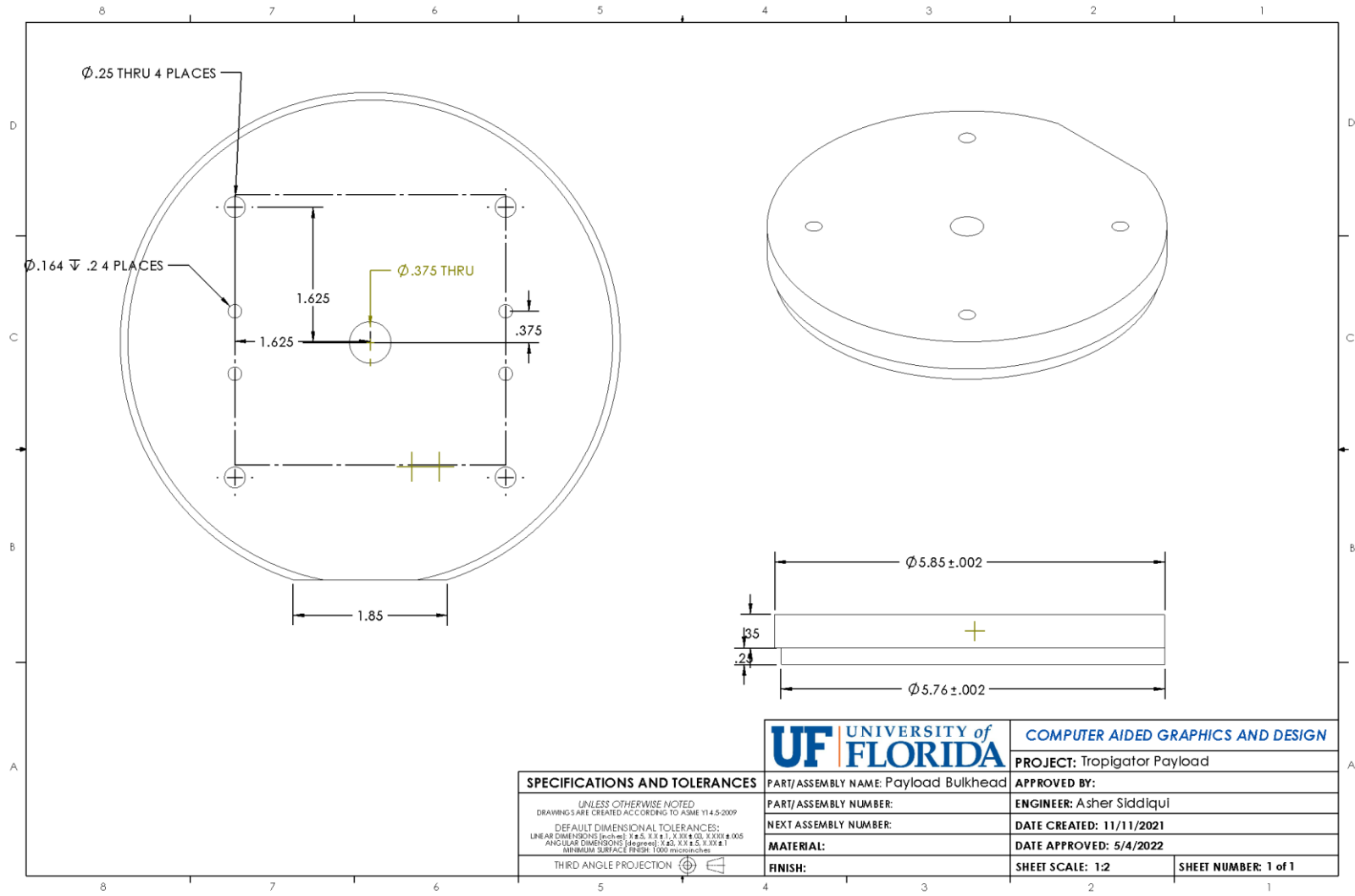
TOLERANCE UNLESS NOTED				TITLE:	
OPERATION	PLACES IN DIMENSION			PAYLOAD BOTTOM PLATE	
	0.0	0.00	0.000	DRAWN	JOSHUA CARSON
MACHINING	±0.050	±0.020	±0.005	DESIGNED	CRISTIAN EDGAR
CUT OFF (SAW, BURN, SHEAR)	±0.1	±0.060		SIZE	DWG. NO.
WELDING	±0.1	±0.060		<b>A</b>	<b>A</b>
ANGULAR DIMS	±5	±2	±0.5	SCALE: 1:1	SHEET 1 OF 1



<b>SPECIFICATIONS AND TOLERANCES</b> <small>UNLESS OTHERWISE NOTED  DRAWINGS ARE CREATED ACCORDING TO ASME Y14.5-2009</small> <small>DEFAULT DIMENSIONAL TOLERANCES:  LINEAR DIMENSIONS (inch): X.X ± .1, X.XX ± .05, X.XXX ± .005  ANGULAR DIMENSIONS (degrees): X.XX ± .1  MINIMUM SURFACE FINISH: 1000 microinches</small> <small>THIRD ANGLE PROJECTION</small>	<b>UNIVERSITY of FLORIDA</b> Swamplaunch IREC Rocket Team
	PROJECT: Tropogator - Payload
PART/ASSEMBLY NAME: Flywheel	APPROVED BY: JOSHUA CARSON
PART/ASSEMBLY NUMBER:	ENGINEER: Shridhar Shanbhag
NEXT ASSEMBLY NUMBER:	DATE CREATED: 12/3/2021
MATERIAL:	DATE APPROVED: 3/22/2022
FINISH:	SHEET SCALE: 1:1
	SHEET NUMBER: 1 of 1



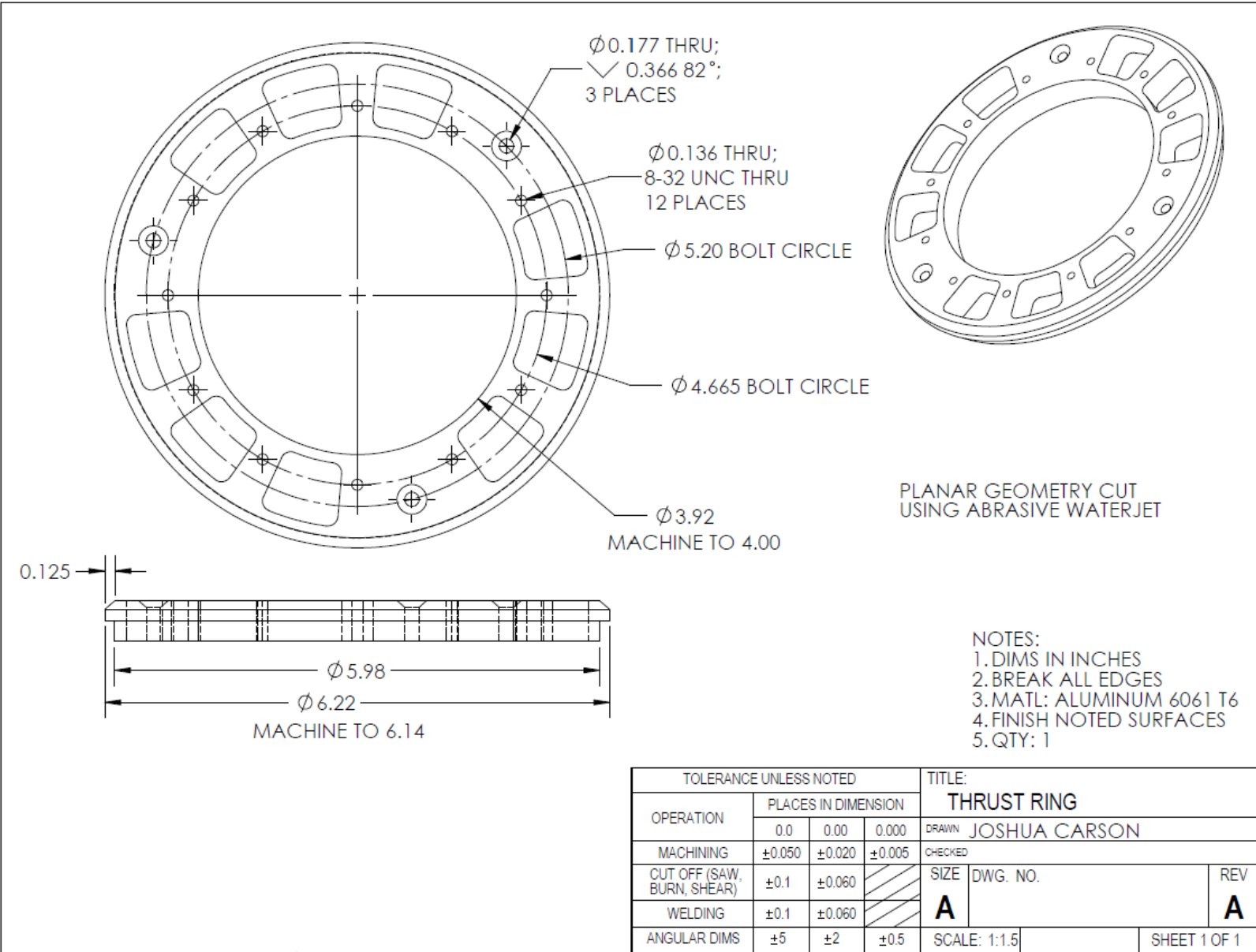
<b>SPECIFICATIONS AND TOLERANCES</b>	<small>UNLESS OTHERWISE NOTED DRAWINGS ARE CREATED ACCORDING TO ASME Y14.5-2009</small> <small>DEFAULT DIMENSIONAL TOLERANCES: LINEAR DIMENSIONS (Inches): X <math>\pm</math> .5, X <math>\pm</math> .1, X <math>\pm</math> .05, X <math>\pm</math> .02, X <math>\pm</math> .002 <math>\pm</math> .005 ANGULAR DIMENSIONS (Degrees): X <math>\pm</math> .5, X <math>\pm</math> .1 MINIMUM SURFACE FINISH: 1000 microinches</small>	<b>UF UNIVERSITY of FLORIDA</b>	<b>COMPUTER AIDED GRAPHICS AND DESIGN</b>
		<b>PART/ASSEMBLY NAME:</b> Payload Bulkhead	<b>PROJECT:</b> Tropigator Payload
	<b>PART/ASSEMBLY NUMBER:</b>	<b>APPROVED BY:</b>	
	<b>NEXT ASSEMBLY NUMBER:</b>	<b>ENGINEER:</b> Asher Siddiqui	
	<b>MATERIAL:</b>	<b>DATE CREATED:</b> 11/11/2021	
<b>THIRD ANGLE PROJECTION</b>	<b>FINISH:</b>	<b>DATE APPROVED:</b> 5/11/2022	
		<b>SHEET SCALE:</b> 1:2	<b>SHEET NUMBER:</b> 1 of 1



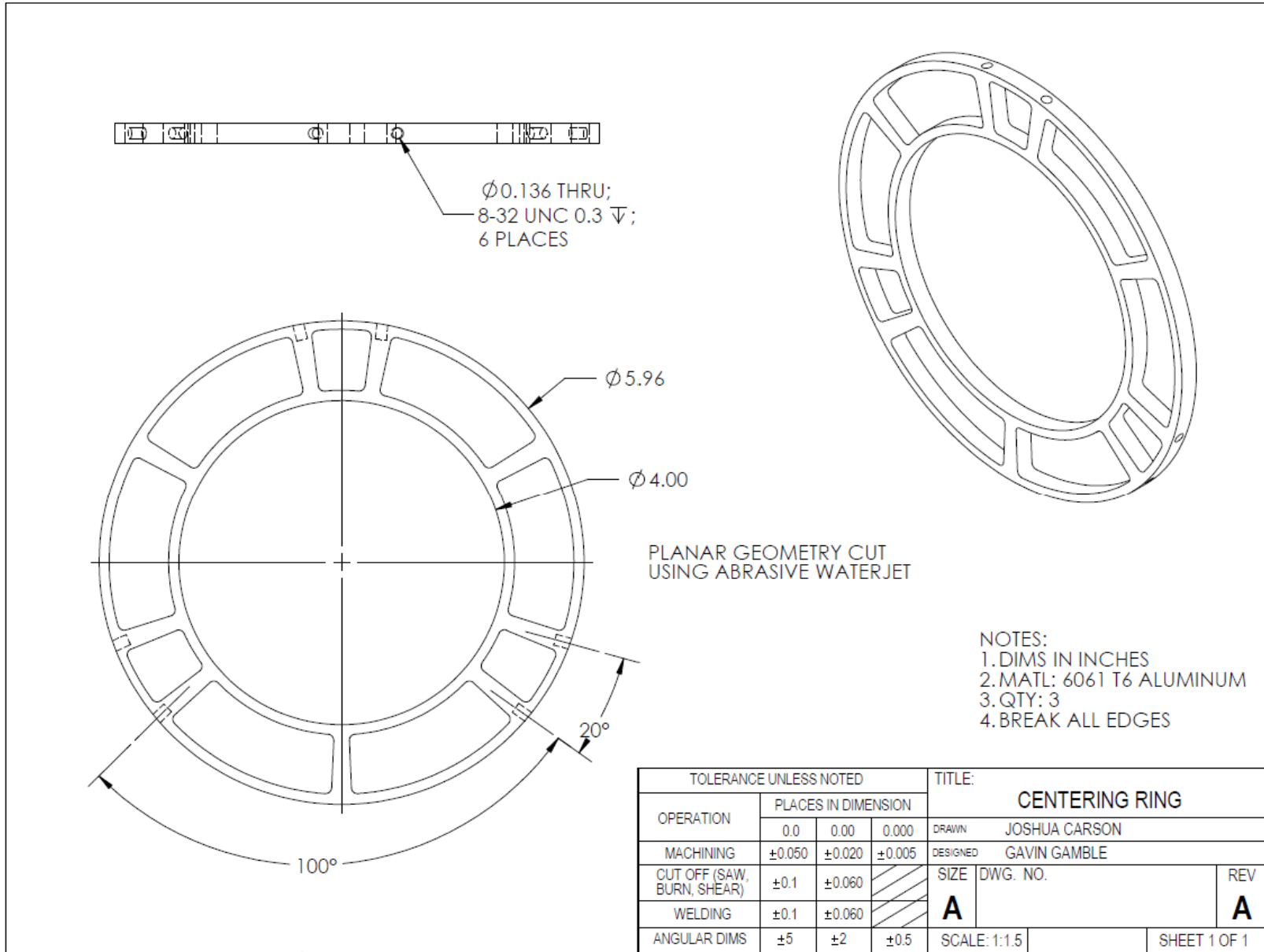
**SPECIFICATIONS AND TOLERANCES**  
 UNLESS OTHERWISE NOTED  
 DRAWINGS ARE CREATED ACCORDING TO: ASME Y14.5-2009  
 DEFAULT DIMENSIONAL TOLERANCES:  
 LINEAR DIMENSIONS (inches): X.X ± .1, X.XX ± .01, X.XXX ± .005  
 ANGULAR DIMENSIONS (degrees): X ± .5, X.X ± .1  
 MINIMUM SURFACE FINISH: 1000 microinches

	COMPUTER AIDED GRAPHICS AND DESIGN	
	PROJECT: Tropigator Payload	
PART/ASSEMBLY NAME: Payload Bulkhead	APPROVED BY:	
PART/ASSEMBLY NUMBER:	ENGINEER: Asher Siddiqui	
NEXT ASSEMBLY NUMBER:	DATE CREATED: 11/11/2021	
MATERIAL:	DATE APPROVED: 5/4/2022	
THIRD ANGLE PROJECTION	FINISH:	SHEET SCALE: 1:2
		SHEET NUMBER: 1 of 1

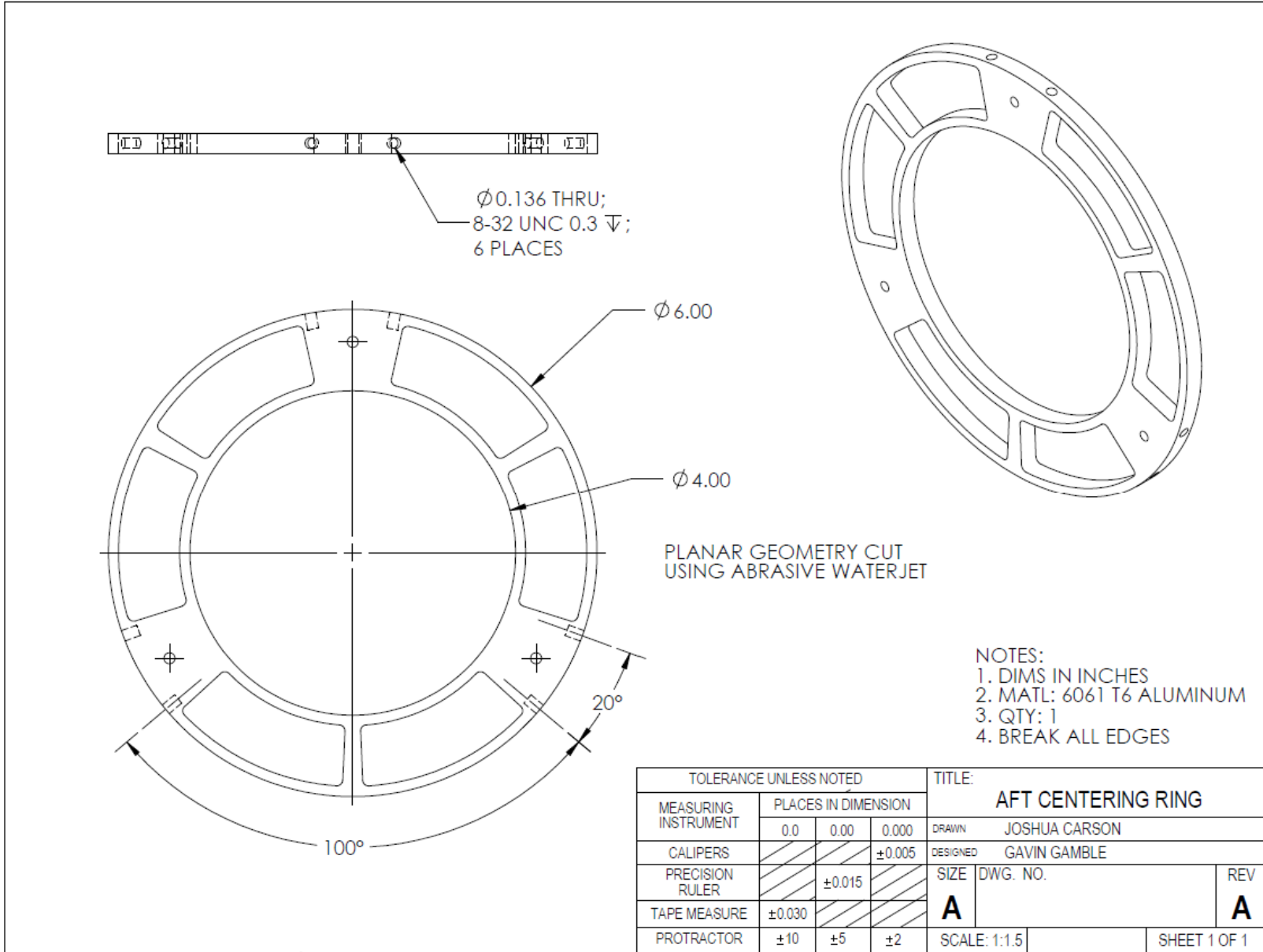




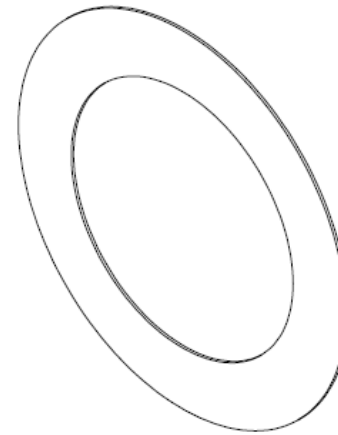
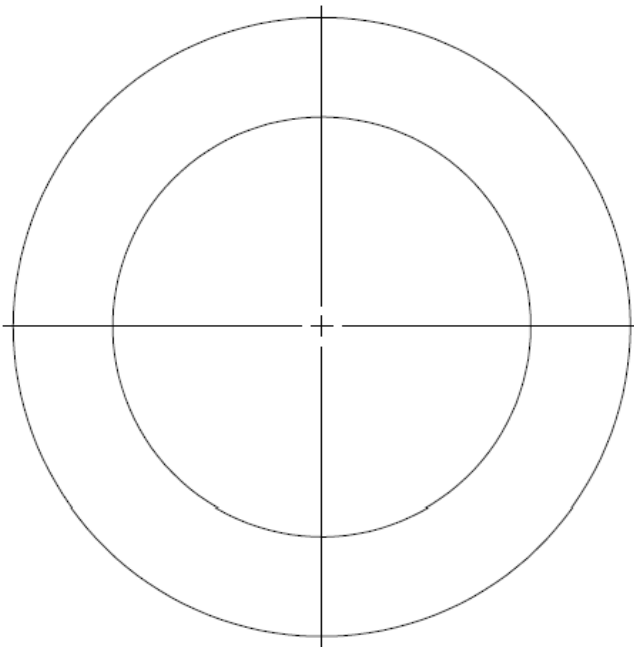
SOLIDWORKS Educational Product. For Instructional Use Only.



SOLIDWORKS Educational Product. For Instructional Use Only.



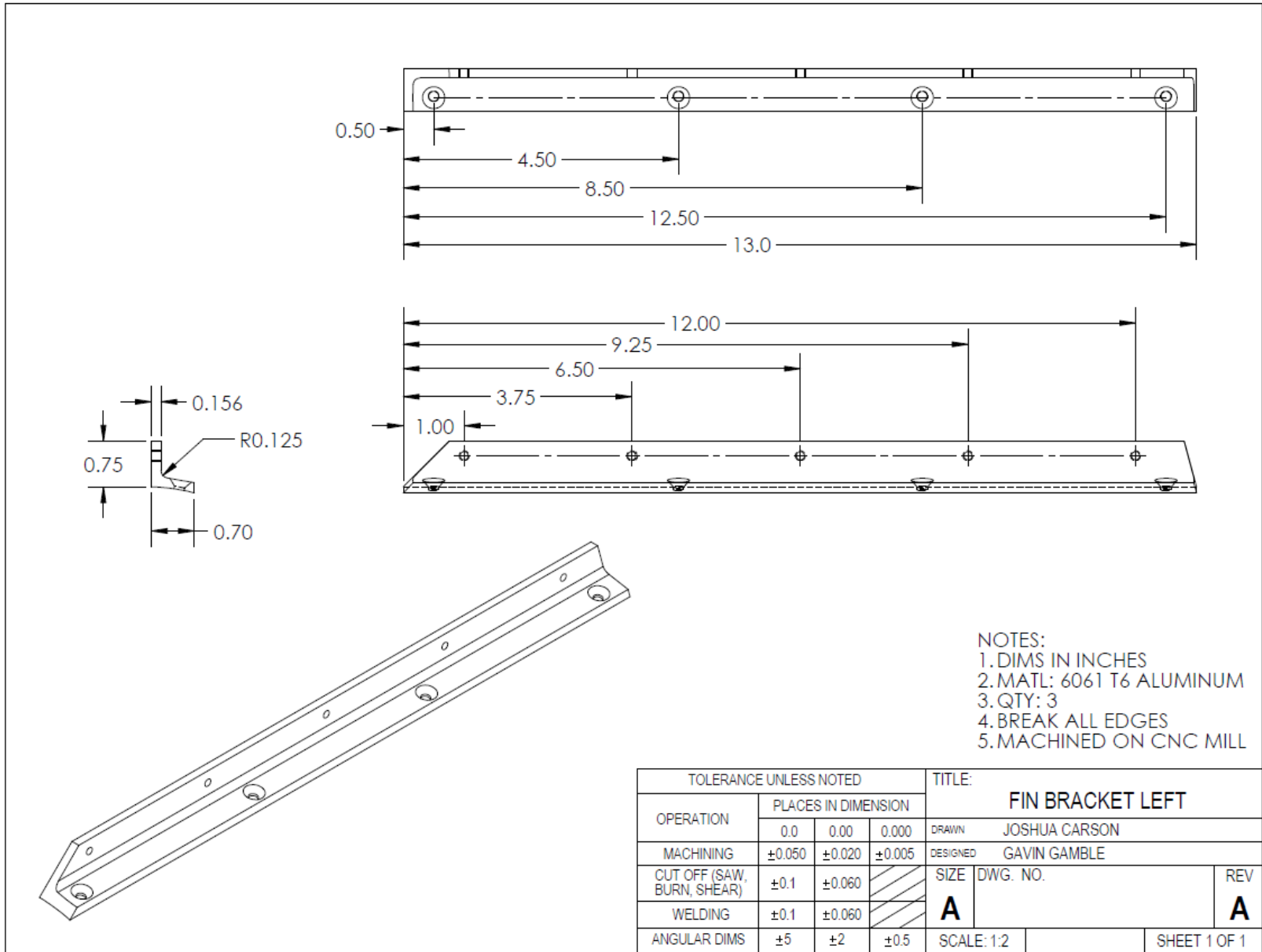
SOLIDWORKS Educational Product. For Instructional Use Only.



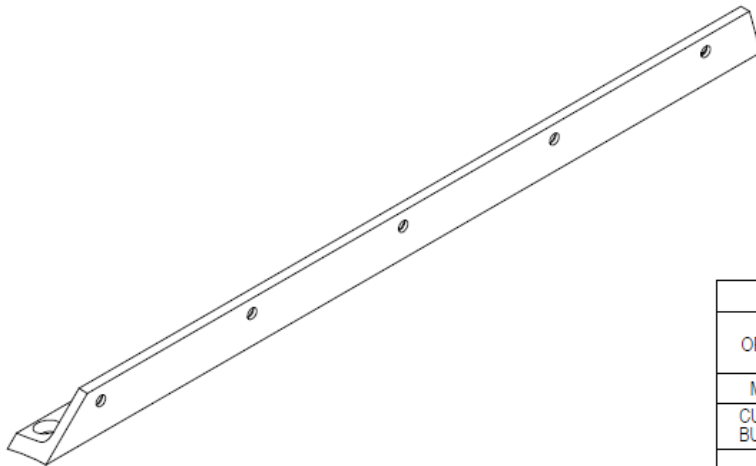
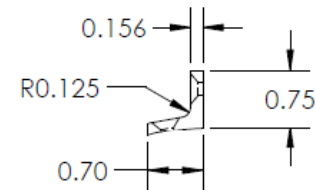
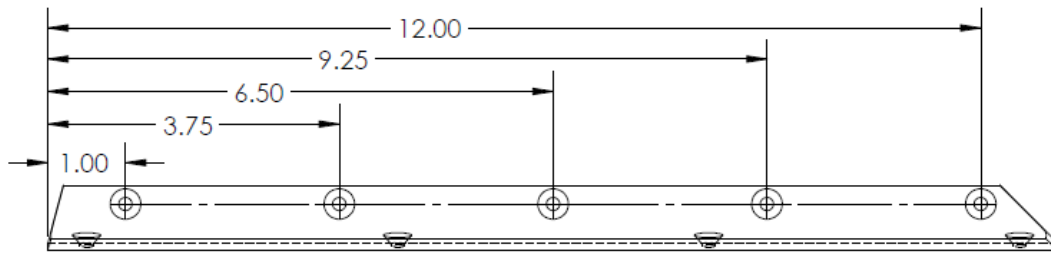
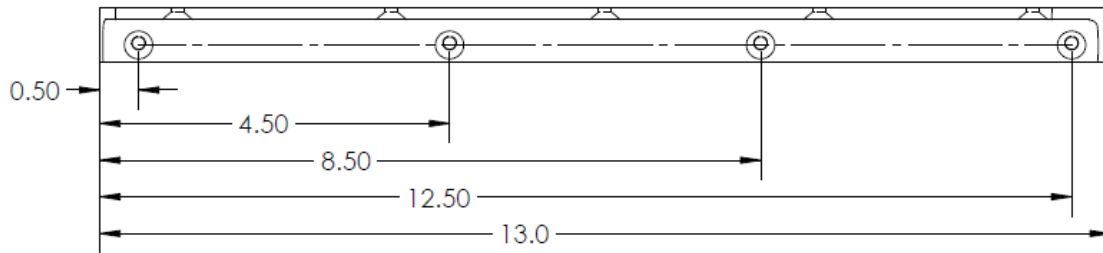
ALL PLANAR GEOMETRY CUT  
USING ABRASIVE WATERJET

- NOTES:  
 1. DIMS IN INCHES  
 2. MATL: CARBON FIBER  
 3. QTY: 1  
 4. BREAK ALL EDGES

TOLERANCE UNLESS NOTED				TITLE:	
OPERATION	PLACES IN DIMENSION			FORWARD CARBON CENTERING RING	
	0.0	0.00	0.000	DRAWN	JOSHUA CARSON
MACHINING	±0.050	±0.020	±0.005	DESIGNED	GAVIN GAMBLE
CUT OFF (SAW, BURN, SHEAR)	±0.1	±0.060		SIZE	DWG. NO.
WELDING	±0.1	±0.060		<b>A</b>	<b>A</b>
ANGULAR DIMS	±5	±2	±0.5	SCALE:1:1.5	SHEET 1 OF 1



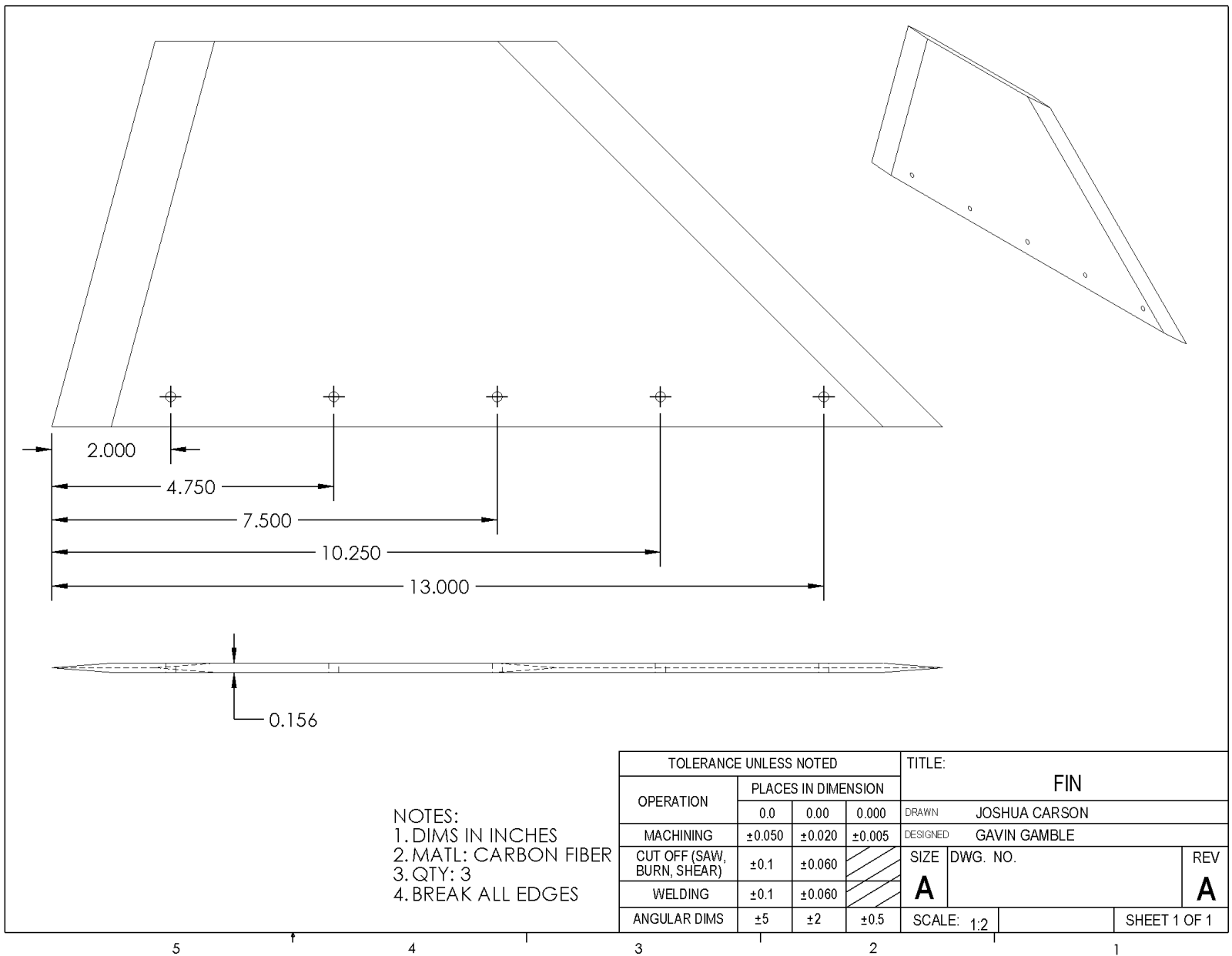
SOLIDWORKS Educational Product. For Instructional Use Only.



- NOTES:  
 1. DIMS IN INCHES  
 2. MATL: 6061 T6 ALUMINUM  
 3. QTY: 3  
 4. BREAK ALL EDGES  
 5. MACHINED ON CNC MILL

TOLERANCE UNLESS NOTED				TITLE:	
OPERATION	PLACES IN DIMENSION			FIN BRACKET RIGHT	
	0.0	0.00	0.000	DRAWN	JOSHUA CARSON
MACHINING	±0.050	±0.020	±0.005	DESIGNED	GAVIN GAMBLE
CUT OFF (SAW, BURN, SHEAR)	±0.1	±0.060		SIZE	DWG. NO.
WELDING	±0.1	±0.060		<b>A</b>	<b>A</b>
ANGULAR DIMS	±5	±2	±0.5	SCALE: 1:2	SHEET 1 OF 1

SOLIDWORKS Educational Product. For Instructional Use Only.



NOTES:  
 1. DIMS IN INCHES  
 2. MATL: CARBON FIBER  
 3. QTY: 3  
 4. BREAK ALL EDGES

5 4 3 2 1

### Acknowledgments

Swamp Launch IREC thanks the team mentor, Jimmy Yawn, for his extensive assistance at launch sites and mentorship in designing a launch vehicle for the IREC 22'.

Swamp Launch IREC thanks the team advisor, Dr. Sean Niemi, for guidance in design for manufacturing and presentation techniques.

Swamp Launch IREC thanks the safety reviewer, Matthew Reppa, for providing feedback on the launch vehicle design.

Swamp Launch IREC thanks the team co-advisor, Dr. Richard Lind, for payload design suggestions.

Swamp Launch IREC thanks former Swamp Launch members for feedback during design reviews.

Swamp Launch IREC thanks Aerojet Rocketdyne for their donation to the team.

Swamp Launch IREC thanks the UF Student Government for funding of the Fall semester.





## References

- [1] S. Niskanen, *OpenRocket, Ver. 15.03*, 2015.
- [2] C. A. Hinds, "Do Different Fin Designs Affect a Rocket's Maximum Altitude?," *CALIFORNIA STATE SCIENCE FAIR*, 2004.
- [3] AeroRocket, *AeroFinSim 10, Ver 5.7 LITE*, 2022.
- [4] V. Knowles, "Ejection Charge Sizing," Vern's Rocketry, 2007. [Online].
- [5] E. J. F. H. H. R. H. Oberg, *Machinery's Handbook*, 30th ed.,, South Norwalk: Industrial Press, Inc., 2016.
- [6] Arduino, "Mahony," May 2022. [Online].
- [7] "Material Property Data," Matweb, [Online]. Available: <https://www.matweb.com/>.
- [8] PJRC, "PJRC.com/store/teensy41," May 2022. [Online].
- [9] Adafruit, "Adafruit.com/product/3387," May 2022. [Online].
- [10] Adafruit, "Adafruit.com/product/3880," May 2022. [Online].
- [11] Apogee, "TeleGPS," May 2022. [Online].
- [12] Apogee, "Teledongle," May 2022. [Online].
- [13] Tenergy, "Tenergy Li-ion 14.8V 2600mAh Rechargeable Battery Pack w/ PCB," May 2022. [Online].
- [14] ATO, "30 W DC Gear Motor, 3000 rpm, 12V/24V," May 2022. [Online].
- [15] KSADBOSSBO, "Mini Hidden Spy Camera Portable Small 1080P Wireless Cam," May 2022. [Online].
- [16] PerfectFile, "Stratalogger SL100 Altimeter," May 2022. [Online].
- [17] A. Systems, "Featherwight Raven Flight Computer 3," August 2010. [Online].
- [18] FreeCadWeb, "Rocket Ejection Charge Calculator," 2022. [Online].